II. REMARKS

Applicants respectfully request reconsideration of the present application in view of the foregoing amendments and in view of the reasons that follow.

Claim 42 is currently being amended to clarify the claimed subject matter. Claim 42 now recites that the IKK protein complex is autophosphorylated at a T loop of the IKK subunit beta (β). Support for the amendment is found in paragraphs [0029], [0048], [0071] and [0073] of the specification as originally filed.

This amendment changes a claim in this application. A detailed listing of all claims that are, or were, in the application, irrespective of whether the claim(s) remain under examination in the application, is presented, with an appropriate defined status identifier. The amendment to the claim is made without prejudice or disclaimer to Applicants' right to pursue the same or similar subject claims in a related application.

The amendment presents the finally rejected claims in better form for allowance or consideration upon appeal. They were not made earlier as Applicants believe the claims as previously amended presented patentable subject matter. Therefore, this amendment complies with 37 C.F.R. § 1.116. Entry of the amendment is respectfully requested. After amending the claims as set forth above, claims 2, 5-7, 17-19, 21-23 and 42 are now pending in this application.

37 C.F.R. § 1.131 Supplemental Declaration

With respect to the Supplemental Declaration Under 37 C.F.R. § 1.131, the Office alleged that the Declaration did not make clear what was done in each experiment and what each gel shows. However, the Office acknowledged that the Declaration stated that similar gels and results are shown in Figure 3 and described in the specification. The Office also acknowledged that the experiments of the declaration appear essentially the same as the experiments of Figure 3, and the brief description of Figure 3 is clear as to what was done. In view of the above interpretation, the

Declaration was deemed sufficient, but the Office stated that if the interpretation is incorrect, Applicants should so state on the record and the rejection will be reinstated unless Applicants provide further explanation of what the experiments of the declaration show.

Applicants agree with the Office's interpretation of the Declaration and state for the record that the experiments of Figure 3 are essentially the same as the experiments of the Declaration.

35 U.S.C. § 112, Second Paragraph

Claims 5-7, 17-19, 21-23 and 42 stand rejected under 35 U.S.C. § 112, second paragraph as allegedly indefinite on the ground that the term "said IKK gamma (γ) gene solely regulates activation of said IKK protein complex" is unclear.

Without conceding to the correctness of the Office's position and in a sincere effort to advance prosecution of the application, claim 42 has been amended to remove the offending language. Claim 42 now recites in its place that the IKK subunit (β) is autophosphorylated at the T loop. Support for the amendment is recited above. Claims 5-7, 17-19 and 21-23 depend from claim 42. In view of the preceding amendment, reconsideration and withdrawal of the rejection is respectfully requested.

35 U.S.C. § 112 First Paragraph

Claims 5-7, 17-19, 21-23 and 42 stand rejected under 35 U.S.C. § 112, first paragraph as allegedly failing to comply with the written description requirement. The Office alleged that the specification fails to provide support for IKK gamma being the sole means of activating the IKK protein complex.

Without conceding to the correctness of the rejection and in a sincere effort to advance prosecution of the application, claim 42 has been amended to recite that the IKK subunit (β) is autophosphorylated at the T loop. Claim 42, as amended, has

sufficient written description support from the specification as originally filed. For example, paragraph [0029] of the specification provides that "IKKγ regulates the autophosphorylation of the T loop residues in the kinase domain of IKKβ. When the T loop residues are phosphorylated, the kinase is active." Claims 5-7, 17-19 and 21-23 depend from claim 42. Therefore, in view of the preceding amendment and remarks, reconsideration and withdrawal of the rejection is respectfully requested.

35 U.S.C. § 103(a)

Claims 2, 5-7, 17-19, 21-23 and 42 stand rejected under 35 U.S.C. § 103(a) as allegedly obvious over Rothwarf et al. in view of Traincard et al. and Epinat et al.

The Office alleged that Rothward et al. teaches that IKK complex can be activated by overexpression of NIK or MEKK1 in mammalian cells and Applicants' argument did not provide reason for believing that overexpression of NIK or MEKK1 wouldn't have the same effect on the IKK complex in yeast cells. The Office further alleged that autophosphorylation of the IKK complex was known in the prior art. Furthermore, the Office alleged that a skilled artisan would clearly expect that the IKK α, β, γ subunits to have all inherent functions when they are coexpressed in any eukaryotic system and, hence, production of substantially homogenous and biologically functional IKK protein in yeast would be expected from the teaching of the prior art.

1. Rothwarf et al. does not teach that IKK complex can be activated by NIK or MEKK1 in yeast

Applicants provided in the response to the Non-Final Office Action mailed October 15, 2008, that Rothwarf et al. does not teach that IKK complex can be activated by NIK or MEKK1 in yeast systems. The Office alleged that this statement is insufficient to overcome the explicit teaching by Rothwarf et al. that overexpression of NIK and MEKK2 can be used for activation of the IKK complex. The Office alleged that the disclosure of Rothwarf et al. that IKK- α/β can be activated by overexpression of

NIK and MEKK1 in mammalian cells suggests that overexpression of these genes have the same effect on IKK complex in the yeast cells. Applicants respectfully disagree.

Applicants submit that the disclosure in Rothwarf et al. that IKK- α/β can be activated by NIK or MEKK1 in human cells does not teach or suggest that the same reaction can take place in yeast, because yeast lack the upstream regulatory elements believed necessary for expression and activation of the complex. Taking NIK as an example, in order for NIK to active IKK- α/β, all of the following must occur: **1)** NIK is activated, **2)** NIK's cofactor is present and binds to NIK, and **3)** NIK's substrate, IKK, is in a suitable condition for activation. As explained in detail below, these requirements are present in a human cell but not in a yeast cell. Moreover, only human cells and artificial human systems were studied in the cited prior art. The claimed yeast expression system was neither made nor studied until Applicants' invention.

1) NIK requires activation

NIK is a member of the MAP3K-related serine-threonine kinase family (Ling et al. (1997) Proc. Natl. Acad. Sci. USA 95, 3791-7 (attached as Exhibit A), page 3796, first column second paragraph). MAP3K enzymes are not functional until activated, such as Raf-1, which is phosphorylated and activated when binding to Ras. The molecular mechanisms by which NIK is activated were not known (Ling et al., page 3792, second column, first paragraph), and it was speculated that NIK was activated by a complex involving TRAF and/or RIP proteins (Ling et al., page 3797, first column, second paragraph). Therefore, in order for NIK to activate IKK, NIK needs to be activated.

2) NIK requires cofactors

NIK was first identified as a TRAF2 interacting protein (Malinin et al. (1997) Nature 385:540-4, Abstract, attached as Exhibit B). This suggests that in order for NIK to activate IKK, TRAF2 needs to be present and bind to NIK.

3) NIK requires IKK to be bound to NEMO

NEMO binds to a serine-rich region of the C-terminus of IKK-β. In the absence of NEMO, IKK-β is autophosphorylated at the serine-rich region, making itself refractory to TNFα-induced signal (U.S. Patent No. 6,864,355, as cited by the Office, the '355 Patent) and thus can not be activated by NIK. Therefore, in order for NIK to activate IKK, NEMO needs to be present and bind to IKK.

Additionally, as of the effective filing date of the current application, it was known that yeast lacks the TNF-α and NF-κB signaling pathways (see Specification of the present application at paragraph [0024]), to which the biological reactions between IKK and NIK or MEKK1 belong. Therefore, there was a general understanding by one of skill in the art that it was difficult to reconstruct all or even part of the TNF-α and NF-κB signaling pathway in yeast. This general understanding is further evidenced by scientific references published even after the effective filing date of the current application.

For example, it was reported that TRAF6 recruits and activates NIK, and TAK1, TAB1 and TAB2 also may act upstream of NIK (Li et al. (2006) J. Bio. Chem. 281(3):1495-505 (attached as Exhibit C), at page 1495, second column, second paragraph). Li et al. (2006) also discloses that H_2O_2 plays an important role in NIK activation following IL-1β stimulation, by promoting TRAF6 association with NIK (Li et al, page 1496, first column, fourth paragraph).

Binding to TRAF proteins is essential for NIK's function because a point mutation in NIK's TRAF-binding region eliminated NIK's ability to activate IKK (Yin et al. (2001) "Defective lymphotoxin-β receptor-induced NF-κB transcriptional activity in NIK-deficient mice," Science 291:2162-65, attached as Exhibit D). Also, NIK is a component of the EGF/heregulin receptor signaling complexes which include ErbB4 and Grb7 (Chen et

al. (2003) Oncogene 22(28):4348-55, Abstract, attached as Exhibit E). These findings further confirm that NIK cannot act alone.

Additionally, NIK undergoes degradation when its binding to Hsp90 is inhibited, suggesting that Hsp90 is specifically involved in the folding and stabilization of NIK (Qing et al. (2007) Cell Res. 17(6):520-30, Abstract, attached as Exhibit F).

Therefore, in order for NIK to activate IKK, at the minimum, NIK needs to be recruited and activated by TRAF6, bind to TRAF2, be stabilized by Hsp90, and bind to IKK in the presence of NEMO. Some of these proteins or their counterparts, such as Hsp90, may be present in yeast, but most are not. Even in the case of Hsp90, which is more selective than other chaperones, it was unknown whether the yeast Hsp90 has the same specificity or function as the human counterpart.

In a human cell, all of these proteins are constantly present, therefore overexpression of NIK can tilt the balance of the biochemical reaction towards IKK activation even when other proteins in the pathway are unaltered. However, at the time of the effective filing date of the application, it would not have been expected to one of ordinary skill in the art that mere overexpression of NIK, without the presence of the TRAF6, TRAF2, Hsp90, or NEMO, would be able to activate IKK.

Applicants further note that even with the presence of TRAF6, TRAF2, Hsp90, and NEMO in a yeast cell, it was still unknown whether NIK would be able to activate IKK in a yeast cell since it was unknown whether each of these proteins require its own activation and cofactors for proper functioning.

The molecular mechanisms by which MEKK1 activates IKK is even less well understood. As of the effective filing date, it was suspected that MEKK1 does not directly activate IKK (Karin et al. (1998) Proc. Natl. Acad. Sci. USA 95:9067-9, attached as Exhibit G, at page 9067, second column, second to the last sentence, and Figure 1). For the same reasons recited for NIK, an observation that overexpression of MEKK1

activates IKK in a human cell does not suggest that MEKK1 can activate IKK in a yeast cell.

Thus, in sum, Applicants submit that one cannot rely on the teaching that IKK was expressed and activated in human cells to expect that IKK can be similarly expressed and activated in yeast, because the comparison of the two systems is one of apples to oranges.

Indeed, many of the findings based on human or mammalian-expressed IKK are inherently tainted by the heterogeneity of the IKK complexes produced in these cells, *i.e.*, the IKK complex produced by one research group and reported in one reference was unlikely to be identical as the IKK produced by another research group and reported in another reference as evidenced by the existence of widely varying and inconsistent findings. Therefore absent an analysis of the complex produced, studied and reported in each reference, the teachings cannot be combined as to obviate or draw any reasonably definite conclusions.

Therefore, the disclosure in Rothwarf et al. that IKK can be activated by overexpression of NIK and MEKK1 does not teach or suggest that IKK can be activated in yeast by these proteins.

2. U.S. Patent No. 6,864,355 does not teach that IKK complex can be autophosphorylated and activated

The Office alleged that IKK autophosphorylation is taught in U.S. Patent No. 6,864,355 ("the '355 Patent). Applicants note that the '355 Patent teaches that IKK-β is autophosphorylated at a serine-rich region of the C-terminus (the '355 Patent, at column 24, lines 53 to 63). However, this "autophosphorylation serves to down-regulate TNFα-induced IKKβ activity by causing conformational changes within the protein" and autophosphorylated IKKβ is "refractory to TNFα-induced signals" (the '355 Patent, at column 25, lines 40 to 48, emphasis added).

To the contrary, autophosphorylation as described and claimed in the current application occurs at a T loop of the N-terminus of IKK-β and results in activation of IKK. As disclosed in the application (see, e.g., paragraphs [0046]) and further explained in Schomer-Miller et al. (2006) J. Bio. Chem. 281(22):15268-76 (attached as Exhibit H), IKK with autophosphorylation at the C-terminus of IKK-β only has basal level activity. Upon stimulation, IKK-β is dephosphorylated at the C-terminus. IKK is then activated by autophosphorylation at the T loop of the N-terminus (see, e.g., paragraph [0029] of the Specification, and Schomer-Miller et al. Abstract and Figure 5).

Therefore, the '355 Patent does not teach that IKK complex can be autophosphorylated **and** activated.

3. **Activated IKK is not an expected inherent result of coexpression of the α, β, and γ subunits**

The Office alleged that production of substantially homogenous and biologically functional IKK protein is expected because they are inherent functions of the α, β, and γ subunits. However, the claims, as both previously presented and currently amended, are directed to methods for preparing substantially homogenous, biologically functional and activated IKK protein complex.

Applicants note that it was known in the art, at the time the application was filed, that IKK-β can be autophosphorylated and basally active in human and mammalian cells. It was unknown that IKK can be activated in yeast. "Activated", refers "a state of being more than usually active" (Blood and Studdert (1999) Saunders Comprehensive Veterinary Dictionary, 2nd Ed. WB Saunders). "Basal", on the other hand, refers to "of, relating to, or being essential for maintaining the fundamental vital activities of an organism : MINIMAL" (Webster's Ninth New Collegiate Dictionary (1988) Merriam-Webster Inc. Emphasis in original). An activated IKK is clearly different from a basally active IKK-β. Therefore, an activated IKK is not an expected inherent result of coexpression of the α, β, and γ subunits.

For the reasons explained above, claims 2, 5-7, 17-19, 21-23 and 42 are not obvious over Rothwarf et al. in view of Traincard et al. and Epinat et al, because the prior art in combination does not teach or suggest that the IKK protein complex can be activated in yeast.

4. **Claim 42**

Claim 42 has been currently amended to clarify the claimed subject matter. Claim 42 recites that the IKK protein complex is autophosphorylated at a T loop of the IKK subunit beta (β). The autophosphorylation and activation of the IKK protein complex, as explained above, is not taught or suggested by any of the cited prior art references or in any combination. Therefore, claim 42 is not obvious over the prior art.

In view of the preceding amendments and remarks, Applicants submit that the cited references do not teach as alleged by the Office and that given the deficiencies of the basic teachings, the references alone or in combination, fail to render obvious the claimed subject matter. Thus, reconsideration and withdrawal of the rejections under 35 U.S.C. §103, is respectfully requested.

[The rest of the page is intentionally left blank.]

III. CONCLUSION

Applicants believe that the present application is now in condition for allowance. Favorable reconsideration of the application as amended is respectfully requested.

The Examiner is invited to contact the undersigned by telephone if it is felt that a telephone interview would advance the prosecution of the present application.

The Commissioner is hereby authorized to charge any additional fees which may be required regarding this application under 37 C.F.R. §§ 1.16-1.17, or credit any overpayment, to Deposit Account No. 19-0741. Should no proper payment be enclosed herewith, as by the credit card payment instructions in EFS-Web being incorrect or absent, resulting in a rejected or incorrect credit card transaction, the Commissioner is authorized to charge the unpaid amount to Deposit Account No. 19-0741. If any extensions of time are needed for timely acceptance of papers submitted herewith, Applicant hereby petitions for such extension under 37 C.F.R. §1.136 and authorizes payment of any such extensions fees to Deposit Account No. 19-0741.

Respectfully submitted,

Date: July 28, 2009

By 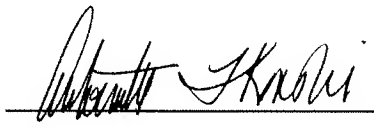

FOLEY & LARDNER LLP
Customer Number: 38706
Telephone: (650) 251-1129
Facsimile: (650) 856-3710

Antoinette F. Konski
Attorney for Applicants
Registration No. 34,202

Alex Y. Nie
Attorney for Applicants
Registration No. 60,523

EXHIBIT A

Proc. Natl. Acad. Sci. USA
Vol. 95, pp. 3792–3797, March 1998
Immunology

NF-κB-inducing kinase activates IKK-α by phosphorylation of Ser-176

LEI LING, ZHAODAN CAO, AND DAVID V. GOEDDEL*

Tularik, Inc., Two Corporate Drive, South San Francisco, CA 94080

Contributed by David V. Goeddel, January 29, 1998

ABSTRACT **Activation of the transcription factor NF-κB by inflammatory cytokines involves the successive action of NF-κB-inducing kinase (NIK) and two IκB kinases, IKK-α and IKK-β. Here we show that NIK preferentially phosphorylates IKK-α over IKK-β, leading to the activation of IKK-α kinase activity. This phosphorylation of IKK-α occurs specifically on Ser-176 in the activation loop between kinase subdomains VII and VIII. A mutant form of IKK-α containing alanine at residue 176 cannot be phosphorylated or activated by NIK and acts as a dominant negative inhibitor of interleukin 1- and tumor necrosis factor-induced NF-κB activation. Conversely, a mutant form of IKK-α containing glutamic acid at residue 176 is constitutively active. Thus, the phosphorylation of IKK-α on Ser-176 by NIK may be required for cytokine-mediated NF-κB activation.**

Many of the common proinflammatory properties of tumor necrosis factor (TNF) and interleukin 1 (IL-1) are mediated by the transcription factor NF-κB (1–3). Under normal conditions, NF-κB exists in a cytoplasmic complex with an inhibitor protein IκB (1–3). The activation of NF-κB requires phosphorylation of IκB-α at Ser-32 and Ser-36 (4). This phosphorylation targets IκB-α for ubiquitination and proteosome-mediated degradation, thereby releasing NF-κB to enter the nucleus and activate a series of genes involved in the inflammatory response (5).

It is now known that NF-κB activation by TNF and IL-1 involves signal transduction cascades containing several intermediate signaling proteins. TNF initiates its signaling by binding to and trimerizing the type 1 TNF receptor, TNF-R1 (6, 7). Several cytoplasmic proteins, including TNF-R1-associated death domain protein (TRADD) (6), TNF receptor-associated factor (TRAF2) (8), and receptor-interacting protein (RIP) (9), are then recruited to the intracellular domain of TNF-R1 where they form an active signaling complex. Overexpression of each of these proteins can activate the signaling cascade leading to NF-κB activation. On the other hand, IL-1 induces the formation of a complex including two distinct receptor chains, IL-1RI and IL-1RAcP (10), the adaptor protein MyD88 (11), and the protein kinase IRAK (12). Following its activation, IL-1 receptor-associated kinase (IRAK) is released from the receptor complex (11) and associates with TRAF6 (13).

These distinct TNF and IL-1 pathways merge at the level of the protein kinase NF-κB-inducing kinase (NIK) (14). NIK, which is a member of the mitogen-activating protein (MAP) kinase kinase kinase (MAP3K) family, was originally identified as a TRAF2-interacting protein. NIK activates NF-κB when overexpressed, and kinase-inactive mutants of NIK behave as dominant-negative inhibitors that suppress NF-κB activation mediated by TNF, IL-1, TRADD, RIP, TRAF2, TRAF5, and TRAF6 (14, 15). Thus, NIK is a common mediator in the NF-κB signaling cascades triggered by TNF and IL-1 that acts downstream of the receptor complexes. However, NIK is not involved in TNF and IL-1-stimulated kinase pathways that lead to the activation of the Jun N-terminal kinase (15). The details of the molecular mechanism(s) by which NIK itself becomes activated are not yet understood.

In an effort to identify downstream targets of NIK, conserved helix–loop–helix ubiquitous kinase (CHUK) was isolated in a yeast two-hybrid screen (16). CHUK was also biochemically purified from TNF-treated HeLa cells by DiDonato *et al.* (17) and by Mercurio *et al.* (18). CHUK is an 85-kDa protein kinase of previously unknown function (19). CHUK directly associates with, and specifically phosphorylates IκB-α on Ser-32 and -36 (16, 17). A catalytically inactive mutant of CHUK is a dominant-negative inhibitor of TNF-, IL-1, TRAF2-, TRAF6-, and NIK-induced NF-κB activation and CHUK kinase activity is stimulated by cytokine treatment (16, 17). Based on these results, CHUK has been redesignated as IκB kinase-α (IKK-α). Cells cotransfected with NIK and IKK-α display elevated IKK-α activity (16). A second IKK, IKK-β, with 52% amino acid identity to IKK-α, was also recently identified (18, 20, 21). IKK-α and IKK-β exist in a heterocomplex form that is able to interact with NIK (20). Thus, IKK-α and IKK-β may both represent downstream targets of NIK, and all three of these kinases are likely present in a large IκB kinase complex of 700–900 kDa (17, 20, 22).

Because NF-κB can be activated by numerous stimuli, the IKK complex may serve as an integration point for signals emanating from many different pathways. Although the molecular mechanism for activation of this kinase complex is not known, IKK-α is likely a downstream target of NIK, because NIK coexpression stimulates the ability of IKK-α to phosphorylate IκB-α. Additionally, a dominant negative form of IKK-α blocks NIK-induced NF-κB activation (16, 20). Because NIK is a member of the MAP3K family, it may activate downstream kinases by specific phosphorylation events similar to other MAP3K family members. In this study, we report that IKK-α is a better substrate than IKK-β for phosphorylation by NIK. The primary site of IKK-α phosphorylation by NIK is Ser-176 in the kinase activation loop. Phosphorylation of this residue correlates with activation of IKK-α.

MATERIALS AND METHODS

Cell Culture and Biological Reagents. Recombinant human TNF and IL-1 were provided by Genentech, Inc. (South San Francisco). The anti-FLAG mAb M2 affinity resin and purified FLAG peptide were purchased from Eastman Kodak. Rabbit anti-FLAG and anti-Myc polyclonal antibodies were from Santa Cruz Biotechnology. Human embryonic kidney

The publication costs of this article were defrayed in part by page charge payment. This article must therefore be hereby marked "*advertisement*" in accordance with 18 U.S.C. §1734 solely to indicate this fact.

Abbreviations: NIK, NF-κB-inducing kinase; IKK, IκB kinase; TNF, tumor necrosis factor; IL, interleukin; MAP, mitogen-activating protein; MAP3K, MAP kinase kinase kinase; β-gal, β-galactosidase.

*To whom reprint requests should be addressed. e-mail: goeddel@tularik.com.

293 cells, 293/IL-1R1 cells (12) and HeLa cells were maintained as described (6).

Expression Vectors. Mammalian cell expression vectors encoding wild-type and kinase-inactive versions of NIK, IKK-α, and IKK-β have been described (15, 16, 20). IKK-α(KA) and IKK-β(KA) signify lysine to alanine changes at amino acid 44 of IKK-α and IKK-β, respectively. NIK(KA) represents lysine to alanine changes at amino acids 429 and 430 of NIK. The control expression plasmid pRK5, the NF-κB-dependent E-selectin-luciferase reporter gene plasmid and plasmid RSV-β-galactosidase were also described (23, 24). Expression vectors encoding IKK-α and IKK-β mutants with alanine or glutamic acid replacing serine and threonine residues in the activation loop of IKK-α and IKK-β [IKK-α(S176A), IKK-α(KA)S176A, IKK-α(S176E), IKK-α(T179A), IKK-α(KA)T179A, IKK-α(S180A), IKK-α(KA)S180A, IKK-β(S177A)] were constructed using Stratagene Quickchange site-directed mutagenesis kit. All the mutations were verified by DNA sequencing analysis.

Immunoprecipitation, Western Blot Analysis and *in Vitro* Kinase Assays. 293 cells or HeLa cells were transiently transfected with expression plasmids by using calcium phosphate as described (6). Between 24–36 hr later, cells were washed with cold PBS and lysed in Nonidet P-40 lysis buffer containing 50 mM Hepes (pH 7.6), 250 mM NaCl, 10% glycerol, 1 mM EDTA, 0.1% Nonidet P-40, and Complete protease inhibitors (Boehringer Mannheim) (16, 20). Cell lysates were cleared and incubated for 2–4 hr at 4°C with anti-FLAG M2 antibody resin (Kodak), washed extensively with lysis buffer and eluted with FLAG peptide (300 μg/ml, Kodak) or not eluted. *In vitro* kinase assays were performed with eluted proteins or immune complexes and bacterially synthesized IκB-α (amino acids 1–250) proteins (16) in 20 μl kinase buffer containing 20 mM Tris·HCl (pH7.6), 10 mM MgCl2, 0.5 mM DTT, 100 μM ATP, and 5 μCi of [γ-^{32}P]ATP (1 Ci = 37 GBq) at room temperature for 30 min (16). Samples were analyzed by 10% SDS/PAGE and autoradiography. Immunoblotting analyses were performed with rabbit polyclonal antibodies and detected by alkaline phosphatase-conjugated goat-anti-rabbit secondary antibody.

Reporter Assays. For reporter gene assays, 293 cells, 293/IL-1R1 cells, or HeLa cells were seeded into six-well plates. Cells were transfected the following day by the calcium phosphate precipitation method with 0.5 μg E-selectin-luciferase reporter gene plasmid, 1 μg pRSV-β-gal plasmid, and various amounts of each expression construct. The total DNA transfected (4.5 μg) was kept constant by supplementation with the control vector pRK5. In the NIK and IKK-α synergy experiments, 0.01 μg of NIK, IKK-α(WT), and IKK-α(S176A) were used for each 35-mm well. After 24 hr, cells were either left untreated or stimulated with IL-1 (10 ng/ml), or TNF (100 ng/ml) for 5 hr prior to harvest. Reporter gene activity was determined with the Luciferase Assay System (Promega). The results were normalized for transfection efficiency on the basis of β-gal expression.

RESULTS

***In Vitro* Phosphorylation of IKK-α by NIK.** NIK directly interacts with IKK-α and IKK-β, and the phosphorylation of IκB-α by IKK-α and IKK-β is enhanced by NIK coexpression (16, 20). These results suggest that IKK-α and IKK-β may be NIK-activated IκB-α kinases that link TNF-and IL-1-induced kinase cascades to NF-κB activation. To investigate if IKK-α and IKK-β can be phosphorylated by NIK, we transiently expressed FLAG epitope-tagged wild-type or kinase-inactive mutants of NIK, IKK-α, and IKK-β in human embryonic kidney 293 cells (Fig. 1). The epitope-tagged proteins were immunoprecipitated with an anti-FLAG antibody, and incubated with [γ-^{32}P]ATP. In these assays, wild-type IKK-α, IKK-β, and NIK become autophosphorylated when expressed individually, while mutants of all three kinases containing lysine-to-alanine (KA) substitutions in their ATP-binding sites were not autophosphorylated (16). The IKK-α(KA) and IKK-

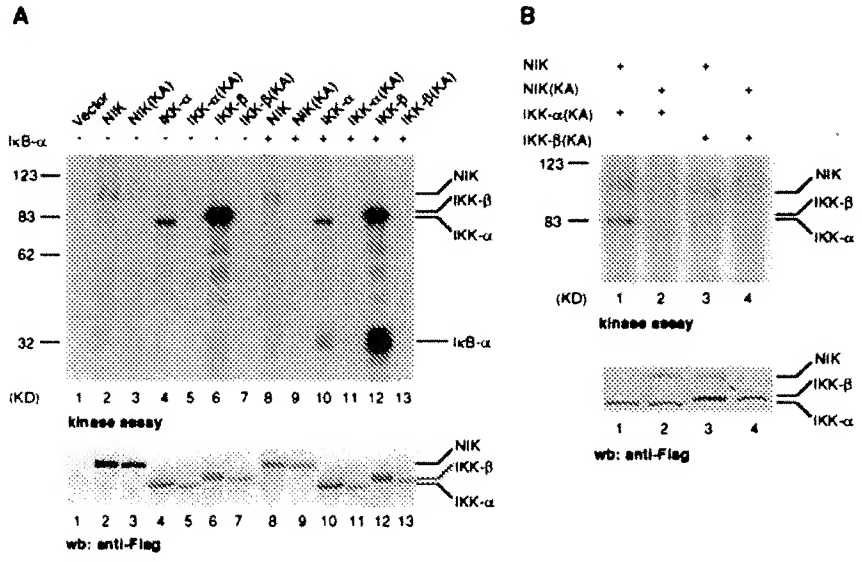

FIG. 1. In vitro phosphorylation of IKK-α by NIK. (*A*) Autophosphorylation and phosphorylation of IκB-α by various kinases. 293 cells were transiently transfected with expression plasmids encoding FLAG epitope-tagged wild-type or KA mutants of NIK, IKK-α and IKK-β. Thirty-six hours after transfection, extracts were immunoprecipitated with anti-FLAG mAb affinity resin and FLAG-tagged proteins were purified as described in *Materials and Methods*. Purified proteins were incubated with [γ-^{32}P]ATP in the presence or absence or bacterially synthesized protein IκB-α (amino acids 1–250), resolved by SDS/PAGE, and analyzed by autoradiography. The amounts of proteins used in the reactions were determined by immunoblotting (wb) with anti-FLAG polyclonal antibodies (*Lower*). The positions of IKK-α, IKK-β, and NIK are indicated. (*B*) Phosphorylation of IKK-α(KA) and IKK-β(KA) by NIK. 293 cells were transiently transfected with expression plasmids encoding FLAG epitope-tagged wild-type NIK, IKK-α(KA), or IKK-β(KA). Purified proteins were incubated with [γ-^{32}P]ATP, resolved by SDS/PAGE, and analyzed by autoradiography. The amounts of proteins used in the reactions were determined by immunoblotting (wb) with anti-FLAG polyclonal antibodies (*Lower*). The positions of IKK-α, IKK-β, and NIK are indicated.

β(KA) mutants were also unable to phosphorylate IκB-α (Fig. 1*A*).

To examine its ability to phosphorylate IKK-α and IKK-β, we coexpressed NIK with the catalytically inactive IKK mutants. We found that NIK can phosphorylate IKK-α(KA), but only weakly phosphorylates IKK-β(KA) (Fig. 1*B*, compare lanes 1 and 3). The kinase-inactive NIK does not phosphorylate IKK-α(KA) or IKK-β(KA) (Fig. 1*B*, lanes 2 and 4). In addition, we found that purified, baculovirus-expressed IKK-α(KA) can be phosphorylated by baculovirus-expressed NIK, but not by baculovirus-expressed NIK(KA) (data not shown).

Ser-176 of IKK-α Is Phosphorylated by NIK. Because NIK is a MAP3K-related kinase, it may activate a downstream kinase or kinases in a manner similar to other members of the MAP3K family. MAP3Ks activate MAP2Ks (such as MEK1) by phosphorylating serine and threonine residues in the "activation loop" between kinase subdomains VII and VIII (25–27). Therefore, we examined serine and threonine residues in the activation loop of IKK-α as we have no evidence for IKK-α being tyrosine-phosphorylated (unpublished data).

There are two serines (residues 176 and 180) and a threonine (residue 179) in the activation loop of IKK-α (Fig. 2). To test if Ser-176, Thr-179, or Ser-180 are phosphorylated by NIK, each of these three residues was mutated to alanine in the background of the inactive IKK-α(KA) mutant to eliminate IKK-α autophosphorylation activity, and tested for phosphorylation by NIK. Mutation of Ser-176 to alanine [IKK-α(S176A)] significantly reduced the phosphorylation of IKK-α by NIK, while the T179A and S180A mutants were still efficiently phosphorylated (Fig. 3). These results indicate that Ser-176 represents the major site of IKK-α phosphorylation by NIK.

Loss of Activation of IKK-α(S176A) by NIK. Because NIK can phosphorylate Ser-176 in the activation loop of IKK-α and stimulate IκB-α phosphorylation by IKK-α, it is possible that Ser-176 phosphorylation may be required for IKK-α activity. If so, the phosphorylation of IκB-α by IKK-α should be greatly impaired when Ser-176 of wild-type IKK-α is mutated to alanine. IKK-α(S176A) was expressed, purified, and found to have greatly reduced activity as measured by both its autophosphorylation and its ability to phosphorylate IκB-α (Fig. 4*A*). In contrast, mutation of the equivalent serine in IKK-β results in a kinase, IKK-β(S177A), that is fully active in autophosphorylation and in phosphorylation of IκB-α (Fig. 4*B*).

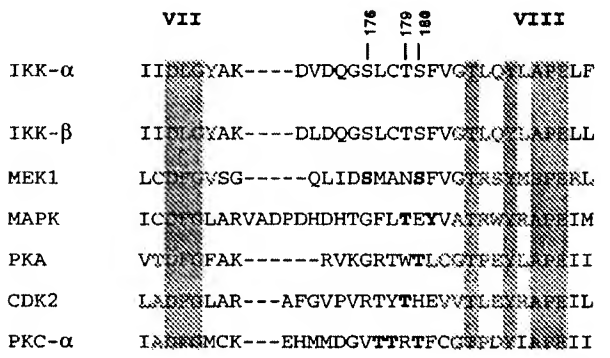

FIG. 2. Alignment of IKK-α amino acid sequences with several kinases in the activation loop region. The D(F/L)G and (A/S)PE residues that are characteristic of kinase subdomains VII and VIII are shaded. The conserved threonine and tyrosine residues in the TXXY motif adjacent to subdomain VIII are also shaded. The activating phosphorylation sites in MEK1 (25, 26), MAPK (30), PKA (31), CDK2 (32), and PKC-α (33) are shown in boldface. The position of the serine and threonines residues of IKK-α are indicated. The sequence of the activation loop of IKK-β is also included.

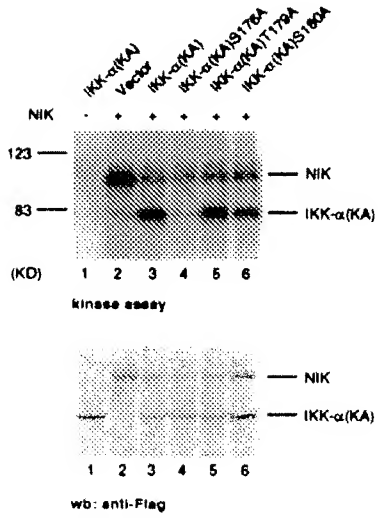

FIG. 3. Ser-176 in the activation loop of IKK-α is a major site of phosphorylation by NIK. Individual serine and threonine residues in the activation loop of IKK-α kinase domain were mutated to alanine. Each IKK-α mutant protein also contained the KA mutation in the ATP-binding site to prevent autophosphorylation. 293 cells were transiently transfected with expression plasmids encoding the indicated FLAG epitope-tagged proteins. Thirty-six hours after transfection, immunopurified proteins were incubated with [γ-^{32}P]ATP, resolved by SDS/PAGE, and analyzed by autoradiography. The amount of protein used in each reaction was determined by immunoblotting (wb) with anti-FLAG polyclonal antibodies (*Lower*).

To determine whether IKK-α(S176A) is also defective in NF-κB activation, we compared IKK-α and IKK-α(S176A) in an NF-κB reporter gene assay in transiently transfected HeLa cells. As expected (16), expression of IKK-α modestly activated the NF-κB luciferase reporter gene in a dose-dependent manner. Mutation of Ser-176 to alanine abrogated the ability of IKK-α to activate NF-κB, similar to the IKK-α(KA) mutant (Fig. 4*C*).

If phosphorylation of Ser-176 is required to activate IKK-α, then mutation of this site should impair the ability of IKK-α to be activated by NIK. To test this, we coexpressed either FLAG epitope-tagged IKK-α or IKK-α(S176A) with Myc epitope-tagged wild-type NIK. We then specifically immunopurified the FLAG epitope-tagged IKK-α proteins and assayed them for IκB-α phosphorylation activity in an *in vitro* kinase assay. The phosphorylation of IκB-α by IKK-α was significantly enhanced when IKK-α was stimulated by NIK, but NIK failed to activate IKK-α(S176A) kinase activity to a similar extent (Fig. 5*A*).

The inability of NIK to activate IKK-α(S176A) is not only reflected by *in vitro* kinase assay but is also observed in tissue culture cells by using an NF-κB reporter gene assay. As shown in Fig. 5*B*, low levels of NIK and IKK-α synergistically activated the NF-κB luciferase reporter gene when coexpressed. This synergy was not observed when NIK is coexpressed with IKK-α(S176A).

IKK-α(S176A) Is a Dominant Negative Inhibitor of IL-1- and TNF-Induced NF-κB Activation. IKK-α associates with both NIK and IKK-β (16, 20). Because the IKK-α(S176A) mutant is inactive in both kinase and NF-κB reporter assays, it might compete with endogenous IKK-α for binding to NIK, IKK-β, or IκB-α and thereby block the activation of NF-κB. To test this, we determined the effect of IKK-α(S176A) on IL-1- and TNF-induced NF-κB activation in reporter gene assays in 293/IL-1RI cells. As shown in Fig. 6, overexpression of IKK-α(S176A) blocked both IL-1- and TNF-induced reporter gene activation in a dose-dependent manner. In addition, overexpression of IKK-α(S176A) blocked NIK-, TRAF2-, and

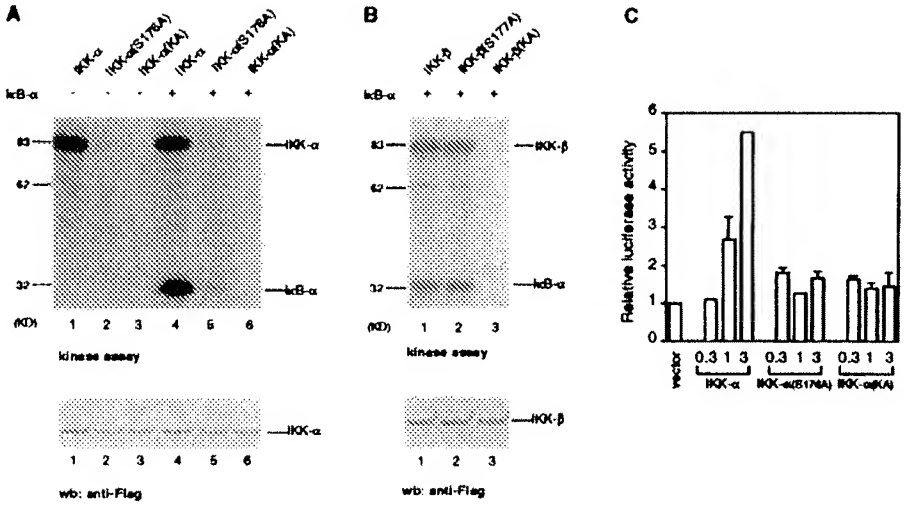

FIG. 4. IKK-α(S176A) has reduced kinase activity and NF-κB activation. (*A*) IKK-α(S176A) has reduced kinase activity. 293 cells were transiently transfected with the indicated epitope-tagged expression vectors. Thirty-six hours after transfection, IKK-α proteins were immunopurified with anti-FLAG mAb affinity resin and used in *in vitro* kinase reactions with IκB-α and [γ-^{32}P]ATP. (*Lower*) The protein expression in each lane is shown. (*B*) IKK-β(S177A) has similar kinase activity as IKK-β. 293 cells were transiently transfected with the indicated epitope-tagged expression vectors. Thirty-six hours after transfection, IKK-β proteins were immunopurified with anti-FLAG mAb affinity resin and used in *in vitro* kinase reactions with IκB-α and [γ-^{32}P]ATP. (*Lower*) The protein expression in each lane is shown. (*C*) IKK-α(S176A) is defective in NF-κB activation. HeLa cells were transiently cotransfected with an E-selectin-luciferase reporter gene plasmid and vector control or IKK-α expression vector as indicated. Twenty-four hours after transfection, luciferase activities were determined and normalized on the basis of β-gal expression. The values shown are averages (±SEM) of duplicate samples for one representative experiment.

TRAF6-induced reporter gene activation in a dose-dependent manner (data not shown).

Mutation of Ser-176 to Glutamic Acid Activates IKK-α. Phosphorylation of IKK-α at Ser-176 introduces negative charge into this portion of the protein and results in kinase activation. It has been shown that substitution with negatively charged amino acids in the activation loop of other kinases can mimic activation (26, 27). Therefore we constructed an IKK-α(S176E) mutant, which contains glutamic acid at position 176. We expressed different doses of IKK-α or IKK-α(S176E) in HeLa cells, and measured the ability of immunopurified IKK-α or IKK-α(S176E) to phosphorylate IκB-α. At equivalent levels of expression, IKK-α(S176E) had significantly greater kinase activity than IKK-α, as measured by either autophosphorylation or phosphorylation of IκB-α (Fig. 7*A*). We also compared IKK-α and IKK-α(S176E) in an NF-κB reporter gene assay in transiently transfected HeLa cells. Mutation of Ser-176 to glutamic acid significantly enhanced the ability of IKK-α to activate NF-κB (Fig. 7*B*).

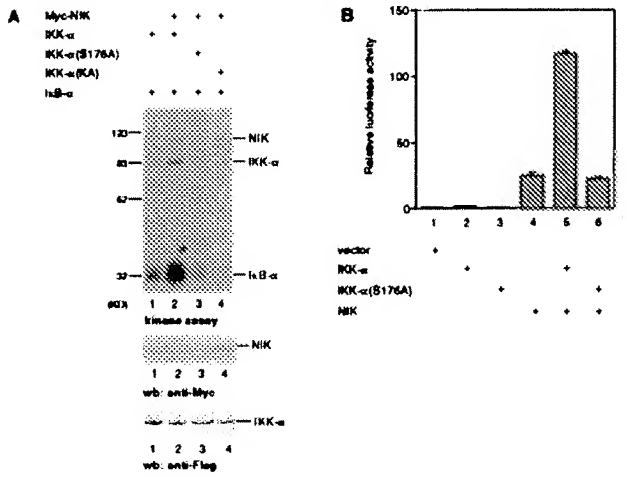

FIG. 5. Loss of IKK-α(S176A) activation by NIK. (*A*) Loss of IKK-α(S176A) activation by NIK in kinase assay. 293 cells were transiently transfected with expression plasmids for FLAG epitope-tagged IKK-α or IKK-α(S176A) and Myc-epitope-tagged NIK. IKK-α proteins (and coprecipitating Myc-NIK proteins) were purified with anti-FLAG antibodies, and *in vitro* phosphorylation reactions were carried out by using bacterially expressed IκB-α and [γ-^{32}P]ATP. The amounts of protein used were determined by immunoblotting with anti-Myc polyclonal antibodies (*Middle*), and with anti-FLAG polyclonal antibodies (*Bottom*). (*B*) Loss of IKK-α(S176A) activation by NIK in an NF-κB reporter gene assay. 293 cells were transiently cotransfected with an E-selectin-luciferase reporter gene plasmid and vector control or IKK-α and NIK expression vectors as indicated. Thirty to 36 hr after transfection, luciferase activities were determined and normalized on the basis of β-gal expression. The values shown are averages (±SEM) of duplicate samples for one representative experiment.

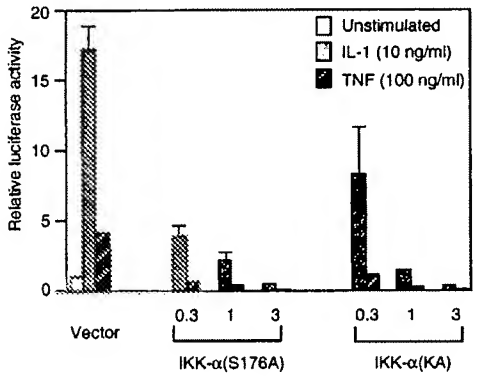

FIG. 6. IKK-α(S176A) is a dominant negative inhibitor of IL-1 and TNF-induced NF-κB activation. 293/IL-1RI cells were transiently cotransfected with an E-selectin-luciferase reporter gene plasmid and vector control or IKK-α(S176A) expression vector as indicated. Twenty-four hours after transfection, cells were either left untreated, or stimulated for 6 hr with IL-1 (10 ng/ml) or TNF (100 ng/ml) prior to harvest. Luciferase activities were determined and normalized on the basis of β-gal expression. The values shown are averages (±SEM) of duplicate samples for one representative experiment.

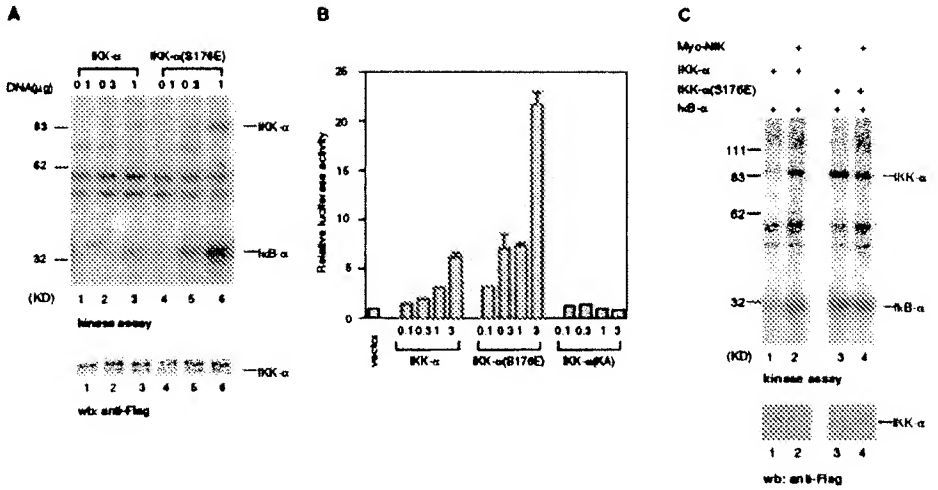

FIG. 7. IKK-α(S176E) is constitutively active. (*A*) IKK-α(S176E) has significantly greater activity than IKK-α in kinase assay. HeLa cells were transiently transfected with expression plasmids for FLAG epitope-tagged IKK-α or IKK-α(S176E) at different doses. Thirty hours later, IKK-α proteins were purified with anti-FLAG antibodies, and *in vitro* phosphorylation reactions were carried out with bacterially expressed IκB-α and [γ-^{32}P]ATP. The amounts of protein used were determined by immunoblotting with anti-FLAG antibodies (as shown in the lower panel). (*B*) IKK-α(S176E) has significantly greater activity than IKK-α in an NF-κB reporter gene assay. HeLa cells were transiently cotransfected with an E-selectin-luciferase reporter gene plasmid and vector control or IKK-α expression vector as indicated. Twenty-four hours after transfection, luciferase activities were determined and normalized on the basis of β-gal expression. The values shown are averages (±SEM) of duplicate samples for one representative experiment. (*C*) IKK-α(S176E) activity is independent of NIK activation. HeLa cells were transiently transfected with expression plasmids for FLAG epitope-tagged IKK-α or IKK-α(S176E) and Myc-epitope-tagged NIK. IKK-α proteins were purified with anti-FLAG antibodies, and *in vitro* phosphorylation reactions were carried out by using bacterially expressed IκB-α and [γ-^{32}P]ATP. The amounts of IKK-α protein used were determined by immunoblotting with anti-FLAG antibodies (*Lower*).

The IKK-α(S176E) mutant is more active than wild-type IKK-α in both kinase assay and reporter assay. However, it is still important to know whether the IKK-α(S176E) mutant can be further activated by the upstream kinase NIK. In the experiments shown in Fig. 7*C*, we expressed FLAG epitope-tagged wild-type IKK-α or the IKK-α(S176E) mutant together with Myc epitope-tagged NIK in HeLa cells. We then measured the ability of the immunopurified IKK-α to phosphorylate recombinant IκB-α. The activity of wild-type IKK-α was strongly enhanced upon activation by the coexpressed NIK kinase. In contrast, IKK-α(S176E) mutant was similarly active when expressed either with or without NIK, suggesting that IKK-α(S176E) activity is independent of upstream activation.

DISCUSSION

The TNF- and IL-1-induced NF-κB activation pathways converge at NIK, a MAP3K-related serine/threonine kinase (14). NIK forms a complex with two IKKs, IKK-α and IKK-β (16, 20). IKK-α and IKK-β are serine/threonine kinases that phosphorylate members of the IκB family on two specific serine residues in a signal-induced process that is required for IκB degradation and NF-κB activation (16–18, 20, 21). In this study, we have shown that IKK-α is activated via serine phosphorylation by the upstream kinase NIK. NIK phosphorylates IKK-α on Ser-176 that lies in the activation loop (28) between subdomains VII and VIII. Mutation of Ser-176 to alanine results in a kinase-inactive form of IKK-α that is impaired not only in phosphorylating IκB-α and activating an NF-κB reporter gene, but which also can no longer be activated by NIK. Conversely, replacement of Ser-176 with glutamic acid results in a constitutively active IKK-α whose activity in both kinase and NF-κB reporter assays is independent of upstream kinase NIK. The importance of Ser-176 is further suggested by the ability of the IKK-α(S176A) mutant to block IL-1- and TNF-induced NF-κB activation. Although IKK-α can be activated via NIK-mediated phosphorylation on Ser-176, it is possible that other kinases may exist that can also phosphorylate and activate IKK-α.

The site of the NIK-activating phosphorylation of IKK-α lies between kinase subdomains VII and VIII. This phosphorylation and activation of IKK-α by NIK is reminiscent of the MAP kinase pathway in which the upstream kinases Raf and MEKK activate MEK via phosphorylation on Ser-218 and Ser-222 between kinase subdomains VII and VIII (25–27). MEK then activates MAPK by phosphorylating its corresponding activation loop on Thr-183 and Tyr-185 (30). The crystal structure of MAP kinase demonstrates that the activation loop lies in a solvent-exposed portion of the protein and phosphorylation of residues in this region can stabilize the kinase in an active conformation (28, 29). The spatial conservation of the sites activating kinase activity suggests that this mode of regulation is strongly conserved, especially among kinases found in signal transduction cascades. Activation sites in other related kinases might thus be inferred by homology to this region.

Although IKK-α and IKK-β share 52% identity, they are differentially phosphorylated by NIK. NIK appears to phosphorylate IKK-α better than IKK-β. However, we do not know if this difference is reflected in biological differences in the signaling processes affected by these two kinases. Recent experiments suggest that IKK-α and IKK-β form a heterocomplex that interacts directly with the upstream kinase NIK (18, 20, 21). IKK-β may be an inherently better IκB-α kinase than IKK-α and therefore might not need to be further activated by NIK phosphorylation. It is also possible IKK-β may become activated by autophosphorylation when overexpressed. Alternatively, IKK-β may also require phosphorylation by IKK-α or another kinase to be activated. Mercurio *et al.* (16) recently reported that an IKK-β(SS177, 181EE) mutant is constitutively active, supporting the view that phosphorylation also plays an important role in the activation of IKK-β.

IKK-α can be activated by a variety of external stimuli (17). Although the activation mechanism of IKK-α is emerging, little is known about the IKK-α inactivation process that occurs rapidly following the activation (17). It is possible that a phosphatase specifically dephosphorylates Ser-176 and inac-

tivates IKK-α, or that additional sites on IKK-α become dephosphorylated, resulting in enzyme inactivation.

We can now fill in additional details to the pathway by which TNF binding on the cell surface results in NF-κB activation in the nucleus. TNF interaction with TNF-R1 results in receptor trimerization and subsequent association with the adaptor molecule TRADD via the death domains of both proteins. TRADD then recruits TRAF2, RIP, and other signaling molecules, resulting in the formation of the TNF-R1 signaling complex. In a step that is not yet understood and that may require RIP and/or TRAF proteins, NIK becomes activated. NIK then phosphorylates IKK-α (or the α subunit of an IKK-α/IKK-β heterodimer) on Ser-176 in the IKK-α activation loop. Once activated by NIK, IKK-α phosphorylates Ser-32 and Ser-36 of IκB-α, signaling IκB-α for degradation, and allowing NF-κB translocation to the nucleus.

We thank Keith Williamson for DNA sequencing and Catherine Regnier, Mike Rothe, John Woronicz, and Ho Yeong Song for expression vectors. We thank Patrick Baeuerle, Catherine Regnier, Lin Wu, Xiong Gao, and Csaba Lehel for helpful discussions and Patrick Baeuerle, Mike Rothe, and Vijay Baichwal for comments on the manuscript.

1. Baeuerle, P. A. & Henkel, T. (1994) *Annu. Rev. Immunol.* **12,** 141–179.
2. Baeuerle, P. A. & Baltimore, D. (1996) *Cell* **87,** 13–20.
3. Verma, I. M., Stevenson, J. K., Schwarz, E. M., Van Antwerp, D. & Miyamoto, S. (1995) *Genes Dev.* **9,** 2723–2735.
4. Traenckner, E. B., Pahl, H. L., Henkel, T., Schmidt, K. N., Wilk, S. & Baeuerle, P. A. (1995) *EMBO J.* **14,** 2876–2883.
5. Thanos, D. & Maniatis, T. (1995) *Cell* **80,** 529–532.
6. Hsu, H., Xiong, J. & Goeddel, D. V. (1995) *Cell* **81,** 495–504.
7. Tartaglia, L. A. & Goeddel, D. V. (1992) *Immunol. Today* **13,** 151–153.
8. Hsu, H., Huang, J., Shu, H. B., Baichwal, V. & Goeddel, D. V. (1996) *Immunity* **4,** 387–396.
9. Hsu, H., Shu, H. B., Pan, M. G. & Goeddel, D. V. (1996) *Cell* **84,** 299–308.
10. Huang, J., Gao, X., Li, S. & Cao, Z. (1997) *Proc. Natl. Acad. Sci. USA* **94,** 12829–12832.
11. Wesche, H., Henzel, W. J., Shillinglaw, W., Li, S. & Cao, Z. (1997) *Immunity* **7,** 837–847.
12. Cao, Z., Henzel, W. J. & Gao, X. (1996) *Science* **271,** 1128–1131.
13. Cao, Z., Xiong, J., Takeuchi, M., Kurama, T. & Goeddel, D. V. (1996) *Nature (London)* **383,** 443–446.
14. Malinin, N. L., Boldin, M. P., Kovalenko, A. V. & Wallach, D. (1997) *Nature (London)* **385,** 540–544.
15. Song, H. Y., Regnier, C. H., Kirschning, C. J., Goeddel, D. V. & Rothe, M. (1997) *Proc. Natl. Acad. Sci. USA* **94,** 9792–9796.
16. Regnier, C. H., Song, H. Y., Gao, X., Goeddel, D. V., Cao, Z. & Rothe, M. (1997) *Cell* **90,** 373–383.
17. DiDonato, J. A., Hayakawa, M., Rothwarf, D. M., Zandi, E. & Karin, M. (1997) *Nature (London)* **388,** 548–554.
18. Mercurio, F., Zhu, H., Murray, B. W., Shevchenko, A., Bennett, B. L., Li, J., Young, D. B., Barbosa, M., Mann, M., Manning, A. & Rao, A. (1997) *Science* **278,** 860–866.
19. Connelly, M. A. & Marcu, K. B. (1995) *Cell. Mol. Biol. Res.* **41,** 537–549.
20. Woronicz, J. D., Gao, X., Cao, Z., Rothe, M. & Goeddel, D. V. (1997) *Science* **278,** 866–869.
21. Zandi, E., Rothwarf, D. M., Delhase, M., Hayakawa, M. & Karin, M. (1997) *Cell* **91,** 243–252.
22. Chen, Z. J., Parent, L. & Maniatis, T. (1996) *Cell* **84,** 853–862.
23. Schall, T. J., Lewis, M., Koller, K. J., Lee, A., Rice, G. C., Wong, G. H., Gatanaga, T., Granger, G. A., Lentz, R., Raab, H., *et al.* (1990) *Cell* **61,** 361–370.
24. Schindler, U. & Baichwal, V. R. (1994) *Mol. Cell. Biol.* **14,** 5820–5831.
25. Zheng, C. F. & Guan, K. L. (1994) *EMBO J.* **13,** 1123–1131.
26. Yan, M. & Templeton, D. J. (1994) *J. Biol. Chem.* **269,** 19067–19073.
27. Alessi, D. R., Saito, Y., Campbell, D. G., Cohen, P., Sithanandam, G., Rapp, U., Ashworth, A., Marshall, C. J. & Cowley, S. (1994) *EMBO J.* **13,** 1610–1619.
28. Zhang, F., Strand, A., Robbins, D., Cobb, M. H. & Goldsmith, E. J. (1994) *Nature (London)* **367,** 704–711.
29. Canagarajah, B. J., Khokhlatchev, A., Cobb, M. H. & Goldsmith, E. J. (1997) *Cell* **90,** 859–869.
30. Payne, D. M., Rossomando, A. J., Martino, P., Erickson, A. K., Her, J. H., Shabanowitz, J., Hunt, D. F., Weber, M. J. & Sturgill, T. W. (1991) *EMBO J.* **10,** 885–892.
31. Shoji, S., Titani, K., Demaille, J. G. & Fischer, E. H. (1979) *J. Biol. Chem.* **254,** 6211–6214.
32. Gould, K. L., Moreno, S., Owen, D. J., Sazer, S. & Nurse, P. (1991) *EMBO J.* **10,** 3297–3309.
33. Cazaubon, S. M. & Parker, P. J. (1993) *J. Biol. Chem.* **268,** 17559–17563.

EXHIBIT B

from non-expressors by flow cytometry. Quantitative cell-surface expression of integrins was determined by flow cytometry[29] using human α_5 antibody 6F4 at 1:4 dilution of hybridoma supernatant to assay α_5 expression and non-inhibitory $\alpha_{IIb}\beta_3$ antibody D57 at 1:200 dilution of mouse ascites to assay $\alpha_{IIb}\beta_3$ expression. Cells expressing α_5 were sorted into three populations with different relative expression levels, and cells expressing $\alpha_{IIb}\beta_3(\beta_{1-2})$ were sorted into similar surface-expression profiles to $\alpha_{IIb}\beta_3$ transfected cells. Both $\alpha_{IIb}\beta_3$ and $\alpha_{IIb}\beta_3(\beta_{1-2})$ were activated to the high-affinity state by incubation with 100 μg ml^{-1} monoclonal antibody 62 (anti-LIBS2 antibody).

Adhesion assay. CHO cells were incubated on silaned fibrinogen- or fibronectin (Sigma)-coated glass slides for 20 min in serum-free OptiMEM 1 (GIBCO-BRL). The slide was placed in a shear-stress flow chamber[19], which produces a linear gradient in shear with position along the centre line: $\tau_w = (6\mu Q/h^2 w_1)/(1 - (z/L))$ where τ_w is the surface shear stress, ν the fluid viscosity, Q the flow rate, h the channel height, w_1 the channel width at the origin of the flow field, z the distance from the origin along the centre line, and L the length of the flow field. PBS with Ca^{2+} and Mg^{2+}, heated to 37 °C, flowed through the chamber for 5 min to detach the cells. Cells in 20 fields along the slide were counted before and after flow detachment. Shear stress was calculated for each field and converted to shear force (F_s) by approximating cell morphology as a hemispherical cap, such that $F_s = 2.15\pi(r_p^2 + h^2)\tau_w$ where r_p is the hemispherical cap radius and h the height. The fraction of cells detached as a function of shear force was fit to the integrals of logarithmic normal probability density-function distributions to determine the mean shear force for detachment of 50% of the cells. Five detachment assays were performed for each cell type at each extracellular-matrix concentration, and mean detachment forces were averaged.

Migration assay. CHO cells were incubated on silaned, fibrinogen- or fibronectin-coated coverslips for 3 h in serum-free OptiMEM 1. Real-time digital image processing was used to acquire images and calculate cell centroid position as a function of time. The image-processing software (Engineering Technology Center, Mystic, CT) identifies cell boundaries from phase-contrast images and measures cell centroid position. We scanned 5–10 cells per field in 10 different fields every 15 min for 12 h. The mean-squared displacement of the cell centroid as a function of time was calculated for each cell using non-overlapping time intervals. The mean-squared displacements were averaged and fit to a persistent random walk model[30] to calculate cell speed, S, and persistence time, P: $\langle d^2(t)\rangle = 2S^2P[t - P(1 - e^{-t/P})]$.

Received 13 November; accepted 19 December 1996.

1. Hynes, R. O. *Cell* **69**, 11–25 (1992).
2. Cheresh, D. A. *Adv. Mol. Cell Biol.* **6**, 225–252 (1993).
3. Schwartz, M. A., Schaller, M. D. & Ginsberg, M. H. *Annu. Rev. Cell Dev. Biol.* **11**, 549–599 (1995).
4. Lauffenburger, D. A. & Horwitz, A. F. *Cell* **84**, 359–369 (1996).
5. Goodman, S. L., Risse, G. & van der Mark, K. *J. Cell Biol.* **109**, 799–809 (1989).
6. DiMilla, P. A., Stone, J. A., Quinn, J. A., Albelda, S. A. & Lauffenburger, D. A. *J. Cell Biol.* **122**, 729–737 (1993).
7. Bauer, J. S., Schreiner, C. L., Giancotti, F. G., Ruoslahti, E. & Juliano, R. L. *J. Cell Biol.* **116**, 477–487 (1992).
8. Giancotti, F. G. & Ruoslahti, E. *Cell* **60**, 849–859 (1990).
9. Keely, P. J., Fong, A. M., Zutter, M. M. & Santoro, S. A. *J. Cell Sci.* **108**, 595–607 (1995).
10. Duband, J.-L., Dufour, S., Yamada, S. S., Yamada, K. M. & Thiery, J. P. *J. Cell Sci.* **98**, 517–532 (1991).
11. Kuijpers, T. W. *et al. J. Exp. Med.* **178**, 279–284 (1993).
12. Huttenlocher, A., Ginsberg, M. H. & Horwitz, A. F. *J. Cell Biol.* **134**, 1551–1562 (1996).
13. Huttenlocher, A., Sandborg, R. R. & Horwitz, A. F. *Curr. Opin. Cell Biol.* **7**, 697–706.
14. DiMilla, P. A., Barbee, K. & Lauffenburger, D. A. *Biophys. J.* **60**, 15–37 (1991).
15. Regen, C. M. & Horwitz, A. F. *J. Cell Biol.* **119**, 1347–1359 (1992).
16. Palecek, S. P., Schmidt, C. E., Lauffenburger, D. A. & Horwitz, A. F. *J. Cell Sci.* **109**, 941–952 (1996).
17. Bajt, M. L., Loftus, J. C., Gawaz, M. P. & Ginsberg, M. H. *J. Biol. Chem.* **267**, 22211–22216 (1992).
18. Frelinger, A. L., Du, X., Plow, E. F. & Ginsberg, M. H. *J. Biol. Chem.* **266**, 17106–17111 (1991).
19. Powers, M. J., Rodriguez, R. E. & Griffith, L. G. *Biotechnol. Bioeng.* (in the press).
20. Oliver, T. N., Lee, J. & Jacobson, K. *Semin. Cell Biol.* **5**, 139–147 (1994).
21. Abercrombie, M., Heaysman, J. E. M. & Pegrun, S. M. *Exp. Cell Res.* **59**, 393–398 (1970).
22. Marks, P. W., Hendey, B. & Maxfield, F. R. *J. Cell Biol.* **112**, 149–158 (1991).
23. Jay, P. Y., Pham, P. A., Wong, S. A. & Elson, E. L. *J. Cell Sci.* **108**, 387–393 (1995).
24. Wessels, D., Vawter-Hugart, H., Murray, J. & Soll, D. R. *Cell Motil. Cytoskeleton* **27**, 1–12 (1994).
25. Cary, L. A., Chang, J. F. & Guan, J. *J. Cell Sci.* **109**, 1787–1794 (1996).
26. Varner, J. A. & Cheresh, D. A. *Curr Opin. Cell Biol.* **8**, 724–730 (1996).
27. Langer, R. & Vacanti, J. *Science* **260**, 920–926 (1993).
28. Argraves, W. S. *et al. J. Cell Biol.* **105**, 1183–1190 (1987).
29. Loftus, J. C. *et al. Science* **249**, 915–918 (1990).
30. Dunn, G. A. *Agents Actions* (suppl.) **22**, 14–33 (1983).

Acknowledgements. We thank R. Isberg for 6F4 antibody, L. Reichardt for α, cDNA, and R. Juliano for CHO B2 cells. This work was supported by grants from the NIH to D.A.L., A.F.H., J.C.L. and M.H.G., and a Whitaker Foundation graduate fellowship in Biomedical Engineering to S.P.P.

Correspondence and requests for materials should be addressed to D.A.L. (e-mail: lauffen@mit.edu).

MAP3K-related kinase involved in NF-κB induction by TNF, CD95 and IL-1

Nikolai L. Malinin, Mark P. Boldin, Andrei V. Kovalenko & David Wallach

Department of Membrane Research and Biophysics, The Weizmann Institue of Science, 76100 Rehovot, Israel

Several members of the tumour-necrosis/nerve-growth factor (TNF/NGF) receptor family activate the transcription factor NF-κB through a common adaptor protein, Traf2 (refs 1–5), whereas the interleukin 1 type-I receptor activates NF-κB independently of Traf2 (ref. 4). We have now cloned a new protein kinase, NIK, which binds to Traf2 and stimulates NF-κB activity. This kinase shares sequence similarity with several MAPKK kinases. Expression in cells of kinase-deficient NIK mutants fails to stimulate NF-κB and blocks its induction by TNF, by either of the two TNF receptors or by the receptor CD95 (Fas/Apo-1), and by TRADD, RIP and MORT1/FADD, which are adaptor proteins that bind to these receptors. It also blocked NF-κB induction by interleukin-1. Our findings indicate that NIK participates in an NF-κB-inducing signalling cascade common to receptors of the TNF/NGF family and to the interleukin-1 type-I receptor.

NF-κB, a ubiquitously expressed transcription factor comprising a homo- or heterodimer of DNA-binding proteins related to the proto-oncogene c-Rel, controls the expression of many immune- and inflammatory-response genes. In most cells NF-κB exists in a

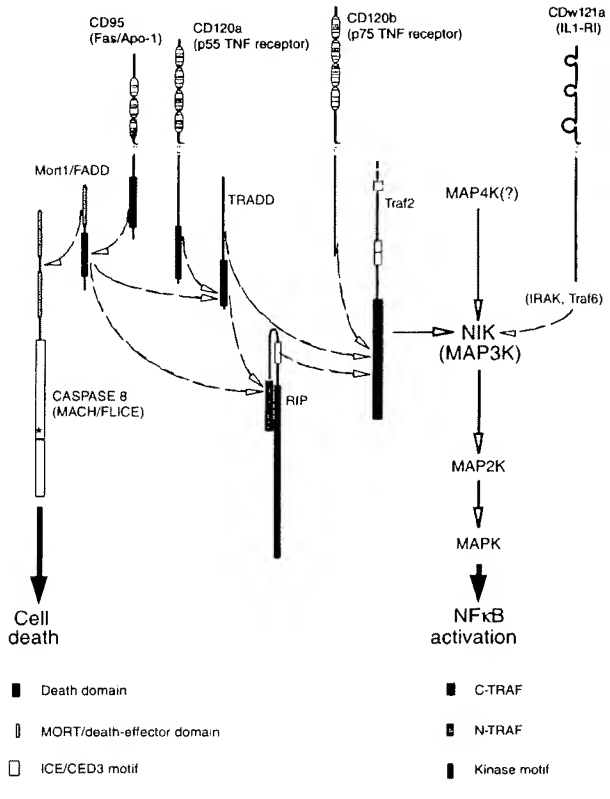

Figure 1 The known protein-protein interactions through which the TNF receptors (p55, or CD120a, and p75, or CD120b), CD95 (Fas/Apo-1) and CDw121a (the IL-1 type-I receptor) might affect the activity of NIK.

latent state in the cytoplasm bound to inhibitory proteins (collectively called IκB) that mask its nuclear localization signal. The latent form can be activated by inducing agents, including several cytokines that signal for phosphorylation and subsequent degradation of IκB (reviewed in ref. 6). Several adaptor proteins are involved in the events associated with this cytokine-induced effect, including the TRAF proteins (for TNF-receptor-associated factors). These proteins share sequence homology at their C-terminal receptor-binding regions (TRAF domain), although their binding properties and activities differ. One of them, Traf2, binds to the p55 (CD120a) and p75 (CD120b) TNF receptors, as well as to several other receptors of the TNF/NGF receptor family, either directly or through other adaptor proteins (Fig. 1). Traf2 is crucial for the activation of NF-κB by these receptors[5]; Traf3 inhibits activation of NF-κB by some receptors of the TNF/NGF family[2], whereas Traf6 is required for the induction of NF-κB by interleukin-1 (IL-1)[7], a cytokine with activities similar to TNF, although it uses a structurally unrelated receptor. None of the TRAF molecules has enzymatic activity.

Here we describe a new protein with serine/threonine kinase activity that binds to Traf2 and takes part in the activation of NF-κB by the TNF receptors, by CD95 (also known as Fas/Apo-1, a receptor belonging to the TNF/NGF receptor family), and by the type-I IL-1 receptor (CDw121a). This protein has marked sequence similarity to several kinases that participate in MAP kinase cascades and may itself act in a kinase cascade.

A partial complementary DNA of this new protein was cloned by two-hybrid screening of a human B-cell cDNA library[8,9] using Traf2 as bait. Employing several steps of the polymerase chain reaction (PCR), we then cloned the full-length cDNA from cDNA libraries. This cDNA was 4,596 nucleotides long, with an open reading frame of 2,841 nucleotides, of which 972 were present in the initially cloned partial cDNA. In view of the kinase activity of the protein and its ability to stimulate NF-κB (see below), we called it NIK, for NF-κB-inducing kinase.

Two-hybrid testing of the binding properties of NIK (Fig. 2) revealed that the initially isolated partial clone of NIK (NIK624–947) binds specifically to the C-terminal region (TRAF domain) of Traf2. By contrast, binding of full-length NIK to Traf2 involved both the TRAF domain and the region upstream of it. NIK did not bind to Traf3. Moreover, a chimaeric molecule comprising the TRAF domain of Traf2 and the N-terminal part of Traf3 bound NIK624–947 but not full-length NIK, confirming that binding of full-length NIK to Traf2 involves both the N- and C-terminal regions of Traf2. NIK did not self-associate, neither did it bind to the intracellular domain of either of the two TNF receptors, nor to CD40 or CD95 (two receptors that belong to the TNF/NGF family). It did not bind to TRADD, MORT1/FADD or RIP, which share a motif (the 'death' domain) that differs from the TRAF domain. These three adaptor proteins are involved in the function of the TNF receptors and of CD95 and trigger induction of NF-κB (see below), apparently by interacting with Traf2 (Fig. 1).

NIK also bound Traf2 in transfected mammalian cells, where its expression was markedly increased upon deletion of its 3′ non-coding region (Fig. 3).

Northern blot analysis revealed a single transcript of NIK, expressed in various tissues at different and rather low levels, whose size (~5,000 nucleotides) was similar to that of cloned NIK cDNA (Fig. 4a).

Examination of the predicted amino-acid sequence of NIK (Fig. 4b) revealed that this protein contains a serine/threonine protein-kinase motif, resembling several MAP kinase kinase kinases (MAPKKK[9]; Fig. 4c). *In vitro* testing of NIK kinase activity indicated that the protein can be autophosphorylated, but not when the active-site lysine and an adjacent lysine are replaced with alanine (NIK KK429–430AA in Fig. 5).

Overexpression of NIK in 293 EBNA cells induced NF-κB, and to

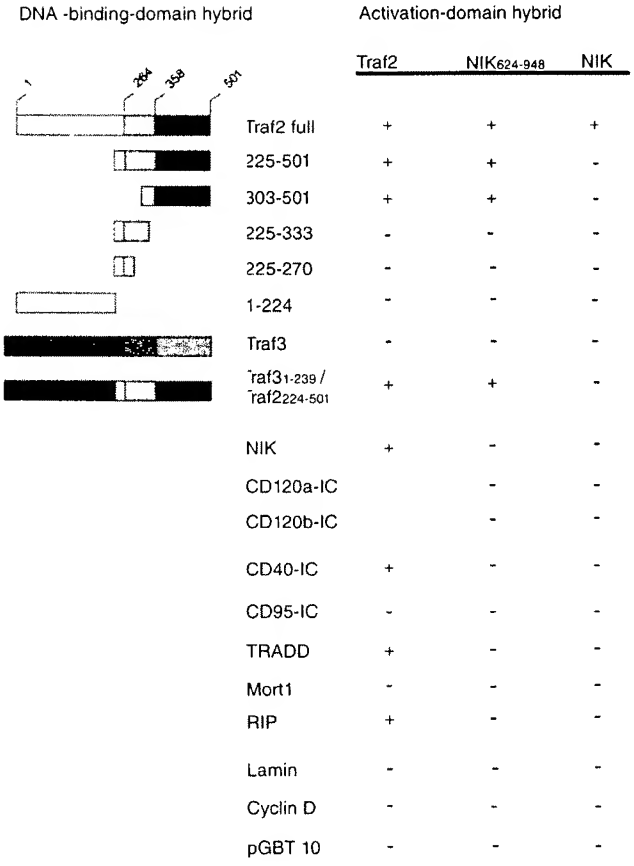

Figure 2 Interaction of NIK with Traf2 in transfected yeast. The binding of NIK and its partial clone NIK624-947 to Traf2, Traf2 deletion mutants, Traf3, a chimaera of Traf3 (residues 1-239) and Traf2 (residues 224-501), and to specificity controls encoded in transfected SFY526 yeast by the Gal4 DNA-binding-domain and activation-domain constructs (pGBT10 and pGAD-GH) was assessed by two-hybrid β-galactosidase filter assay[15]. Plus and minus signs indicate that strong colour develops within 3 h and no colour develops within 24 h, respectively. IC, intracellular domain.

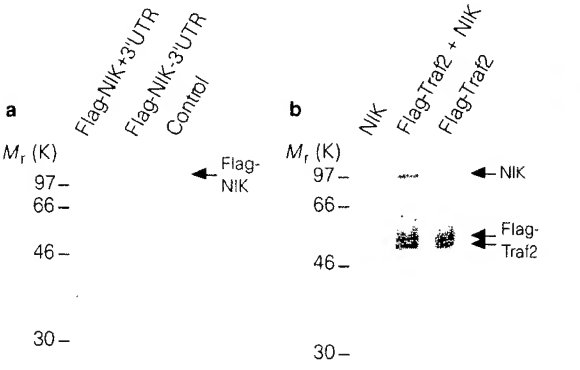

Figure 3 Interaction of NIK with Traf2 within transfected 293-EBNA cells. **a**, Effect of the NIK 3′ untranslated region (UTR) on its expression. NIK was expressed and metabolically labelled with ^{35}S in 293-EBNA cells, with or without its 3′ UTR, as a fusion protein with the Flag epitope. Immunoprecipitation of the fusion protein using anti-Flag antibody is shown. **b**, Interaction of NIK with Traf2, showing the immunoprecipitation of Traf2 fused at its N terminus to the Flag epitope (Flag-Traf2), which was expressed alone or with NIK and metabolically labelled.

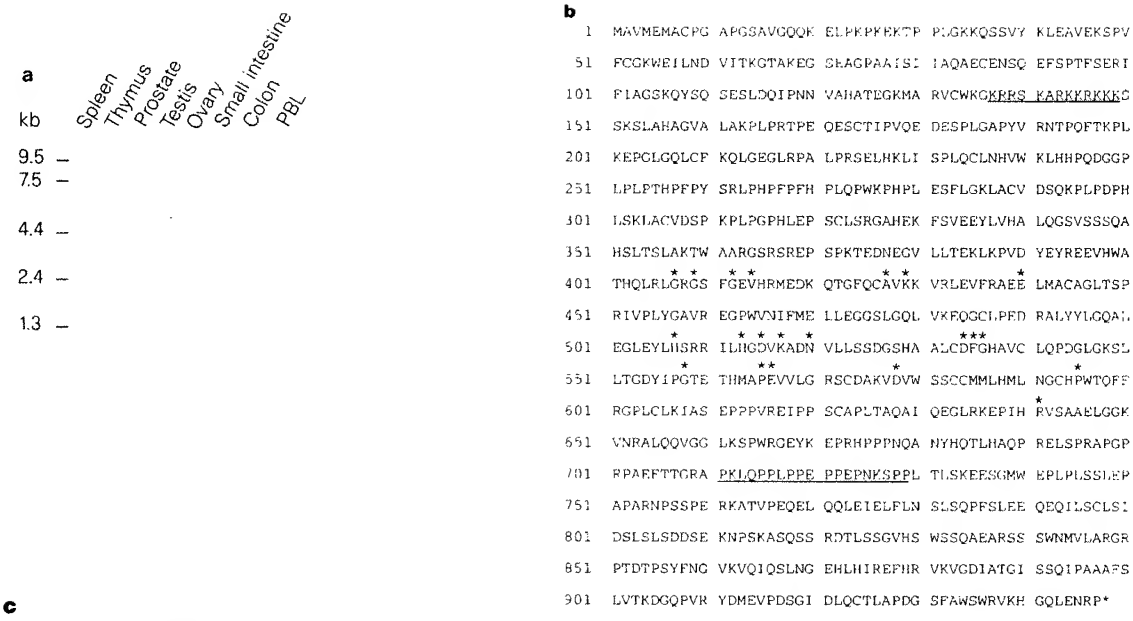

Figure 4 NIK transcript and its encoded protein. **a**, Northern blot of poly(A)$^+$ RNA (2 μg per lane) from human tissues (Clontech) probed with a cDNA corresponding to nucleotides 1,259–2,150 in NIK. PBL, peripheral blood leukocytes. **b**, Deduced amino-acid sequence of NIK. Conserved residues in the kinase domain[19] are indicated by asterisks. A proline-rich region downstream of the kinase domain and an upstream lysine-rich region (which may act as a nuclear localization signal) are underlined. **c**, Collinear amino-acid sequence alignment of the kinase domains in NIK, the mouse MEKK1 (ref. 20) and the proteins of cluster 2032.9 in the CRSeqAnnot database[21] which includes Ste11 (ref. 22), Bck1 (ref. 23) and Ste8 (also called Byr2; refs 24, 25), yeast proteins that serve as MAPKKK, the yeast proteins Cdc7 (ref. 26) and Ssc3 (SwissProt P25390), the mammalian oncogene *cot* (also called the Ewing's sarcoma oncogene or Tpl-2; refs 27, 28) which acts as MAPKKK[29], and the tobacco Ste11 homologue NPK1 (ref. 30).

a greater extent than did overexpression of Traf2. However, NF-κB was not activated in cells expressing NIK624–947 or NIK KK429–430AA (Fig. 6a, b), indicating that induction by the native molecule depends on its kinase function. NIK differs in this respect from RIP, which also contains a protein kinase domain yet can still induce NF-κB when its kinase activity is abolished by mutation (Fig. 6b).

The activation of NF-κB upon overexpression of NIK was indistinguishable from that produced by treatment of cells with TNF. As with TNF or Traf2 (ref. 2) overexpression, the principal components of NIK-activated NF-κB were p50 and p65 (Fig. 7a). NIK overexpression caused degradation of IκBα, and blocking this degradation by N-acetyl-Leu-Leu-norleucinal (ALLN) resulted, as with TNF, in the accumulation of IκB molecules that migrated more slowly in SDS–PAGE and might correspond to phosphorylated IκBα (Fig. 7b, c).

As shown in Fig. 6, NF-κB can be activated in 293-EBNA cells by TNF, as well as by overexpression of CD120a or CD120b, or of CD120a with its intracellular domain replaced by that of CD95 (CD120a-CD95). It can also be activated by overexpression of Traf2, TRADD, RIP or MORT1/FADD, but not by a MORT1/FADD

deletion mutant lacking the region upstream of the death domain. Expression of NIK KK429–430AA or of NIK624–947 in 293-EBNA cells blocked induction of NF-κB by all of these agents, indicating that NIK activity is involved in the induction (Fig. 6). This inhibition correlated with less IκB reduction (Fig. 7c).

NF-κB is activated by IL-1 as well. This effect, unlike that of the TNF receptors and CD95, is little affected by expression of a Traf2 dominant-negative mutant[4] (Fig. 6b, right), but is inhibited by expression of NIK mutants (Fig. 6b, left). However, the NF-κB activity observed upon overexpression of the p65 Rel homologue in 293-EBNA cells was unaffected by coexpression of kinase-deficient NIK mutants, indicating that NIK does not affect the function of Rel proteins directly, but participates in their receptor-induced activation.

The cytotoxic activity of TNF, which is apparently mediated by a Mort1/FADD-associated ICE/Ced3 protease (caspase 8/MACH/

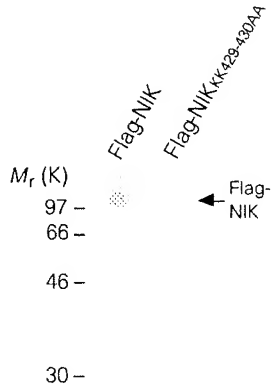

Figure 5 NIK kinase activity. Autoradiography of SDS–PAGE to assess the *in vitro* autophosphorylation of Flag-NIK and Flag-NIK KK429–430AA, immunoprecipitated from lysates of 293-EBNA cells that transiently express these proteins.

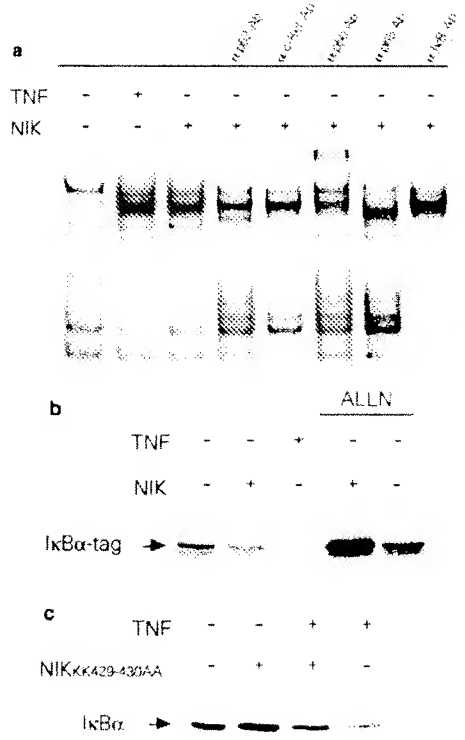

Figure 7 Rel and IκB molecules affected by NIK. **a**, Effects of antibodies against different Rel homologues on the NIK-induced NF-κB complex. Antisera against Rel proteins or, as a control, against IκBα were added in aliquots of 1 μl per electromobility-shift assay reaction. **b** and **c**, Western blot analysis of IκBα expression showing degradation of IκBα or, in cells treated with *N*-acetyl-Leu-Leu-norleucinal (ALLN; 100 mM for 3 h), accumulation of phosphorylated IκBα, in response to NIK expression (**b**), and inhibition of the degradation of IκBα, induced by TNF (3,000 U m^{-1} for 30 min) in cells expressing NIK KK429–430AA (**c**).

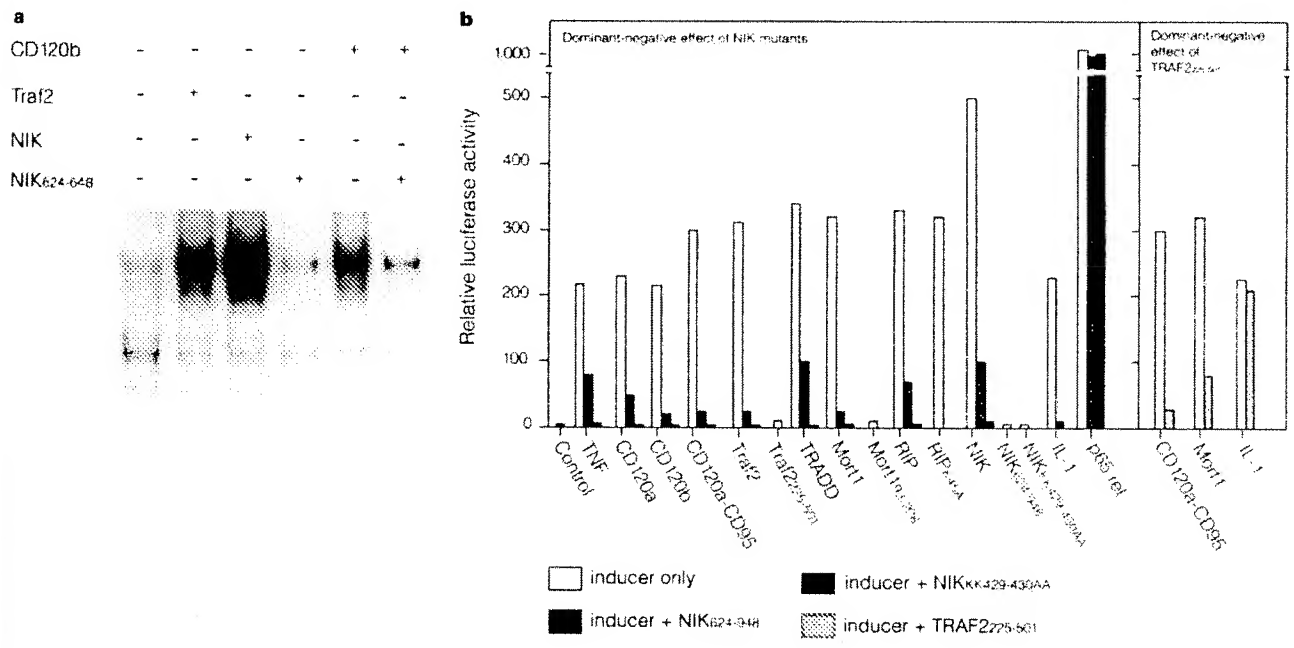

Figure 6 NIK mediates NF-κB induction by the TNF receptors, CD95 and IL-1. **a**, Electromobility shift assay of NF-κB binding activity demonstrating the activation of NF-κB by overexpression of Traf2, NIK or CD120b in 293-EBNA cells, and inhibition of the CD120b-induced effect by coexpression of the kinase-deficient partial clone NIK624–947. **b**, NF-κB-dependent reporter gene activity (HIV LTR-luciferase) in 293-EBNA cells treated with TNF (300 U ml^{-1}) or IL-1α (300 U m^{-1}) for 6 h, or in 293-EBNA cells overexpressing the TNF receptors, CD120a-CD95 or their adaptor proteins, or p65 NF-κB subunit; effects of coexpression of NIK KK429–430AA or NIK624–947 (left panel), or Traf2 225–501 (right panel). Data are from one of five experiments with similar qualitative results. They are presented in terms of luciferase activity relative to that in cells transfected with empty vector

FLICE; Fig. 1), is subject to negative regulation by some NF-κB-inducible genes (see ref. 10 for example). The antagonizing consequences of NF-κB-mediated gene induction and caspase 8/MACH/FLICE activation may explain why TNF itself, as well as IL-1 (both activate NF-κB), can induce cellular resistance to TNF cytotoxicity[11,12]. In line with this, we found that expression of NIK dominant-negative mutants in 293-EBNA cells significantly increased their susceptibility to killing by TNF, and that overexpression of wild-type NIK inhibited their killing by TNF or as a result of overexpression of CD120a (data not shown).

Our findings indicate that the kinase activity of NIK is part of a signalling cascade that is responsible for NF-κB activation and is common to the TNF receptors CD95 and IL-1, although its exact role in this process is not clear. Binding of NIK to Traf2 may allow NIK to be affected by both TNF receptors and by CD95 (refs 2,4; Fig. 1). By analogy with the MAP kinase cascades, NIK may serve as substrate for a kinase (MAPKKKK) upon being recruited with Traf2 to the stimulated receptors, so that when it is phosphorylated it phosphorylates and hence activates other kinase(s). The IL-1-induced activation of NF-κB, however, is independent of TRAF2. Perhaps activation of NIK by the IL-1 receptor is mediated by IRAK, a serine/threonine kinase that is recruited to the IL-1 receptor after stimulation[13], and by Traf6, which binds IRAK[7]. The target of NIK, or of a cascade of kinases activated by it, might be IκB, whose phosphorylation facility is unknown. Alternatively, NIK may phosphorylate TRAF proteins or regulatory proteins that bind to them, for example TANK/I-TRAF[3,14], creating docking sites for other proteins. Identification of the cellular substrates of NIK will shed more light on its mechanism of action and its functional relationship to known MAP kinase cascades. □

Methods

Metabolic labelling, immunoprecipitation and kinase assay. Proteins were expressed by transfecting pcDNA3 expression constructs with the indicated cDNAs into human embryonic kidney 293-EBNA cells (5×10^6 cells per sample). Extracts were prepared 24 h after transfection. Except where otherwise indicated, NIK cDNA was expressed without its 3′ UTR. Metabolic labelling and immunoprecipitation were done as described[15], using cells transfected with 10 μg NIK expression vector. For analysis of NIK autophosphorylation, cells were lysed in 25 mM Tris-HCl, pH 5.7, 150 mM NaCl, 1% Triton X-100, 1 mM EDTA, 1 mM EGTA and 20 mM NaF. Flag-tagged proteins were immunoprecipitated with anti-Flag affinity gel and then incubated for 20 min at 30 °C in a buffer containing 50 mM Tris-HCl, pH 7.5, 100 mM NaCl, 6 mM $MgCl_2$, 1 mM $MnCl_2$, 1 mM DTT and 100 mM [γ^{32}P]ATP (150 mCi μmol^{-1}), followed by SDS–PAGE.

NF-κB activity measurements. Electromobility-shift assay was done as described[16], using a radiolabelled double-stranded oligonucleotide of sequence 5′-GATGCCATTGGGGATTTCCTCTTTTGAC-3′. For the reporter gene assay, cells were cotransfected with the HIV LTR–luciferase reporter gene plasmid (1 μg) and the NF-κB-inducing-protein (1.5 μg) and NIK-mutant (3 μg) expression vectors. The amount of transfected DNA was kept constant by supplementation with 'empty' vector. Overexpression of kinase-deficient NIK mutants did not affect the activity of coexpressed luciferase linked to the β-actin promoter (not shown), ruling out the possibility that inhibition of NF-κB induction by the mutants reflects a cytotoxic effect.

Western blot analysis of IκB expression. Cells were transfected with expression vectors of NIK or NIK KK429–430AA or with empty vector (3 μg) and, for the experiment shown in Fig. 7b, with 1.5 μg of an expression vector for C-terminally tagged IκBα (pcDNA3-IκB ctag[17]) as well. Cell extracts were analysed by SDS–PAGE (12%) followed by western blot analysis, using the anti-Tag monoclonal antibody SV5-Pk[18] (Fig. 7b), or rabbit anti-IκBα antiserum (Fig. 7c), and the ECL kit (Amersham).

Received 14 November; accepted 23 December 1996.

1. Rothe, M., Wong, S. C., Henzel, W. J. & Goeddel, D. V. *Cell* **78**, 681–692 (1994).
2. Rothe, M., Sarma, V., Dixit, V. M. & Goeddel, D. V. *Science* **269**, 1424–1427 (1995).
3. Cheng, G. & Baltimore, D. *Genes Dev.* **10**, 963–973 (1996).
4. Hsu, H., Shu, H.-B., Pan, M.-G. & Goeddel, D. V. *Cell* **84**, 299–308 (1996).
5. Wallach, D. *Eur. Cyokine Net.* **7**, 713–724 (1996).
6. Miyamoto, S. & Verma, I. M. *Adv. Cancer Res.* **66**, 255–292 (1995).
7. Cao, Z., Xiong, J., Takeuchi, M., Kurama, T. & Goeddel, D. V. *Nature* **383**, 443–446 (1996).
8. Durfee, T. *et al. Genes Dev.* **7**, 555–569 (1993).
9. Boldin, M. P., Goncharov, T. M., Goltsev, Y. V. & Wallach, D. *Cell* **85**, 803–815 (1996).
9. Seger, R. & Krebs, E. G. *FASEB J.* **9**, 726–735 (1995).
10. Beg, A. A. & Baltimore, D. *Science* **274**, 782–784 (1996).
11. Hahn, T. *et al. Proc. Natl Acad. Sci. USA* **82**, 3814–3818 (1985).
12. Holtmann, H., Hahn, T. & Wallach, D. *Immunobiology* **177**, 7–22 (1988).
13. Cao, Z., Henzel, W. J. & Gao, X. *Science* **271**, 1128–1131 (1996).
14. Rothe, M. *et al. Proc. Natl Acad. Sci. USA* **93**, 8241–8246 (1996).
15. Boldin, M. P. *et al. J. Biol. Chem.* **270**, 7795–7798 (1995).
16. Schreiber, E., Matthias, P., Muller, M. M. & Schaffner, W. *Nucleic Acids Res.* **17**, 6419 (1989).
17. Rodriguez, M. S., Michalopoulos, I., Arenzana-Seisdedos, F. & Hay, R. T. *Mol. Cell. Biol.* **15**, 2413–2419 (1995).
18. Hanke, T., Szawlowski, P. & Randall, R. E. *J. Gen. Virol.* **73**, 653–660 (1992).
19. Hanks, S. K., Quinn, A. M. & Hunter, T. *Science* **241**, 42–52 (1988).
20. Lange-Carter, C. A., Pleiman, C. M., Gardner, A. M., Blumer, K. J. & Johnson, G. L. *Science* **260**, 315–319 (1993).
21. Worley, K. C., Wiese, B. A. & Smith, R. F. *Genome Res.* **5**, 173–184 (1995).
22. Rhodes, N., Connell, L. & Errede, B. *Genes. Dev.* **4**, 1862–1874 (1990).
23. Lee, K. S. & Levin, D. E. *Mol. Cell. Biol.* **12**, 172–182 (1992).
24. Wang, Y., Xu, H. P., Riggs, M., Rodgers, L. & Wigler, M. *Mol. Cell. Biol.* **11**, 3554–3563 (1991).
25. Styrkarsdottir, U., Egel, R. & Nielsen, O. *Mol. Gen. Genet.* **235**, 122–130 (1992).
26. Fankhauser, C. & Simanis, V. *EMBO J.* **13**, 3011–3019 (1994).
27. Miyoshi, J., Higashi, T., Mukai, H., Ohuchi, T. & Kakunaga, T. *Mol. Cell. Biol.* **11**, 4088–4096 (1991).
28. Patriotis, C., Makris, A., Bear, S. E. & Tsichlis, P. N. *Proc. Natl Acad. Sci. USA* **90**, 2251–2255 (1993).
29. Salmerón, A *et al. EMBO J.* **15**, 817–826 (1996).
30. Banno, H. *et al. Mol. Cell. Biol.* **13**, 4745–4752 (1993).

Acknowledgements. We thank R. Seger for helpful comments; J.-L. Virelizier, Y. Ben-Nenah and I. Alkalay for their advice and for reagents used in the assessment of NF-κB activation; S. J. Elledge for the B-cell cDNA library; and H. Englemann for CD40 cDNA. This work was supported in part by grants from Inter-Lab Ltd, Ness Ziona, Israel, from Ares Trading SA, Switzerland, from the Israeli Ministry of Arts and Sciences and from the Forchheimer Center for Molecular Genetics.

Correspondence and requests for materials should be addressed to D.W. (e-mail: lvwalach@weizmann.weizmann.ac.il). Nucleotide and amino-acid sequence data will appear in the EMBL, GenBank and DDBJ Nucleotide Sequence Databases under accession number Y10256.

Suppression of c-Myc-induced apoptosis by Ras signalling through PI(3)K and PKB

Andrea Kauffmann-Zeh*, Pablo Rodriguez-Viciana*, Eugen Ulrich*, Christopher Gilbert*, Paul Coffer†, Julian Downward* & Gerard Evan*

* *Imperial Cancer Research Fund, 44 Lincoln's Inn Fields, London WC2A 3PX, UK*

† *Department of Pulmonary Diseases, University Hospital Utrecht, Heidelberglaan 100, Utrecht 3584CX, The Netherlands*

The viability of vertebrate cells depends on survival factors which activate signal transduction pathways that suppress apoptosis. Defects in anti-apoptotic signalling pathways are implicated in many pathologies including cancer, in which apoptosis induced by deregulated oncogenes must be forestalled for a tumour to become established. Phosphatidylinositol-3-kinase (PI(3)K) is involved in the intracellular signal transduction of many receptors and has been implicated in the transduction of survival signals in neuronal cells[1]. We therefore examined the role of PI(3)K, its upstream effector Ras[2], and its putative downstream protein kinase effectors PKB/Akt[3,4] and p70^{S6K} (ref. 5) in the modulation of apoptosis induced in fibroblasts by the oncoprotein c-Myc. Here we show that Ras activation of PI(3)K suppresses c-Myc-induced apoptosis through the activation of PKB/Akt but not p70^{S6K}. However, we also found that Ras is an effective promoter of apoptosis, through the Raf pathway. Thus Ras activates contradictory intracellular pathways that modulate cell viability. Induction of apoptosis by Ras may be an important factor in limiting the expansion of somatic cells that sustain oncogenic *ras* mutations.

In mesenchymal cells, induction of apoptosis by the pervasive oncogene c-*myc* is effectively suppressed by two principal cytokines, PDGF and IGF-I (ref. 6). PDGF and IGF-I, along with nerve growth factor (NGF) are also potent survival factors for cells of neuronal

EXHIBIT C

THE JOURNAL OF BIOLOGICAL CHEMISTRY VOL. 281, NO. 3, pp. 1495–1505, January 20, 2006

Interleukin-1β Induction of NFκB Is Partially Regulated by H_2O_2-mediated Activation of NFκB-inducing Kinase*

Received for publication, October 13, 2005 Published, JBC Papers in Press, November 14, 2005, DOI 10.1074/jbc.M511153200

Qiang Li[‡] **and John F. Engelhardt**[‡§¶1]

From the [‡]*Department of Anatomy & Cell Biology,* [§]*Department of Internal Medicine, and* [¶]*Center for Gene Therapy of Cystic Fibrosis and Other Genetic Diseases, College of Medicine, The University of Iowa, Iowa City, Iowa 52242*

Reactive oxygen species (ROS) have been demonstrated to act as second messengers in a number of signal transduction pathways, including NFκB. However, the mechanism(s) by which ROS regulate NFκB remain unclear and controversial. In the present report, we describe a mechanism whereby interleukin-1β (IL-1β) stimulation of NFκB is partially regulated by H_2O_2-mediated activation of NIK and subsequent NIK-mediated phosphorylation of IKKα. IL-1β induced H_2O_2 production in MCF-7 cells and clearance of this ROS through the expression of GPx-1 reduced NFκB transcriptional activation by inhibiting NIK-mediated phosphorylation of IKKα. Although IKKα and IKKβ were both involved in IL-1β-mediated activation of NFκB, only the IKKα-dependent component was modulated by changes in H_2O_2 levels. Interestingly, *in vitro* reconstitution experiments demonstrated that NIK was activated by a very narrow range of H_2O_2 (1–10 μM), whereas higher concentrations (100 μM to 1 mM) inhibited NIK activity. Treatment of cells with the general Ser/Thr phosphatase inhibitor (okadaic acid) lead to activation of NFκB and enhanced NIK activity as a IKKα kinase, suggesting that ROS may directly regulate NIK through the inhibition of phosphatases. Recruitment of NIK to TRAF6 following IL-1β stimulation was inhibited by H_2O_2 clearance and Rac1 siRNA, suggesting that Rac-dependent NADPH oxidase may be a source of ROS required for NIK activation. In summary, our studies have demonstrated that redox regulation of NIK by H_2O_2 is mechanistically important in IL-1β induction of NFκB activation.

Reactive oxygen species (ROS)[2] have been implicated in a number of pro-inflammatory signal transduction cascades activated by IL-1β, TNFα, and lipopolysaccharide (1, 2). In this context, ROS have been considered second messengers. For example, ROS are generated in response to IL-1β, TNFα, and lipopolysaccharide (3–5), and clearance of intercellular ROS can inhibit the ability of these ligands to activate downstream signals, including NFκB (6). However, despite the fact that ROS have been linked to NFκB activation by certain cytokines, the molecular mechanisms remain poorly defined and controversial (7). In the present study, we sought to investigate the molecular mechanism by which ROS regulate IL-1β induction of NFκB.

IL-1β is a potent pro-inflammatory cytokine that plays an important role in immune and inflammatory responses associated with sepsis (8), arthritis (9), and cancer (10). Septic shock is a systematic inflammatory response to infection that leads to the overproduction of a series of pro-inflammatory cytokines. TNFα and IL-1β are two critical cytokines produced during septic shock, which significantly contribute to morbidity associated with this disease (8, 11). IL-1β exerts its pleiotropic effects by binding to its receptor (IL-1R1) on the plasma membrane. This initiates the IL-1β signaling cascade by activating structural changes in the receptor that dock cytoplasmic adaptor and effector proteins on the receptor tail (12). The first set of proteins recruited to the cytoplasmic tail of IL-1R1 following ligand binding include IL-1RacP, MyD88, and Tollip (13–16). In turn, MyD88 plays an obligatory role in mediating the recruitment of interleukin-1 receptor-associated kinase family members via interactions with its N-terminal death domain (15, 17). Once associated with the receptor complex, interleukin-1 receptor-associated kinase subsequently recruits TRAF6, a member of the TNF receptor-associated factor family of adaptor proteins (18). TRAF6 then recruits and activates TAK1 and/or NIK (19), two IKK kinases important in NFκB activation. It has also been suggested that TAK1 and its regulators, TAB1 and -2, might act upstream of NIK (20).

The IL-1β signaling cascade leads to the activation of several key transcription factors that modulate the expression of genes involved in immunity and inflammation. These include NFκB, AP-1, and p38 MAPK (21–23). In this context, NFκB is known for its ability to induce inflammatory cytokines, inhibit apoptotic pathways, and lead to the resolution of inflammation (23–25). NFκB is composed of homo- and hetero-dimers of the Rel family of transcription factors. p65 and p50 subunits represent the most common types of subunits found in the activated NFκB complex. Activation of NFκB is controlled by a family of IκB inhibitory proteins (IκBα, IκBβ, and IκBε) that sequester the NFκB complex in the cytoplasm by masking its nuclear localization signal. Pro-inflammatory stimuli that activate NFκB lead to the phosphorylation of IκBα on two N-terminal serines (Ser-32 and Ser-36). This results in the ubiquitination and degradation of IκBα and the mobilization of NFκB to the nucleus where it activates transcription (26). Two IKK kinases, IKKα and IKKβ, have the ability to phosphorylate these two serines on IκBα (27, 28). IKKα and IKKβ, together with IKKγ, form a large complex within the cell (29).

Kinases known to phosphorylate IKKα and IKKβ include NIK (30), MEKK1 (31), NFκB-activating kinase (32), and TAK1 (19). The NFκB-inducing kinase (NIK) is a member of the MAPK kinase kinase family, which has Ser/Thr kinase activity. NIK was first identified as a TRAF2 interacting protein. Further studies found that it could also associate with TRAF6 and TRAF5 (33). NIK is dedicated to NFκB signaling and contributes to the induction of NFκB by both TNFα and IL-1β (34).

* This work was supported by NIDDK, National Institutes of Health Grant RO1-DK067928, the vector core funded through the Center for Gene Therapy (Grant P30 DK54759), and the Roy J. Carver Chair in Molecular Medicine. The costs of publication of this article were defrayed in part by the payment of page charges. This article must therefore be hereby marked "*advertisement*" in accordance with 18 U.S.C. Section 1734 solely to indicate this fact.

[1] To whom correspondence should be addressed: Dept. of Anatomy and Cell Biology, College of Medicine, Rm. 1-111 BSB, University of Iowa, 51 Newton Rd., Iowa City, IA 52242. Tel.: 319-335-7744; Fax: 319-335-6581; E-mail: john-engelhardt@uiowa.edu.

[2] The abbreviations used are: ROS, reactive oxygen species; IL-1, interleukin-1; TNF, tumor necrosis factor; TRAF6, TNF receptor-associated factor 6; NIK, NFκB-inducing kinase; MAPK, mitogen-activated protein kinase; GPx, glutathione peroxide; SOD, superoxide dismutase; siRNA, small interference RNA; m.o.i., multiplicity of infection; GFP, green fluorescent protein; CMV, cytomegalovirus; PBS, phosphate-buffered saline; GST, glutathione *S*-transferase; MEKK, MAPK/extracellular signal-regulated kinase kinase kinase; OA, okadaic acid; TAK1, transforming growth factor-β-activated kinase 1; H_2DCFDA, 2′,7′-dichlorodihydrofluorescein diacetate; IKK, IκBα kinase; DPI, diphenyleneiodonium.

NIK has been shown to interact with IKKα in yeast two-hybrid systems (35) and has the potential to specifically phosphorylate IKKα (36).

It has been suggested that ROS play an important role in the activation of NFκB (37), however, this concept remains controversial (7). Various forms of ROS, including superoxide anion (O_2^-) and hydrogen peroxide (H_2O_2), have been implicated in cell signaling. ROS are tightly controlled in cells by a group of antioxidant factors, including glutathione peroxide (GPx), superoxide dismutase (SOD), catalase, peroxiredoxins, and small factors such as glutathione and thioredoxin. Among these, GPx is a group of selenoenzymes responsible for reducing various hydroperoxides in the presence of the reduced form of glutathione (38). At least four GPx isoforms have been identified (39). GPx-1 is the isoform that exists in the cytoplasm, and it uses glutathione to degrade H_2O_2 into water.

A number of studies have revealed that ROS are involved in IL-1β signal transduction. For example, IL-1β stimulates ROS generation in a number of cell systems (40–42). In addition, studies that have used chemical antioxidants, such as diamide, *N*-acetyl-L-cysteine, and phenylarsine oxide, have shown significant effects on IL-1β-induced signaling (43, 44). Although there remain disagreements over the applications of these antioxidants that might weaken this argument (7), a number of studies have also used specific ROS modulation enzymes to confirm the importance of ROS. For example, specific antioxidant enzymes, such as GPx-1 and Mn-SOD, have demonstrated strong inhibitory effects on TNFα- or IL-1β-induced signal transduction (6, 45). In addition, factors that control ROS generation by cells have been shown to influence IL-1β induction of NFκB and the transcriptional activation of downstream genes (46, 47). However, the mechanisms of ROS action in the IL-1β pathway remain poorly defined.

In this report, we have investigated the role of cellular H_2O_2 in IL-1β induction of NFκB. Using GPx-1 expression to modulate cellular H_2O_2, we have demonstrated that H_2O_2 plays an important role in NIK activation of IKKα following IL-1β stimulation. We found that H_2O_2 imparts its activation on this cascade by promoting TRAF6 association with NIK and potentially inhibiting phosphatases that inactivate NIK. Reconstitution experiments demonstrated that a very narrow range of H_2O_2 concentration (1–10 μM) facilitate NIK activation, whereas higher levels of H_2O_2 inhibit NIK activity. These findings shed light on the molecular mechanism by which ROS act to regulate NFκB activation by IL-1β.

EXPERIMENTAL PROCEDURES

Recombinant Adenoviral Vector Infection and siRNA Transfection—Adenoviral infections were performed in serum-free medium for 2 h at an m.o.i. of 500 particles/cell, followed by the addition of an equal volume of fresh media containing 20% fetal bovine serum. Cells were fed with fresh media at 24 h and cells were analyzed at 48 h post-infection. These conditions produced >90% transduction with recombinant adenovirus, as assessed with Ad.CMV-GFP reporter gene expression. Eight different types of recombinant adenoviruses were used, including: Ad.BglII (empty control vector that does not express a transgene), Ad.NFκBLuc (a NFκB-responsive luciferase reporter vector) (48), Ad.GPx-1 (GPx-1 tagged with a c-Myc epitope at the N terminus) (6), Ad.IKKα(KM) (a dominant negative mutant form of IKKα) (6), Ad.IKKβ(KA) (a dominant negative mutant form of IKKβ) (6), Ad.NIK(DN) (a truncated dominant negative NIK adenoviral vector kindly provided by Dr. Robert Schwabe at the University of North Carolina) (49, 50), Ad.IκBαAS (an adenoviral vector that expresses the antisense IκBα cDNA and activates NFκB by reducing levels of the IκBα repressor) (51), and Ad.IκBα(S/A) (an adenoviral vector that expresses a dominant negative IκBα mutant (S32/36A) that inhibits NFκB activation by preventing IKK-mediated phosphorylation of IκBα) (52). For NFκB transcriptional luciferase assays, MCF-7 cells were infected with Ad.NFκBLuc at an m.o.i. of 500 particles/cell 24 h prior to experimental treatments. Human NIK siRNA and Rac1 siRNA were purchased from a library of prescreened siRNAs made by Santa Cruz Biotechnology, and transfections were performed following the manufacturer's protocol.

Cell Culture and Treatment—MCF-7 cells (a human breast cancer cell line obtained from ATCC) were chosen for studies due to their low level of endogenous GPx-1. MCF-7 cells were grown in minimal essential medium with Eagle's salts and L-glutamine, 1% minimal essential medium non-essential amino acids, 10% fetal bovine serum, 1% penicillin/streptomycin. For H_2O_2 treatment, concentrated H_2O_2 (30%) (Fisher Scientific, Fair Lawn, NJ) was diluted to 1 M with deionized H_2O and added to fresh medium at a final concentration of 1 mM. The spent medium was removed from MCF-7 cells and quickly replaced with medium containing 1 mM H_2O_2. After incubation at 37 °C for 1 h (or as otherwise indicated), the medium was changed to fresh medium without H_2O_2, and incubation of cells at 37 °C was continued. IL-1β inductions were performed using 1 ng/ml human IL-1β (R&D Systems, Minneapolis, MN) for the indicated times. Control MCF-7 cells were also fed fresh medium but did not receive any treatment. Cells were harvested for luciferase assays at 6 h following H_2O_2 or IL-1β treatments. MCF-7 cells were washed twice with ice-cold PBS and were prepared for each assay accordingly.

Western Blots—Cell lysates were prepared and normalized for protein concentrations using a Bio-Rad Kit (Bio-Rad, Philadelphia, PA). Western blotting was performed using standard protocols. In brief, 50 μg of crude proteins for each condition were separated on a denaturing 10% SDS-PAGE and transferred to nitrocellulose (Hybond C, Amersham Biosciences). The membranes were then blocked and probed with primary antibody for 1 h at room temperature using dilutions suggested by the manufacturer. After being washed with blocking buffer several times, the membranes were probed with the appropriate dilution of secondary antibody. Immunoreactive proteins were detected using either an enhanced chemiluminescence ECL (Amersham Biosciences) and exposure to x-ray film, or an Odyssey Infrared Imaging System (LI-COR Biotech, Lincoln, NE). The antibodies against IKKα, IKKβ, NIK, GST, FLAG, IL-1R1, MEKK1, and TRAF6 were purchased from Santa Cruz Biotechnology (Santa Cruz, CA). Rac1 antibody was purchased from BD Transduction Laboratories (Lexington, KY).

Luciferase Assays—Luciferase activity was measured using a kit from Promega (Madison, WI) according to the manufacturer's instructions. MCF-7 cells were infected with Ad.NFκBLuc 24 h prior to treatment. Ad.NFκBLuc contains the luciferase gene driven by four tandem copies of the NFκB consensus sequence fused to a TATA-like promoter from the herpes simplex virus thymidine kinase gene. 5 μg of total protein from each sample was used to perform the luciferase assays.

Immunoprecipitation—Cell samples were washed with ice-cold PBS twice and were lysed with radioimmune precipitation assay buffer (150 mM NaCl, 50 mM Tris, pH 7.2, 1% deoxycholate, 1% Triton X-100, 0.1% SDS) at 4 °C for 30 min. Protein concentrations were determined using a Bio-Rad kit and 500 μg of cellular protein, and 5 μl of primary antibody was mixed with 1 ml of radioimmune precipitation assay buffer at 4 °C for 1 h. Then 50 μl of Protein-A-agarose beads (Santa Cruz Biotechnology) was added to the mixture, and the mixture was rotated for 4 h. The beads were spun down at 5000 rpm for 5 min at 4 °C and washed with ice-cold PBS three times prior to analysis of immunoprecipitates.

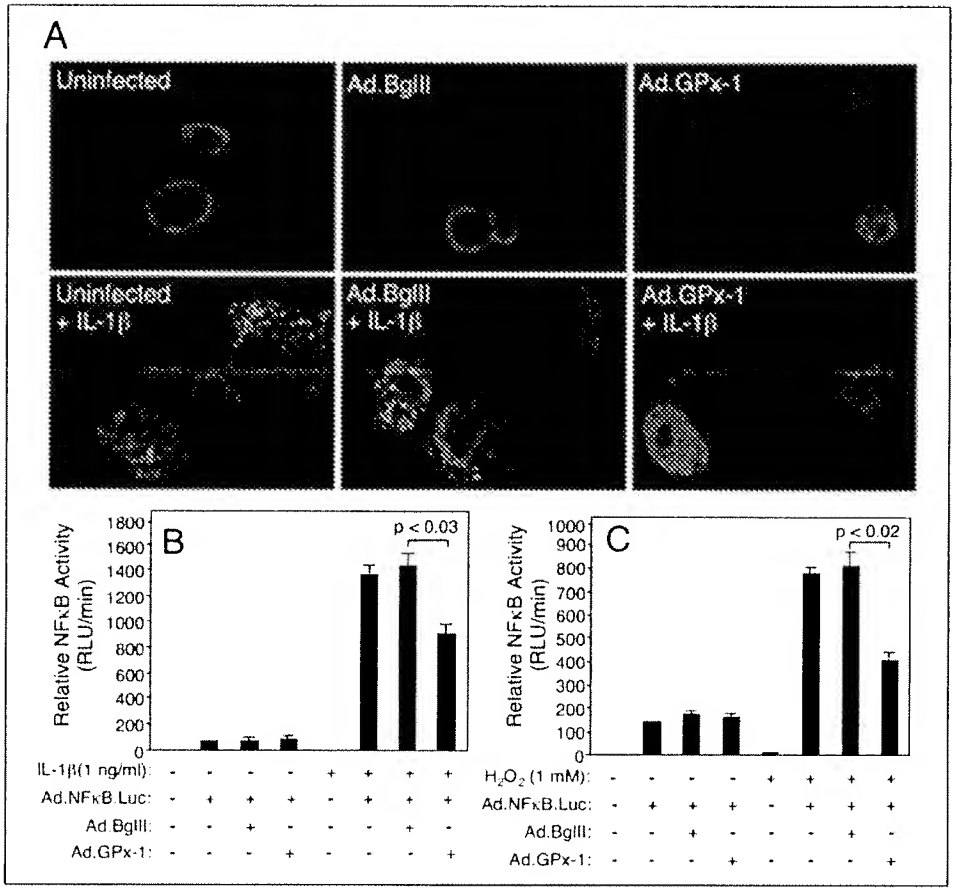

FIGURE 1. **GPx-1 overexpression reduces NFκB transcriptional activity following H_2O_2 or IL-1β treatment of MCF-7 cells.** *A*, MCF-7 cells were infected with Ad.GPx-1 or the control virus Ad.BglII at 500 particles/cell. At 48 h post-infection, cells were treated with IL-1β (1 ng/ml) in the presence of H_2DCFDA (10 μM) to detect H_2O_2 production. Treatment conditions are written in each panel. 4′,6 Diamidino-2-phenylindole was included in the mounting media for identification of nuclei. *B* and *C*, MCF-7 cells were infected with Ad.GPx-1 or the control virus Ad.BglII at 500 particles/cell. At 24 h post-infection, cells were then infected with Ad.NFκBLuc (500 particles/cell). 24 h after the second infection, cells were treated with H_2O_2 (1 mM) or IL-1β (1 ng/ml). Cells were harvested for luciferase activity assays 6 h after IL-1β (*B*) or H_2O_2 (*C*) treatment to quantify NFκB transcriptional activity in 5 μg of protein lysate. Conditions for infection and treatment are indicated below each graph. Results depict the mean relative light units per minute (± S.E., $n = 3$) as an index of relative NFκB activity.

In Vitro Kinase Assay—Kinases (NIK, MEKK1, IKKα, or IKKβ) were immunoprecipitated with their respective antibodies and then mixed with 1 μg of the appropriate protein substrate (IKKα, IKKβ, or IκBα) in 0.3 mM cold ATP, 10 μCi of [γ-^{32}P]ATP, and 10 μl of kinase buffer (40 mM Hepes, 1 mM β-glycerophosphate, 1 mM nitrophenol phosphate, 1 mM Na_3VO_4, 10 mM $MgCl_2$, and 2 mM dithiothreitol). Reaction mixtures were incubated at 30 °C for 30 min (or shorter times as indicated), and reactions were then terminated by the addition of SDS-PAGE loading buffer at 98 °C for 5 min. Proteins were separated by 10% SDS-PAGE and transferred to nitrocellulose membrane and exposed to x-ray film.

Detection of Cellular ROS Production Using H_2DCFDA—Stock solutions of H_2DCFDA (Molecular Probes, Eugene, OR) were generated in Me_2SO at a concentration of 50 μg/ml immediately prior to use. Cells were washed three times with PBS prior to simultaneous treatment with H_2DCFDA (10 μM) and IL-1β (1 ng/ml) for 20 min in PBS at 37 °C in the dark. For samples infected with adenoviral vectors or transfected with siRNAs, this was done 48 h prior to stimulation with IL-1β. When DPI (10 μM) was used to inhibit NADPH oxidases, it was added at the time of IL-1β stimulation. Cells were washed in PBS at 20 min post-stimulation and were then fixed for 10 min in 4% paraformaldehyde. Cells were subsequently mounted in 4′,6-diamidino-2-phenylindole containing antifadent and were examined by fluorescent microscopy for DCF signal. Exposure times were constant for all experimental samples.

RESULTS

Cellular H_2O_2 Influences IL-1β-mediated NFκB Activation—Previous studies have demonstrated that IL-1β stimulation of various cell types leads to cellular ROS production (53–55). Others have also demonstrated that H_2O_2 influences NFκB transcriptional activation following a number of stimuli, including TNF, UV, and IL-1β (3, 6). Furthermore, direct treatment of cells with H_2O_2 has the ability to activate NFκB (6, 56, 57). However, one study has also suggested that NFκB activation by IL-1β occurs in the absence of induced ROS in epithelial cells (42). In the present study, we sought to better understand potential mechanisms by which H_2O_2 influences IL-1β-mediated activation of NFκB. The MCF-7 breast cancer cell line was chosen for these studies, because it expresses a very low level of endogenous GPx-1 (an antioxidant enzyme responsible for degrading cellular H_2O_2 to water) and enables efficient modulation of cellular H_2O_2 levels through the overexpression of recombinant human GPx-1 (6).

We first sought to confirm that IL-1β stimulation of MCF-7 cells led to an increase in cellular H_2O_2. Indeed, our studies demonstrated that IL-1β stimulation of MCF-7 cells enhanced H_2DCFDA fluorescence, suggesting that H_2O_2 is elevated following IL-1β treatment (Fig. 1*A*). Furthermore, infection with recombinant adenovirus expressing GPx-1 (Ad.GPx-1), but not the control Ad.BglII empty vector, significantly attenuated H_2DCFDA fluorescence following IL-1β stimulation (Fig. 1*A*). These findings confirmed that IL-1β stimulates cellular H_2O_2 production in MCF-7 cells and that ectopic expression of GPx-1 could successfully modulate the cellular redox environment.

We next evaluated the extent to which GPx-1 expression could modulate IL-1β induction of NFκB using a NFκB-dependent luciferase reporter. Indeed, we observed that IL-1β induction of NFκB at 6 h was significantly attenuated following infection with Ad.GPx-1 virus, as compared with the infection with an empty adenoviral control vector (Ad.BglII) (Fig. 1*B*). In contrast, ectopic expression of GPx-1 had no effect on baseline transcriptional activity of NFκB. As a control for the ability of GPx-1 expression to modulate H_2O_2 induction of NFκB, we

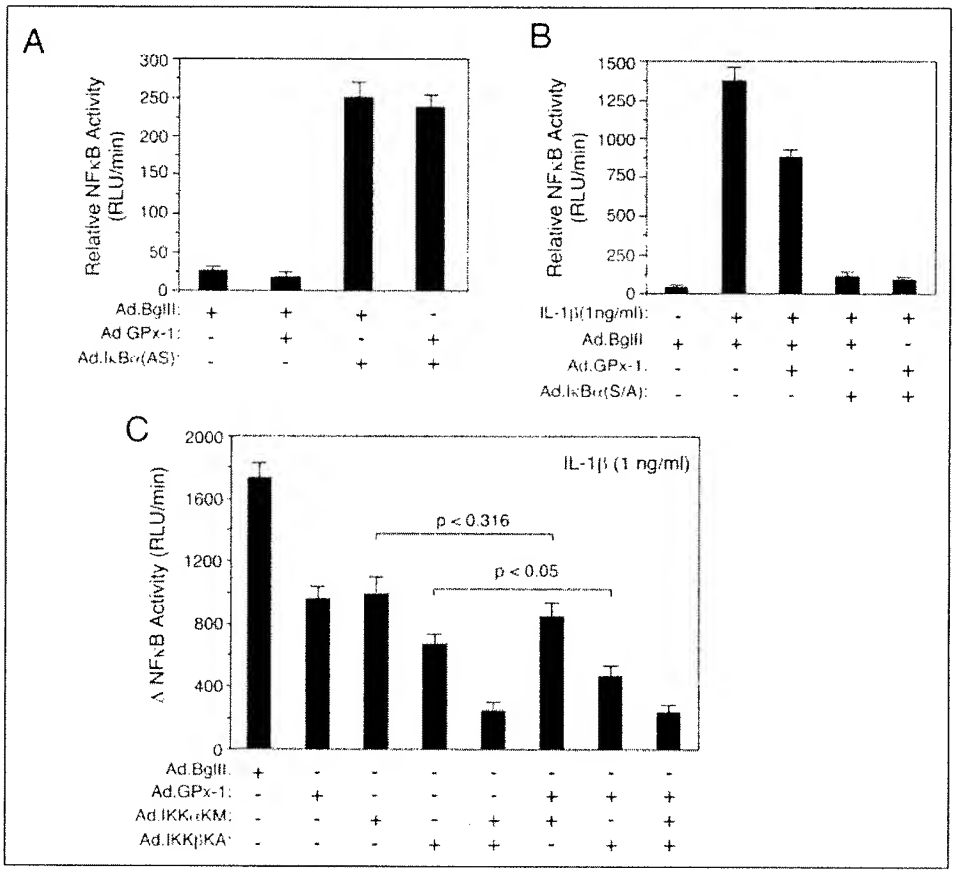

FIGURE 2. **GPx-1-mediated clearance of H_2O_2 inhibits NFκB activation upstream to IκBα stabilization by acting on a pathway that leads to IKKα activation.** MCF-7 cells were infected with the indicated recombinant adenoviral vectors at an m.o.i. of 500 particles/cell for each virus. After 24 h, cells were re-infected with Ad.NFκBLuc for 24 h at 500 particles/cell prior to direct analysis (*A*) or stimulation with IL-1β (1 ng/ml) (*B* and *C*). *A*, the ability of antisense IκBα mRNA expression (Ad.IκBα(AS)) to constitutively induce NFκB transcriptional activation was assessed in the presence of Ad.BglII (control vector) or Ad.GPx-1 co-infection. *B* and *C*, NFκB transcriptional activation was evaluated at 6 h following treatment with IL-1β by assessing the relative luciferase activity in 5 μg of protein lysate. In *panel B*, the mean relative light units (*RLU*/min) (±S.E., $n = 3$) are given for each sample as an index of NFκB transcriptional activation. In *C*, the mean change (±S.E., $n = 3$) in NFκB transcriptional activation following IL-1β stimulation is given (the baseline level of luciferase activity, as determined from Ad.BglII-infected cells in the absence of IL-1β, was subtracted from all experimentally induced values). Statistical comparisons of marked groups using the Student's *t* test are given with *p* values.

performed similar studies in MCF-7 cells transiently treated with 1 mM H_2O_2 for 1 h and assayed for NFκB activation at 6 h. Although GPx-1 expression inhibited direct H_2O_2 induction of NFκB to a greater extent than IL-1β, the level of inhibition was still incomplete (~50%) (Fig. 1*C*). These results suggested that cellular H_2O_2 partially contributes to NFκB activation by IL-1β and that GPx-1 expression more than likely can only partially attenuate H_2O_2 levels in the cell. The ability of GPx-1 expression to only partially block cellular H_2O_2 levels is also supported by H_2DCFDA experiments (Fig. 1*A*).

H_2O_2 Influences NFκB Activation Upstream of IκBα Phosphorylation—We next sought to investigate the molecular mechanism through which H_2O_2 influences IL-1β-mediated NFκB transcriptional activation. IκBα plays a pivotal role in NFκB activation; phosphorylation of IκBα on two serines (Ser-32/Ser-36) leads to its disassociation from NFκB in the cytoplasm, proteasome-dependent degradation of IκBα, and mobilization of NFκB to the nucleus. To evaluate whether H_2O_2 influences NFκB activation downstream of IκBα (*i.e.* after NFκB dissociates from IκBα and moves to the nucleus), we used an antisense IκBα cDNA expressed from recombinant adenovirus (Ad.IκBα(AS)) that represses IκBα protein levels and induces nuclear translocation of NFκB (51). As previously shown in HeLa cells (51), infection with Ad.IκBα(AS) significantly reduced the level of IκBα protein in MCF-7 cells (data not shown) and led to the induction of NFκB transcriptional activity in the absence of cytokine stimulation (Fig. 2*A*). In the presence of antisense IκBα mRNA, overexpression of GPx-1 did not alter NFκB transcriptional activity, suggesting that H_2O_2 levels do not directly influence the transcriptional activity of the NFκB complex once it has been mobilized from IκBα.

We next sought to evaluate whether H_2O_2 might influence IL-1β-dependent NFκB activation by regulating factors that phosphorylate IκBα. Indeed, the majority of NFκB activation following IL-1β stimulation is mediated by IκBα serine phosphorylation, as indicated by a nearly complete block in NFκB activation by adenoviral expression of the dominant negative IκBα mutant (IκBαS32/36A) (Fig. 2*B*). Furthermore, overexpression of GPx-1 and IκBαS32/36A gave a similar level of inhibition as seen with IκBαS32/36A alone, suggesting that GPx-1 regulates components of the NFκB pathway upstream of IκBα. Based on previous reports for other stimuli demonstrating redox-dependent activation of the IKK complex (6, 48, 58–61), we reasoned that H_2O_2 might also influence activation of the IKK complex following IL-1β stimulation.

To approach this question, we used two dominant negative adenoviral vectors that express mutant forms of either the IKKα (Ad.IKKαKM) or IKKβ (Ad.IKKβKA) subunits of the IKK complex. Results from these analyses demonstrated that Ad.IKKαKM or Ad.IKKβKA infection of MCF-7 cells inhibited ~50% of IL-1β-dependent NFκB activation (Fig. 2*C*). The level of inhibition observed by overexpression of GPx-1 was similar to that seen with IKKαKM and slightly less than that seen with IKKβKA. Co-infection with Ad.IKKαKM and Ad.IKKβKA gave nearly complete inhibition of NFκB activation, suggesting that these two subunits of the IKK complex primarily control NFκB activation by IL-1β. To address whether GPx-1-sensitive signaling was directed through IKKα or IKKβ, we performed co-expressing studies with each of these IKK mutants and GPx-1. We reasoned that if H_2O_2 influenced IKKα activation, inhibition of NFκB in the presence of IKKαKM would be unaffected by GPx-1 co-expression. Furthermore, if this hypothesis was true, we would expect to observe enhanced inhibition of NFκB following co-infection with Ad.IKKβKA plus Ad.GPx-1, as compared with Ad.IKKβKA or Ad.GPx-1 infection alone. The reverse scenario would be true if H_2O_2 selectively influenced IKKβ activation (*i.e.* Ad.IKKαKM plus Ad.GPx-1 infection would provide an enhanced level of inhibition,

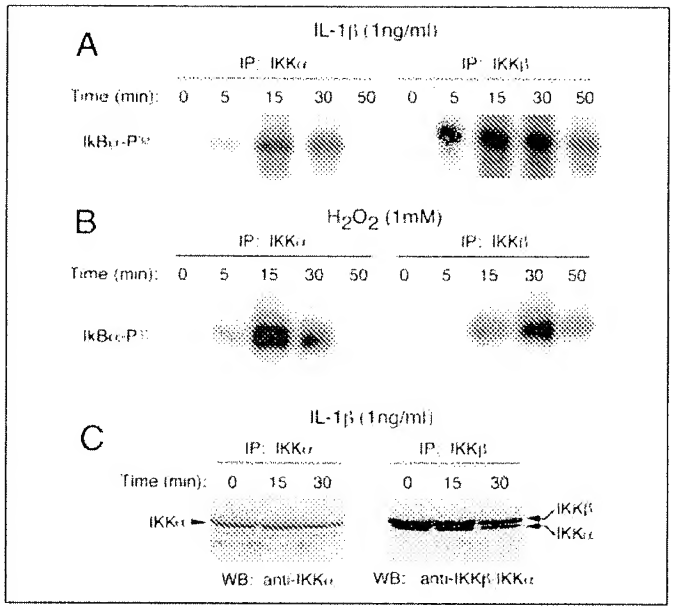

FIGURE 3. **IL-1β or H_2O_2 treatment of MCF-7 cells induces IKKα and IKKβ kinase activity.** *A* and *B*, MCF-7 cells were treated with IL-1β (1 ng/ml, *panel A*) or H_2O_2 (1 mM, *panel B*) and harvested at different time points after treatments for *in vitro* analysis of IKK kinase activities using GST-IκBα as a substrate. Cell lysates were incubated with anti-IKKα or anti-IKKβ antibodies and immunoprecipitates were then incubated with [γ-^{32}P]ATP and GST IκBα for 30 min at 30 °C. The reactions were terminated by the addition of SDS loading buffer and resolved by SDS-PAGE. Gels were transferred to nitrocellulose membrane and analyzed by autoradiography. *C*, Western blots of immunoprecipitated complexes from IL-1β-treated MCF-7 cells in *panel A* using different antibodies that recognize IKKα or both IKKβ/IKKα. Note: anti-IKKα and anti-IKKβ antibodies used in *panels A* and *B* are suitable for immunoprecipitations and specific for IKKα or IKKβ, respectively. The anti-IKKβ antibody used for Western blotting has cross-reactivity with IKKα, whereas the anti-IKKα antibody is specific for IKKα.

as compared with each vector alone). Our results from these experiments (Fig. 2*C*) demonstrated significant synergism in the inhibition of IL-1β-dependent NFκB activation in the presence of both IKKβKA and GPx-1 expression, as compared with each individually. In contrast, inhibition of NFκB was similar following IKKαKM plus GPx-1 overexpression, as compared with expression of IKKαKM or GPx-1 alone (Fig. 2*C*). These findings suggest that GPx-1 acts to inhibit IKKα, but not IKKβ, activation following IL-1β stimulation. Because both IKKα and IKKβ contribute to NFκB activation by IL-1β, we conclude that ROS control only half of the NFκB activation pathways in response to IL-1β.

H_2O_2 Regulates IKK Kinase Activity—Given that GPx-1 expression appeared to modulate IKKα activation following IL-1β stimulation, we next sought to directly confirm that H_2O_2 could activate the IKK complex *in vivo*. To this end, we used *in vitro* kinase assays to monitor IKK activity following IL-1β stimulation and compared these results to that observed following direct H_2O_2 stimulation of MCF-7 cells. This assay utilized immunoprecipitated IKKα or IKKβ, followed by *in vitro* phosphorylation of GST-IκBα in the presence of [γ-^{32}p]ATP. Following IL-1β stimulation, both IKKα and IKKβ kinase activities were substantially increased, peaking at ~15–30 min following stimulation (Fig. 3*A*). The total cellular protein levels of both kinases were also examined, and no changes occurred following IL-1β stimulation (Fig. 3*C*). However, because IKKα and IKKβ form a complex *in vivo* (as evident by immunoprecipitation of IKKα with an IKKβ-specific antibody, Fig. 3*C*), it was impossible to separate the extent to which IKKα and/or IKKβ was activated in the IKK complex. Similar changes in IKKα- and IKKβ-mediated GST-IκBα phosphorylation were seen following treatment of cells with 1 mM H_2O_2 (Fig. 3*B*). Collectively, these studies demonstrated that H_2O_2 can directly activate the IKK complex *in vivo* and suggested a plausible mechanism for IL-1β-induced regulation of NFκB.

H_2O_2-dependent Activation of NIK Contributes to NFκB Activation by IL-1β—We next sought to investigate the molecular mechanism by which H_2O_2 preferentially modulated IKKα following IL-1β stimulation. Previous reports have implicated the redox-dependent activation of NIK following H_2O_2 treatment of cells (62). Furthermore, NIK has previously been demonstrated to preferentially phosphorylate IKKα over IKKβ (36). Hence, NIK was an obvious potential candidate for the redox regulation of NFκB by IL-1β. To investigate the involvement of NIK in NFκB activation following IL-1β stimulation, we utilized a dominant negative NIK mutant (49, 50). Adenovirus-mediated expression of this NIK mutant in MCF-7 cells (Fig. 4*A*) significantly inhibited both H_2O_2- and IL-1β-mediated activation of NFκB (Fig. 4*B*). To evaluate whether the GPx-1-sensitive component of NFκB activation by IL-1β was mediated through NIK, we performed co-infection experiments with Ad.NIK(DN) and Ad.GPx-1 virus. Results from these experiments demonstrated that expression of dominant negative NIK or GPx-1 significantly inhibited NFκB activation to similar extents following H_2O_2 (Fig. 4*C*) or IL-1β stimulation (Fig. 4*D*). Importantly, the level of NFκB inhibition seen following combined infection of cells with Ad.NIK(DN) and Ad.GPx-1 virus was similar to that seen following infection with each vector alone for both H_2O_2 (Fig. 4*C*) and IL-1β (Fig. 4*D*) stimulations. These results support the hypothesis that H_2O_2 activation of NIK plays an important role in NFκB activation by IL-1β.

Redox Activation of NIK Preferentially Regulates IKKα following IL-1β Stimulation—Our data thus far have implicated NIK in the redox-dependent activation of NFκB by IL-1β. Furthermore, our results suggest that activation of IKKα was involved in this pathway of redox activation. To this end, we hypothesized that H_2O_2 activation of NIK enhanced its ability to phosphorylate IKKα. Given the apparent specificity of the redox component of IL-1β signaling for the IKKα subunit of the IKK complex (Fig. 2*C*), we first sought to evaluate whether NIK specifically controlled IKKα activation in response to IL-1β or H_2O_2 stimulation. To this end, we generated bacterial GST fusion proteins for both IKKα and IKKβ and evaluated the ability of NIK to phosphorylate these two proteins following IL-1β or H_2O_2 stimulation. Generation of full-length IKKα and IKKβ GST fusion protein was not successful due to bacterial toxicity. As an alternative strategy, we generated truncated IKKα and IKKβ GST fusion proteins that comprised their respective activation domains phosphorylated by IKK kinases. For IKKα, this region included the sequence between Gly-131 to Trp-205, a 75-amino acid peptide containing Ser-176 and Ser-180 sites known to be phosphorylated and critical for IKKα activity. Similarly, an IKKβ fusion was generated from Ala-132 to Trp-206. This 75-amino acid peptide contained Ser-177 and Ser-181 sites known to be phosphorylated and critical for IKKβ activity (Fig. 5*A*). These two fusion proteins were purified (Fig. 5*B*) and used for *in vitro* kinase assays following H_2O_2 or IL-1β treatment. Results from these studies demonstrated that H_2O_2 and IL-1β treatments stimulated immunoprecipitated NIK to phosphorylate GST-IKKα, but not GST-IKKβ (Fig. 5*C*). Furthermore, the extent of NIK activation by these two stimuli (Fig. 5*C*) was reflected in their respective abilities to activate NFκB in transcriptional assays (Fig. 4*B*) (*i.e.* IL-1β > H_2O_2). To confirm that the inability of NIK to phosphorylate GST-IKKβ was not the result of poor fusion protein quality, we evaluated the ability of MEKK1 to phosphorylate GST-IKKβ following TNFα treatment. MEKK1 has been shown to preferentially phosphorylate IKKβ (36). Indeed, immunoprecipitated MEKK1, from TNFα-treated cells, had a greater ability to phosphorylate GST-IKKβ as compared with GST-IKKα (Fig. 5*C*). These results confirmed that both

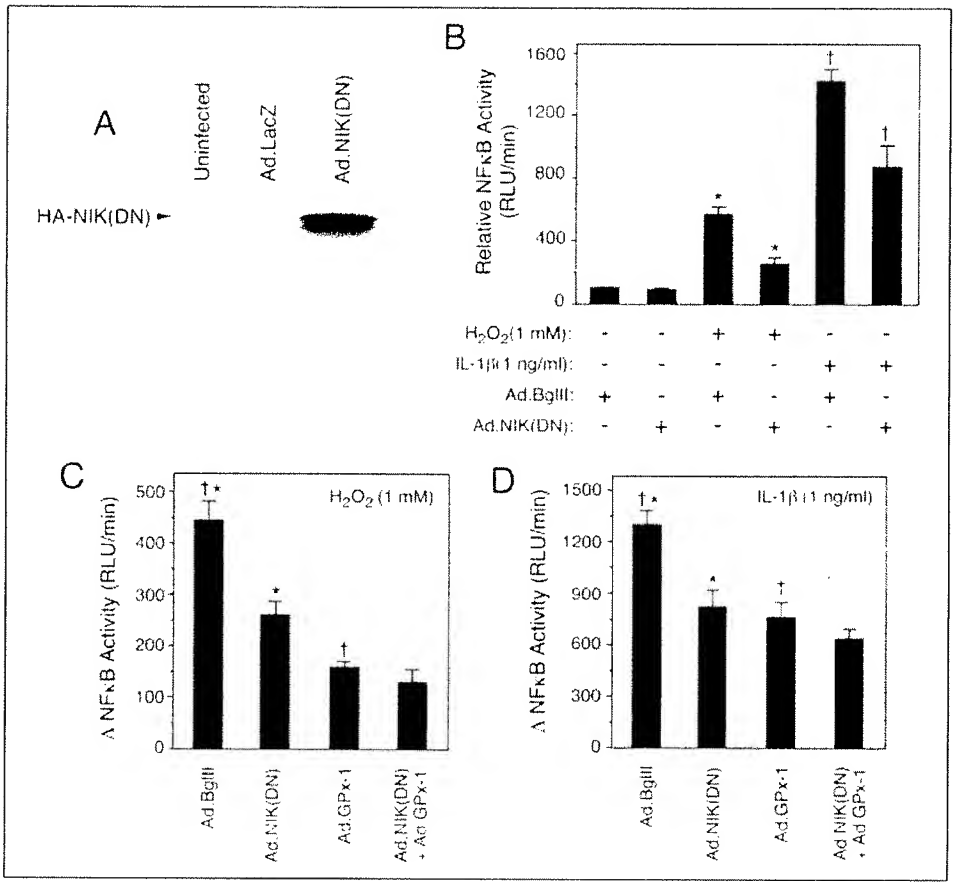

FIGURE 4. **Adenovirus-mediated expression of a dominant negative NIK mutant reduces NFκB transcriptional activation following H_2O_2 or IL-1β treatment of MCF-7 cells.** *A*, MCF-7 cells were infected at an m.o.i. of 500 particles/cell with Ad.NIK(DN) or Ad.LacZ (negative control) adenoviral vectors. At 48 h post-infection, total cell lysates were prepared and analyzed by Western blotting to detect the HA-tagged NIK mutant. *B*, the effect of NIK(DN) overexpression on NFκB transcriptional activation following H_2O_2 or IL-1β treatment was evaluated in MCF-7 cells using a NFκB driving luciferase reporter assay. MCF-7 cells were infected with Ad.NIK(DN) or Ad.BglII (control virus) at 500 particles/cell. At 24 h post-infection, cells were re-infected with Ad.NFκBLuc (500 particles/cell) for an additional 24 h prior to stimulation with H_2O_2 (1 mM) or IL-1β (1 ng/ml). Cells were harvested for luciferase activity assays 6 h after treatments to quantify NFκB transcriptional activity. Results depict the mean relative luciferase units (*RLU*) per minute (±S.E., $n = 3$). *C* and *D*, MCF-7 cells were infected with Ad.BglII, Ad.GPx-1, and/or Ad.NIK(DN) at an m.o.i. of 500 particles/cell of each virus. At 24 h post-infection, cells were re-infected with Ad.NFκBLuc (500 particles/cell) for an additional 24 h prior to stimulation with H_2O_2 (1 mM) or IL-1β (1 ng/ml). Cells were harvested 6 h after treatment, and luciferase activity was determined. Results depict the mean change (±S.E., $n = 3$) in NFκB transcriptional activation following IL-1β and H_2O_2 stimulation. Paired comparisons (*/†) demonstrated significant differences ($p < 0.05$), as assessed by the Student's *t* test.

GST-IKKβ and GST-IKKα were receptive kinase substrates and demonstrated that IL-1β and H_2O_2 treatments stimulate NIK to preferentially phosphorylate IKKα.

To provide further evidence that NIK predominantly signals through IKKα in the context of IL-1β-stimulated NFκB activation *in vivo*, we investigated whether expression of dominant negative NIK enhanced inhibition of NFκB in the presence of IKKαKM or IKKβKA dominant mutants. Results from these experiments (Fig. 5*D*) demonstrated that Ad.NIK(DN) infection was only able to augment inhibition of IL-1β-mediated NFκB activation in the presence of Ad.IKKβKA but not Ad.IKKαKM. These results mirrored those seen following co-infection with the IKK mutants and GPx-1 (Fig. 2*C*), suggesting that NIK acts predominantly through IKKα, but not IKKβ, *in vivo* following IL-1β stimulation to induce NFκB.

To directly evaluate the redox dependence of NIK activation following IL-1β stimulation, we next asked whether GPx-1 overexpression inhibited the ability of NIK to phosphorylate GST-IKKα in an *in vitro* kinase assay. As a control, we first tested whether activation of NIK, following treatment of MCF-7 cells with H_2O_2, would be inhibited by GPx-1 overexpression. Indeed, as shown in Fig. 5*E*, immunoprecipitated NIK from H_2O_2-treated cells had significantly attenuated GST-IKKα kinase activity following Ad.GPx-1 infection. Similarly, IL-1β-stimulated NIK kinase activity was significantly reduced in the presence of GPx-1 expression (Fig. 5*E*). Cumulatively, these data provide strong support that NIK activation following IL-1β stimulation is redox regulated by H_2O_2.

Narrow Ranges of H_2O_2 Facilitate NIK Activation in the Presence of Other Cellular Factors—We hypothesized that H_2O_2 might enhance NIK activation during IL-1β signaling through one of three mechanisms: 1) by direct action of H_2O_2 on NIK to enhance its kinase activity, 2) by activating unknown redox effectors within the cell that activate NIK, and/or 3) through H_2O_2-mediated inhibition of phosphatases that inactivate NIK. To approach the first hypothesis, we attempted to directly activate immunoprecipitated NIK from unstimulated MCF-7 cells with increasing concentrations of H_2O_2. Results from these experiments demonstrated that a very narrow range (1–10 μM) of H_2O_2 was capable of activating NIK to phosphorylate GST-IKKα *in vitro* (Fig. 6*A*, compare *lanes 2* and *3* to *lane 6*). Higher concentrations of H_2O_2 (100 μM and 1 mM) did not give rise to NIK activation in this assay (*lanes 4* and *5*). However, the extent of NIK activation following *in vitro* treatment with 1–10 μM H_2O_2 was still significantly lower than the level of NIK activation seen following direct treatment of MCF-7 cells with 1 mM H_2O_2 for 30 min (Fig. 6*A*, *lane 1*). These findings support the notion that other cellular factors may be required to facilitate the redox-dependent activation of NIK and that these factors are predominantly lost during the immunoprecipitation of inactive NIK.

To test whether other cellular factors were required for the H_2O_2-dependent activation of NIK, we performed *in vitro* NIK activation assays in crude cell lysates harvested from both untreated and H_2O_2 treated MCF-7 cells. Crude lysates were first treated with 1 μM to 1 mM H_2O_2 for 30 min, and then NIK was immunoprecipitated and assayed for its ability to phosphorylate GST-IKKα. Crude lysates generated from cells treated with 1 mM H_2O_2 served as an internal control for the maximal achievable NIK activation at each *in vitro* concentration of H_2O_2 used to stimulate NIK in crude lysates. Several interesting findings emerged from these studies (Fig. 6*B*). First, as seen following *in vitro* exposure of immunoprecipitated NIK (Fig. 6*A*, *lanes 2* and *3*), only 1 and 10 μM concentrations of H_2O_2 were able to activate NIK in crude lysates from

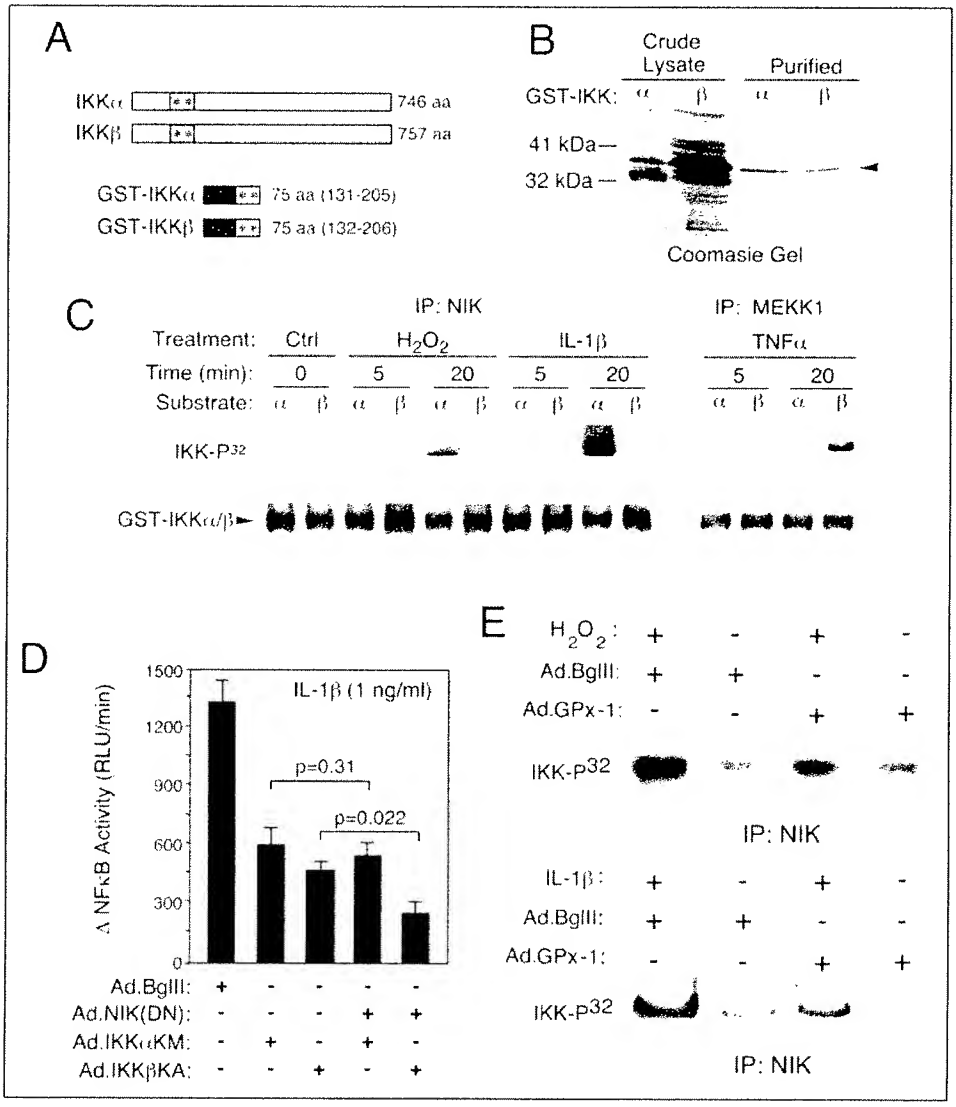

FIGURE 5. **Redox activation of NIK preferentially regulates IKKα-mediated induction of NFκB following H_2O_2 or IL-1β treatment of MCF-7 cells.** *A*, diagram of bacterial-derived GST-IKK fusion proteins used for assessing IKK kinase activities in relationship to the full-length IKK proteins. The activation domains that contain Ser phosphorylation sites (*) are *gray*, and GST is *black*. For IKKα, a 75 amino acid fragment (from Gly-131 to Trp-205) within its activation domain was used (Ser-176 and Ser-180 are phosphorylation sites). For IKKβ, a 75-amino acid fragment (from Ala-132 to Trp-206) in the activation domain was used (Ser-177 and Ser-181 are known phosphorylation sites). *B*, SDS PAGE Coomassie Blue gel of purified GST fusion proteins. *C*, immunoprecipitated (*IP*) NIK or MEKK1 from MCF-7 cells treated with H_2O_2 (1 mM), IL 1β (1 ng/ml), or TNFα (0.5 ng/ml) for the indicated times was used in an *in vitro* kinase assay with [γ-^{32}P]ATP and GST-IKKα or GST-IKKβ. Samples were resolved by SDS-PAGE and transferred to nitrocellulose membrane. Membranes were then analyzed by autoradiography followed by Western blotting with anti-GST. *D*, MCF-7 cells were co-infected with Ad.NIK(DN) and Ad.IKKα(KM) or Ad.IKKβ(KA) at an m.o.i. of 500 particles/cell of each virus. Ad.BglII infection was used as a negative control. At 24 h post-infection, cells were re-infected with Ad.NFκBLuc (500 particles/cell) for an additional 24 h prior to stimulation with IL-1β (1 ng/ml) for 6 h. Cells were then harvested, and luciferase activity was determined as an index of NFκB transcriptional activity. Results depict the mean change (+S.E., $n = 3$) in NFκB transcriptional activation following IL-1β stimulation. Statistical comparisons using the Student's *t* test are marked for *p* value grouped comparisons. *E*, MCF-7 cells were infected with Ad.GPx-1 or Ad.BglII at 500 particles/cell. At 48 h post-infection, cells were treated with H_2O_2 (1 mM) or IL-1β (1 ng/ml) for 30 min and lysates were prepared for *in vitro* kinase assays. NIK was immunoprecipitated and then incubated with [γ-^{32}P]ATP and GST-IKKα for 30 min at 30 °C in kinase buffer. The reactions were analyzed by SDS-PAGE and transferred to nitrocellulose membrane prior to autoradiography.

unstimulated cells (Fig. 6*B*, compare *lanes 8* and *10* to *lane 2*). Exposure of unstimulated crude lysates to 10 μM H_2O_2 (*lane 8*) achieved a similar level of activation as seen following *in vivo* exposure of cells to 1 mM H_2O_2 (*lane 1*). Second, exposure of crude lysates to higher concentrations of H_2O_2 (100 μM and 1 mM), inhibited NIK activation, as evident by a decline in phosphorylated GST-IKKα in samples derived from cells pretreated with 1 mM H_2O_2 (compare *lanes 1*, *7*, and *9* to *lanes 3* and *5*). This inhibition was also evident in lysates derived from untreated cells treated with increasing concentrations of H_2O_2 (compare *lanes 4*, *6*, *8*, and *10*). In summary, these results substantiate the findings that only very narrow ranges of H_2O_2 can activate NIK and that unknown cytoplasmic factors enhance the redox-dependent activation of NIK.

The above studies suggested that H_2O_2 was able to activate NIK to phosphorylate IKKα. However, an alternative possibility was that some other unknown redox-regulated IKKα kinases (*i.e.* TAK1, etc.) might associate with NIK and thereby co-immunoprecipitate in our kinase assays and complicate the assignment of GST-IKKα phosphorylation to NIK. To formally address this possibility, we expressed FLAG-tagged wild type NIK (WT-NIK) or the dominant negative NIK mutant (DN-NIK) and assessed IKKα kinase activity following immunoprecipitation of the FLAG tag from H_2O_2-treated MCF-7 cell lysates. We reasoned that if H_2O_2 activated an alternative IKKα kinase that associated with NIK, this would be revealed as residual H_2O_2-induced IKKα kinase activity in precipitates of the kinase-dead DN-NIK mutant. Results from these experiments are shown in Fig. 6*C*. Immunoprecipitated FLAG-tagged WT-NIK demonstrated a significant increase in its ability to phosphorylate GST-IKKα following H_2O_2 treatment (Fig. 6*C*, compare *lanes 7* to *8*). This level of IKKα kinase activity was similar to what had been seen following immunoprecipitation of endogenous NIK (compare *lanes 1* to *2*). In contrast, FLAG immunoprecipitates from LacZ (negative control without a FLAG tag) or FLAG-tagged DN-NIK transfected cells failed to demonstrate H_2O_2-induced IKKα kinase activity (*lanes 3–6*). These studies suggest that other H_2O_2-activated IKKα kinases likely do not associate with NIK. However, given that the DN-NIK construct is a truncation mutant (49, 50), we cannot currently rule out that an alternative IKKα kinase might associate with the deleted region of NIK. However, we failed to see TAK1 (a known alternative IKKα kinase) association with NIK in MCF-7 cells prior to or following IL-1 or H_2O_2 treatment (data not shown), suggesting that if this occurs it does not involve TAK1.

The third potential mechanism by which H_2O_2 might enhance NIK activation during IL-1β signaling includes H_2O_2-mediated inhibition of phosphatases that inactivate NIK. NIK is known for its ability to autophosphorylate, so redox regulation by phosphatases seems reasonable

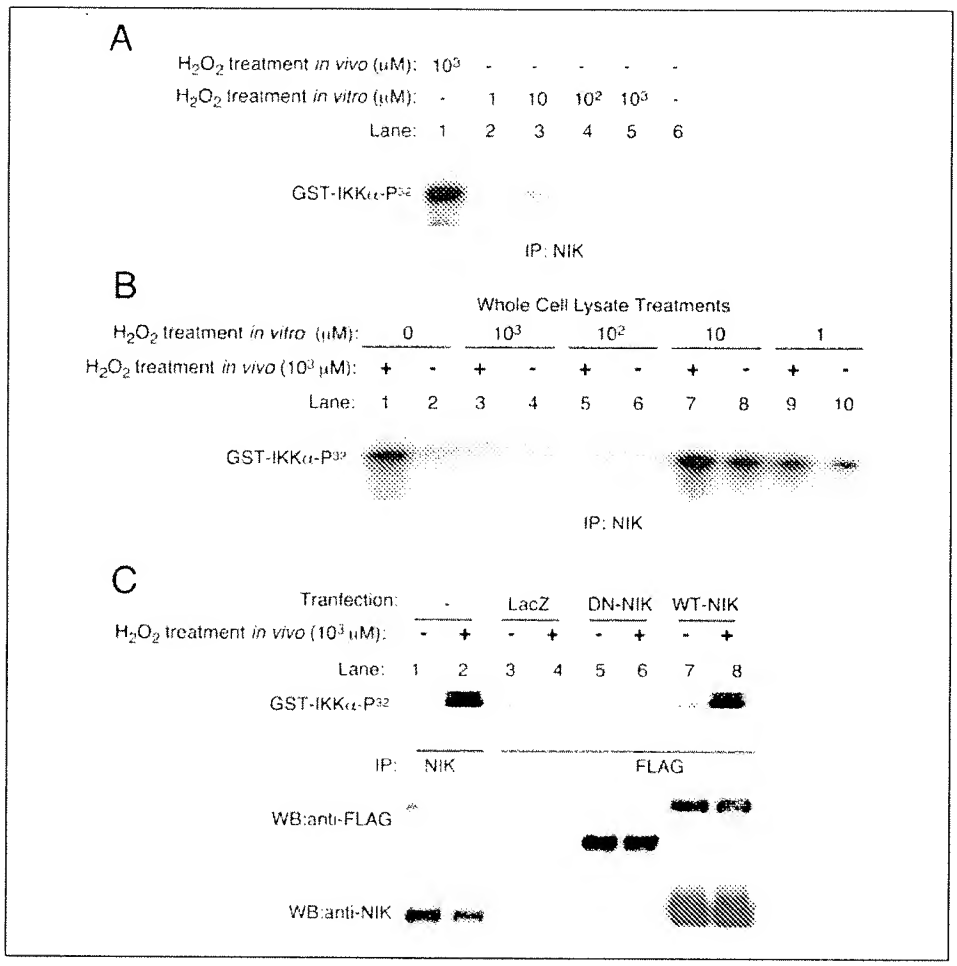

FIGURE 6. **H_2O_2 can directly activate NIK to phosphorylate IKKα in the presence of cellular lysate.** The ability of H_2O_2 to activate IKKα kinase activity of NIK was evaluated using *in vitro* reconstitution experiments with immunoprecipitated NIK. *A*, NIK was immunoprecipitated from untreated MCF-7 cell lysates and exposed to increasing concentrations of H_2O_2 *in vitro* for 30 min prior to performing GST-IKKα kinase assays (*lanes 2–6*). As a positive control, NIK was also immunoprecipitated from MCF-7 cell lysates following an *in vivo* 30 min treatment with 1 mM H_2O_2 (*lane 1*). The reactions were analyzed by SDS-PAGE and transferred to nitrocellulose membrane prior to autoradiography. *B*, whole cell lysates were generated from MCF-7 cells exposed to an *in vivo* 30-min treatment with 1 mM H_2O_2 (*odd-numbered lanes*) or following no treatment (*even-numbered lanes*) as marked. These crude lysates were then exposed to increasing concentrations of H_2O_2 *in vitro* for 30 min as indicated. NIK was then immunoprecipitated and *in vitro* kinase assays were performed in the presence of [γ-^{32}P]ATP and GST-IKKα for 30 min at 30 °C. The reactions were analyzed by SDS-PAGE and transferred to nitrocellulose membrane prior to autoradiography. *C*, MCF-7 cells were transfected with LacZ (negative control), FLAG-tagged wild-type NIK, or FLAG-tagged dominant negative NIK plasmid expression constructs 48 h prior to treatment with H_2O_2 (1 mM) for 30 min. Cell lysates were prepared and endogenous NIK or recombinant NIK was immunoprecipitated with anti-NIK or anti-FLAG antibodies, respectively. Immunoprecipitated NIK was then used for *in vitro* kinase assays with [γ-^{32}P]ATP and GST-IKKα. The reactions were analyzed by SDS PAGE and transferred to nitrocellulose membrane prior to autoradiography and Western blotting to detect FLAG and NIK.

(62). Although it is well recognized that H_2O_2-dependent inactivation of phosphatases plays important roles in signaling (45, 63), information on phosphatase regulation of NIK is lacking. To approach this question we assessed the effects of okadaic acid (a general Ser/Thr phosphatase inhibitor) on both NFκB activation and the activation of NIK to phosphorylate GST-IKKα. Indeed, treatment of cells with increasing concentrations of okadaic acid significantly increased the transcriptional activation of NFκB in MCF-7 cells (Fig. 7*A*). Similarly, okadaic acid treatment of MCF-7 cells significantly enhanced the IKKα kinase activity of immunoprecipitated NIK (Fig. 7*B*) and also enhanced the association of NIK with TRAF6 (Fig. 7*C*, compare *lanes 1* and *7*). These findings suggest that certain Ser/Thr phosphatases may indeed play a role in NIK activation and its association with TRAF6; as such, Ser/Thr phosphatases are potential targets of H_2O_2-mediated inhibition following IL-1β stimulation.

H_2O_2 Modulates NIK Association with TRAF6—Results thus far have demonstrated that IL-1β-mediated activation of NIK leads to enhanced IKKα phosphorylation and is partially responsible for activation of NFκB. *In vitro*, the process of NIK activation by H_2O_2 appears to require unknown cellular factors and may also involve inhibition of phosphatases *in vivo*. TRAF6, which recruits NIK to the IL-1 receptor complex, is an integral part of generating an active IKKα kinase complex following IL-1β stimulation (64). To this end, we sought to investigate whether H_2O_2 modulated the association of NIK with TRAF6. Such a mechanism could explain why cell lysate was required for maximal H_2O_2-mediated activation of immunoprecipitated NIK (Fig. 6, *A* and *B*). We evaluated the extent to which IL-1β or H_2O_2 treatment enhanced the association of NIK with immunoprecipitated TRAF6. Results from these experiments demonstrated that IL-1β or H_2O_2 stimulation of MCF-7 cells increased the association of NIK with TRAF6 (Fig. 7*C*). Furthermore, degradation of H_2O_2 by GPx-1 expression inhibited this association (Fig. 7*C*, *lanes 3 versus 4* and *lanes 5 versus 6*). As expected, the increased association between TRAF6 and NIK promoted by phosphatase inhibition (*i.e.* OA treatment) was unaffected by GPx-1-mediated clearance of H_2O_2 (Fig. 7*C*, *lanes 7 versus 8*). Together with earlier studies, these experiments provide strong support that H_2O_2 regulates NIK activity by modulating the association between NIK and TRAF6.

Rac1 and NADPH Oxidase Control the Redox-dependent Association of NIK with TRAF6—The source of ROS generation following IL-1β stimulation remains complex and controversial. Several studies have indirectly implicated NADPH oxidases as a ROS source, based on the ability of diphenyleneiodonium (a NADPH oxidase inhibitor, DPI) to prevent ROS-dependent activation of IL-1β induced genes such as E-selectin, inducible nitric-oxide synthase, c-*fos*, and collagenase (46, 65, 66). However, others have suggested that 5-lipoxygenase may be involved in IL-1β induction of ROS in lymphoid cells, while NADPH oxidase plays a selective role in monocytic cell-induced ROS following IL-1β stimulation (42). Rac1, a small GTPase, plays a central role in cellular ROS generation through certain NADPH oxidases (67). Rac1 has also been linked to IL-1β induction of p65NFκB in a murine thymoma cell line (47). However, it has been suggested that in epithelial cells, Rac1 and NADPH oxidase do not play a role in NFκB activation by IL-1β (42). Given the controversy surrounding potential sources of ROS following IL-1β stimulation, we sought to investigate the potential role of Rac1/

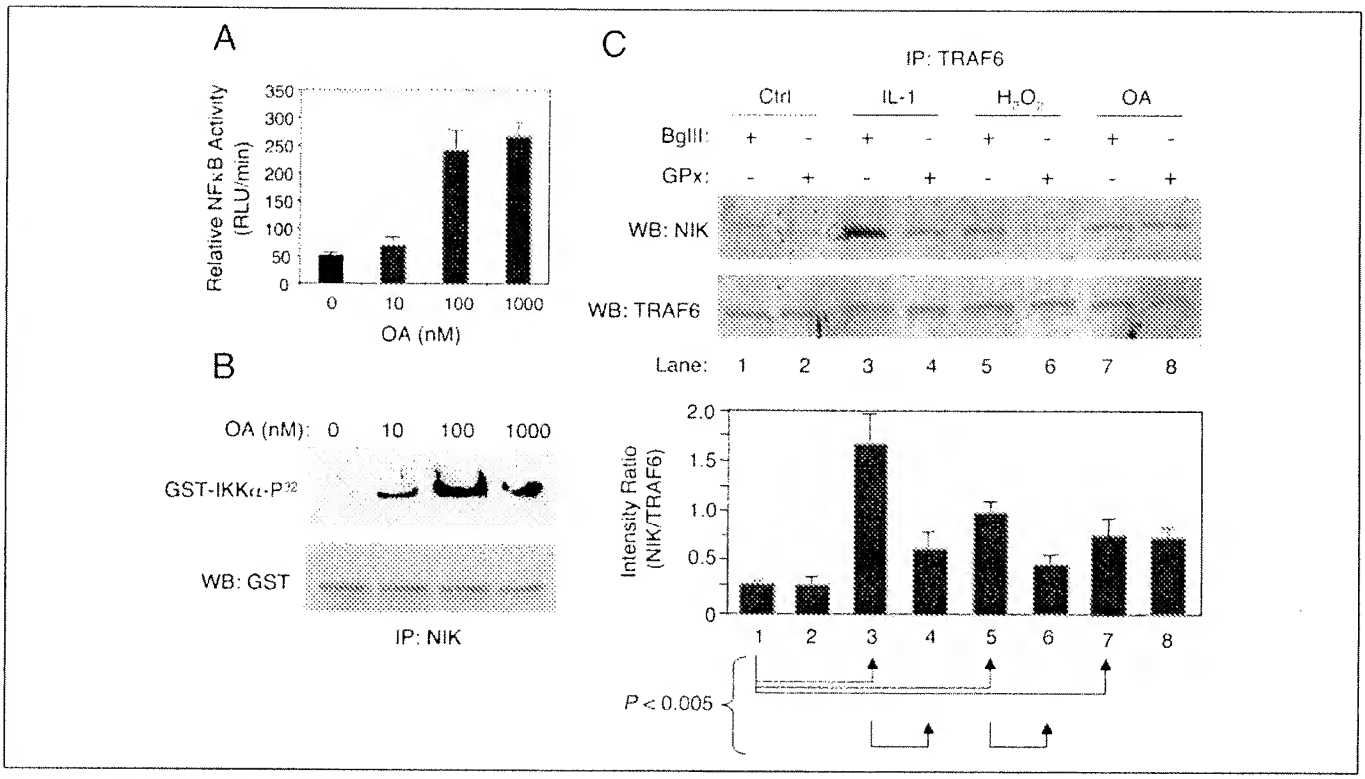

FIGURE 7. **The association of NIK with TRAF6 following IL-1β stimulation is redox-regulated and is also enhanced by inhibition of Ser/Thr phosphatases.** *A* and *B*, MCF-7 cells were infected with Ad.NFκBLuc (500 particles/cell) for 24 h and were then treated with okadaic Acid (*OA*) at the indicated concentrations. Cells were harvested at 6 h post-OA treatment for luciferase activity assays (*A*) or at 30 min post-OA treatment for *in vitro* kinase assays using immunoprecipitated NIK and GST-IKKα as a substrate (*B*). Autoradiography of kinase products on SDS-PAGE were transferred to nitrocellulose membrane, and Western blots of the same membrane to detect GST are shown in *B*. *C*, MCF-7 cells were infected with Ad.GPx-1 or Ad.BglII at 500 particles/cell for 48 h followed by treatment with H_2O_2 (1 mM), IL-1β (1 ng/ml), or OA (100 nM) for 30 min. Cell samples were then harvested and used for immunoprecipitation with anti-TRAF6 antibody. Immunoprecipitates were then analyzed by SDS-PAGE and Western blotting (*top panel*) using anti-TRAF6 and anti-NIK antibodies and infrared dye-conjugated secondary antibodies on an Odyssey infrared imaging system (LI-COR Biotechnology Lincoln, NE). Infrared quantification of NIK·TRAF6 band intensity ratios is plotted in the *lower panel* (mean ± S.E. $n = 3$). The Student's *t* test demonstrated a significant difference ($p < 0.005$) for marked comparisons *below the graph*.

NADPH oxidase in the IL-1β-induced ROS found in MCF-7 mammary epithelial cells.

Using Rac1 siRNA to inhibit Rac1 and DPI to inhibit NADPH oxidase, we investigated the role of Rac1/NADPH oxidase in ROS production following IL-1β stimulation. Results from H_2DCFDA staining demonstrated that both DPI and Rac1 siRNA effectively reduced ROS production in MCF-7 cells following IL-1β stimulation (Fig. 8*A*). No inhibition in ROS was seen following transfection with a scrambled siRNA control. Rac1 siRNA also effectively inhibited total Rac1 protein levels in cell lysates (Fig. 8*B*). These findings provide strong evidence that a Rac1-regulated NADPH oxidase controls ROS production following IL-1β stimulation.

Given that Rac1 was in part required for the stimulation of ROS following IL-1β treatment of MCF-7 cells, we next sought to better understand if Rac1 was also required for NIK recruitment to TRAF6 following IL-1β stimulation. Rac1 siRNA indeed reduced the ability of NIK to associate with TRAF6 following IL-1β stimulation (Fig. 8*C*). However, this inhibition was not seen following transfection with a scrambled siRNA control. Combined with earlier results, these data suggest that Rac1-mediated H_2O_2-dependent activation of NIK, through the inhibition of phosphatases, promotes association of TRAF6 with NIK.

Data demonstrating ligand-independent association of activated NIK with TRAF6 following okadaic acid or H_2O_2 treatment (Fig. 7) suggested that NIK can associate with TRAF6 prior to its recruitment to the receptor. However, it remained unclear if the redox-dependent activation of NIK was required for TRAF6 recruitment to IL-1R1. To address this question, we used NIK and Rac1 siRNAs to modulate the formation of NIK·TRAF6 complex formation following IL-1β stimulation. Results from these experiments demonstrated that NIK siRNA effectively inhibited total NIK in cell lysates (Fig. 8*B*), and as expected, also prevented NIK recruitment to TRAF6 following IL-1β stimulation (Fig. 8*C*). Importantly, inhibition of NIK protein levels had no effect on steady-state levels of TRAF6. To address whether NIK was required for TRAF6 recruitment to IL-1R1, we performed IL-1R1 pull-down assays in the presence of NIK, Rac1, or scrambled siRNAs (Fig. 8*D*). If the redox-sensitive complex formation between TRAF6 and NIK was absolutely required for binding of TRAF6 to IL-1R1, we would anticipate that both NIK and Rac1 siRNAs would prevent TRAF6 recruitment to IL-1R1. As shown in Fig. 8*D*, this was not the case. Rac1 siRNA effectively inhibited both the recruitment of NIK and TRAF6 to IL-1R1. However, NIK inhibition did not alter TRAF6 recruitment to IL-1R1 following IL-1β stimulation. This finding provides strong evidence that NIK binding to TRAF6 is not required for the recruitment of TRAF6 to ligand activated IL-1R1. Given that the association of TRAF6 with NIK can be directly activated by H_2O_2 or okadaic acid in the absence of a ligand signal, our data suggest that redox activation of NIK likely promotes TRAF6·NIK complex formation both prior to and following TRAF6 recruitment to the IL-1 receptor.

DISCUSSION

The mechanism by which ROS stimulates the NFκB pathway remains quite complex and multifaceted. IL-1β induction of the NFκB pathway is one example for which molecular mechanisms of ROS action

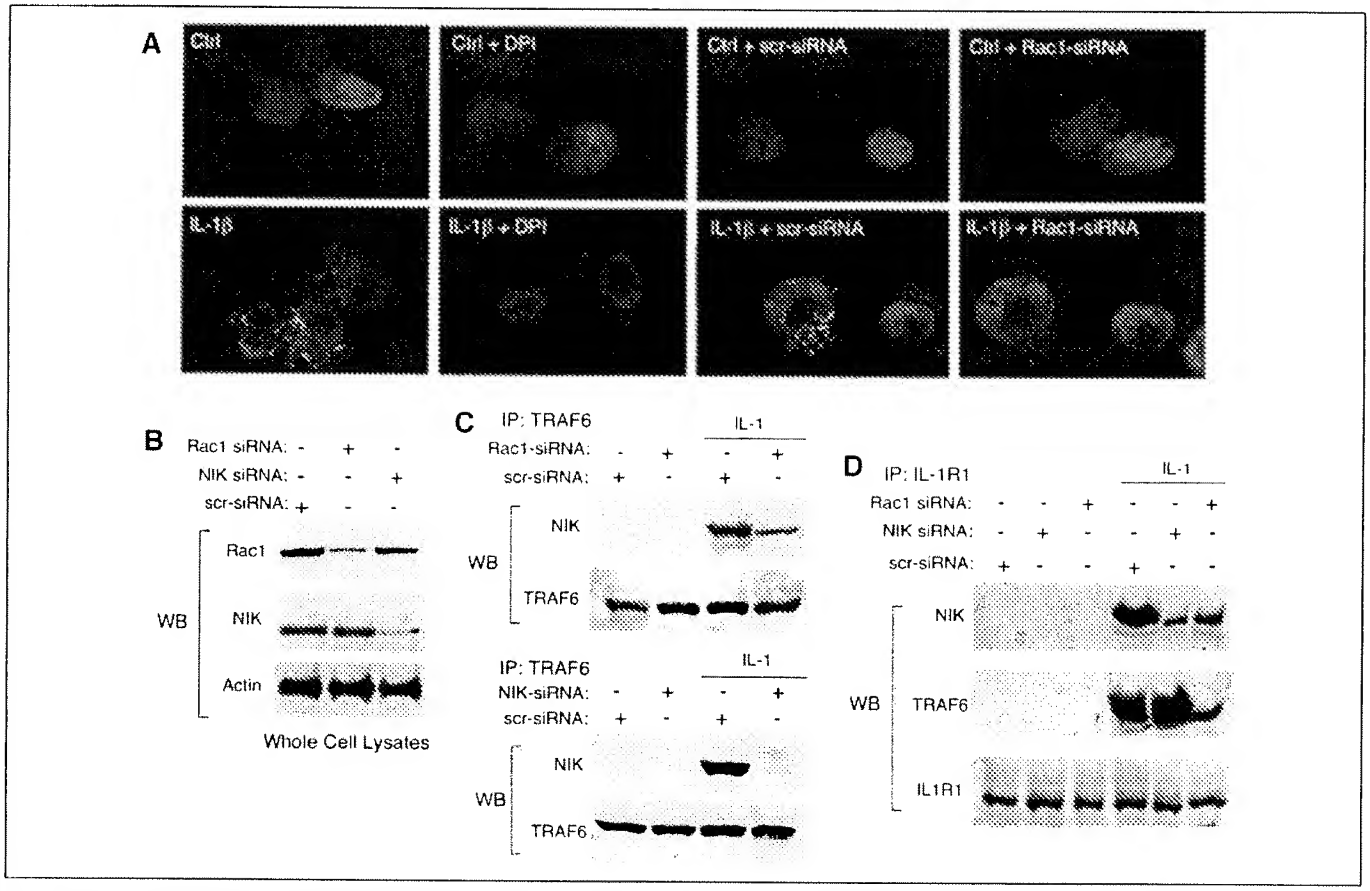

FIGURE 8. **Rac1 regulates NADPH oxidase-mediated ROS production and the recruitment of TRAF6 and NIK to IL-1R1 following IL-1β stimulation.** *A*, MCF-7 cells were assessed for H_2O_2 production following IL-1β (1 ng/ml) stimulation for 20 min in the presence of H_2DCFDA (10 μM). Treatment groups are marked on the fluorescent images and included: 1) transfection with Rac1-siRNA or scrambled siRNA 48 h prior to IL-1β stimulation, and 2) DPI (10 μM) or vehicle (*Ctrl*) treatment at the time of IL-1β stimulation. 4′,6-Diamidino-2-phenylindole was included in the mounting media for identification of nuclei. *B*, MCF-7 cells were transfected with Rac1-siRNA, NIK-siRNA, or scrambled siRNA (*scr-siRNA*). Western blots for total cellular Rac1, NIK, and actin in the absence of IL-1 stimulation are shown at 48 h post-transfection. *C*, MCF-7 cells were transfected with Rac1-siRNA, NIK-siRNA, or scrambled siRNA for 48 h prior to IL-1β (1 ng/ml) stimulation for 20 min. TRAF6 was immunoprecipitated from cell lysates, and Western blots (*WB*) for TRAF6 and NIK are shown. *D*, MCF-7 cells were transfected with Rac1-siRNA, NIK-siRNA, or scrambled siRNA for 48 h prior to IL-1β (1 ng/ml) stimulation for 20 min and immunoprecipitation of IL-1R1. Western blots for NIK, TRAF6, and IL-1R1 are given for the various treatment groups as indicated following immunoprecipitation of IL-1R1.

remain poorly elucidated. In the present study, we have shown that H_2O_2 in part controls NFκB activation by IL-1β by facilitating the activation of NIK and subsequent phosphorylation of IKKα. ROS-mediated events that appear to be important for NIK-mediated activation of NFκB following IL-1β stimulation include NIK association with TRAF6 and the inhibition of Ser/Thr protein phosphatases. Such findings suggest that H_2O_2 may act to promote NIK activation and association with TRAF6 by inhibiting Ser/Thr protein phosphatases.

Rac1 appears to be a central player in the redox control of the IL-1β signaling pathway. The ability of Rac1 siRNA and DPI to inhibit ROS production in cells stimulated by IL-1 implicates Rac1-dependent NADPH oxidases as the cellular ROS source. Rac1 siRNA also inhibited both the redox-dependent formation of a TRAF6·NIK complex and recruitment of both TRAF6 and NIK to IL-1R1. Together with findings that GPx-1 expression inhibited NIK activation and TRAF6·NIK complex formation following IL-1β stimulation, these findings suggest H_2O_2 is the central ROS mediator of this pathway. The importance of Rac1 in IL-1 signaling is supported by previous work demonstrating an association of Rac1 with the IL-1R1 complex through interactions with MyD88 and the IL-1 receptor accessory protein (47). This same study also demonstrated that the dominant negative N17Rac1 mutant prevented IL-1-mediated p65 transactivation. Hence, our studies now clarify that there is a central role for Rac1 in IL-1 signaling via facilitation of the redox activation of downstream effectors.

In vitro reconstitution experiments attempting to directly activate immunoprecipitated NIK with H_2O_2 demonstrated that one or more cellular factors are required for the redox activation of NIK to phosphorylate GST-IKKα (Fig. 6). *In vivo*, H_2O_2 promoted NIK association with TRAF6 in the absence of a ligand signal, and GPx-1 expression inhibited IL-1β-induced TRAF6·NIK association and NIK activation (Figs. 7*C* and 5*E*). Given the close correlation between redox activation of NIK and its association with TRAF6, we anticipate that TRAF6 is a required cellular component necessary for NIK activation as an IKKα kinase. The ability of okadaic acid to directly promote NIK kinase activity and association with TRAF6, in the absence of a ligand signal, suggests that H_2O_2-mediated inhibition of protein phosphatases may be responsible for the redox activation of NIK. Hence, we favor a model whereby TRAF6 must recruit to NIK prior to phosphorylating IKKα. Although NIK binding to TRAF6 may be necessary for an active IKKα kinase complex, this association was not necessary for TRAF6 to recruit to IL-1R1; TRAF6 effectively recruited to IL-1 stimulated IL-1R1 in the absence of NIK.

Cumulatively, these studies place NIK as a central redox-regulated signaling molecule in IL-1-mediated activation of NFκB. We propose a model whereby IL-1 induces Rac1-dependent ROS production through NADPH oxidase, which in turn leads to NIK activation through the inhibition of protein phosphatases and the recruitment of NIK·TRAF6 complexes to the IL-1 receptor.

Acknowledgment—We gratefully acknowledge Mariah Steele for editorial assistance.

REFERENCES

1. Rhee, S. G., Bae, Y. S., Lee, S. R., and Kwon, J. (2000) *Sci. STKE 2000*, PE1
2. Engelhardt, J. F. (1999) *Antioxid. Redox. Signal* **1**, 5–27
3. Brigelius-Flohe, R., Banning, A., Kny, M., and Bol, G. F. (2004) *Arch. Biochem. Biophys.* **423**, 66–73
4. Thannickal, V. J., and Fanburg, B. L. (2000) *Am. J. Physiol.* **279**, L1005–L1028
5. Forman, H. J., and Torres, M. (2002) *Am. J. Respir. Crit. Care Med.* **166**, S4–S8
6. Li, Q., Sanlioglu, S., Li, S., Ritchie, T., Oberley, L., and Engelhardt, J. F. (2001) *Antioxid. Redox. Signal* **3**, 415–432
7. Hayakawa, M., Miyashita, H., Sakamoto, I., Kitagawa, M., Tanaka, H., Yasuda, H., Karin, M., and Kikugawa, K. (2003) *EMBO J.* **22**, 3356–3366
8. Walley, K. R., Lukacs, N. W., Standiford, T. J., Strieter, R. M., and Kunkel, S. L. (1996) *Infect. Immun.* **64**, 4733–4738
9. van den Berg, W. B. (1999) *Z. Rheumatol.* **58**, 136–141
10. Pantschenko, A. G., Pushkar, I., Anderson, K. H., Wang, Y., Miller, L. J., Kurtzman, S. H., Barrows, G., and Kreutzer, D. L. (2003) *Int. J. Oncol.* **23**, 269–284
11. Pinner, R. W., Teutsch, S. M., Simonsen, L., Klug, L. A., Graber, J. M., Clarke, M. J., and Berkelman, R. L. (1996) *J. Am. Med. Assoc.* **275**, 189–193
12. O'Neill, L. A., and Greene, C. (1998) *J. Leukoc. Biol.* **63**, 650–657
13. Burns, K., Clatworthy, J., Martin, L., Martinon, F., Plumpton, C., Maschera, B., Lewis, A., Ray, K., Tschopp, J., and Volpe, F. (2000) *Nat. Cell Biol.* **2**, 346–351
14. Huang, J., Gao, X., Li, S., and Cao, Z. (1997) *Proc. Natl. Acad. Sci. U. S. A.* **94**, 12829–12832
15. Muzio, M., Ni, J., Feng, P., and Dixit, V. M. (1997) *Science* **278**, 1612–1615
16. Wesche, H., Henzel, W. J., Shillinglaw, W., Li, S., and Cao, Z. (1997) *Immunity* **7**, 837–847
17. Li, S., Strelow, A., Fontana, E. J., and Wesche, H. (2002) *Proc. Natl. Acad. Sci. U. S. A.* **99**, 5567–5572
18. Qian, Y., Commane, M., Ninomiya-Tsuji, J., Matsumoto, K., and Li, X. (2001) *J. Biol. Chem.* **276**, 41661–41667
19. Wang, C., Deng, L., Hong, M., Akkaraju, G. R., Inoue, J., and Chen, Z. J. (2001) *Nature* **412**, 346–351
20. Ling, L., Cao, Z., and Goeddel, D. V. (1998) *Proc. Natl. Acad. Sci. U. S. A.* **95**, 3792–3797
21. Fitzgerald, K. A., and O'Neill, L. A. (2000) *Microbes Infect.* **2**, 933–943
22. Uekawa, N., Nishikimi, A., Isobe, K., Iwakura, Y., and Maruyama, M. (2004) *FEBS Lett.* **575**, 30–34
23. Ghosh, S., and Karin, M. (2002) *Cell* **109**, (suppl.) S81–S96
24. Ghosh, S., May, M. J., and Kopp, E. B. (1998) *Annu. Rev. Immunol.* **16**, 225–260
25. Chen, L. W., Egan, L., Li, Z. W., Greten, F. R., Kagnoff, M. F., and Karin, M. (2003) *Nat. Med.* **9**, 575–581
26. Verma, I. M., Stevenson, J. K., Schwarz, E. M., Van Antwerp, D., and Miyamoto, S. (1995) *Genes Dev.* **9**, 2723–2735
27. Woronicz, J. D., Gao, X., Cao, Z., Rothe, M., and Goeddel, D. V. (1997) *Science* **278**, 866–869
28. Zandi, E., Rothwarf, D. M., Delhase, M., Hayakawa, M., and Karin, M. (1997) *Cell* **91**, 243–252
29. Mercurio, F., Murray, B. W., Shevchenko, A., Bennett, B. L., Young, D. B., Li, J. W., Pascual, G., Motiwala, A., Zhu, H., Mann, M., and Manning, A. M. (1999) *Mol. Cell. Biol.* **19**, 1526–1538
30. Hirano, M., Osada, S., Aoki, T., Hirai, S., Hosaka, M., Inoue, J., and Ohno, S. (1996) *J. Biol. Chem.* **271**, 13234–13238
31. Lee, F. S., Hagler, J., Chen, Z. J., and Maniatis, T. (1997) *Cell* **88**, 213–222
32. Tojima, Y., Fujimoto, A., Delhase, M., Chen, Y., Hatakeyama, S., Nakayama, K., Kaneko, Y., Nimura, Y., Motoyama, N., Ikeda, K., Karin, M., and Nakanishi, M. (2000) *Nature* **404**, 778–782
33. Song, H. Y., Regnier, C. H., Kirschning, C. J., Goeddel, D. V., and Rothe, M. (1997) *Proc. Natl. Acad. Sci. U. S. A.* **94**, 9792–9796
34. Malinin, N. L., Boldin, M. P., Kovalenko, A. V., and Wallach, D. (1997) *Nature* **385**, 540–544
35. Regnier, C. H., Song, H. Y., Gao, X., Goeddel, D. V., Cao, Z., and Rothe, M. (1997) *Cell* **90**, 373–383
36. Nakano, H., Shindo, M., Sakon, S., Nishinaka, S., Mihara, M., Yagita, H., and Okumura, K. (1998) *Proc. Natl. Acad. Sci. U. S. A.* **95**, 3537–3542
37. Kabe, Y., Ando, K., Hirao, S., Yoshida, M., and Handa, H. (2005) *Antioxid. Redox. Signal* **7**, 395–403
38. Brigelius-Flohe, R. (1999) *Free Radic. Biol. Med.* **27**, 951–965
39. Ursini, F., Maiorino, M., Brigelius-Flohe, R., Aumann, K. D., Roveri, A., Schomburg, D., and Flohe, L. (1995) *Methods Enzymol.* **252**, 38–53
40. Meier, B., Radeke, H. H., Selle, S., Younes, M., Sies, H., Resch, K., and Habermehl, G. G. (1989) *Biochem. J.* **263**, 539–545
41. Finkel, T. (2001) *IUBMB Life* **52**, 3–6
42. Bonizzi, G., Piette, J., Schoonbroodt, S., Greimers, R., Havard, L., Merville, M. P., and Bours, V. (1999) *Mol. Cell. Biol.* **19**, 1950–1960
43. Bol, G. F., Jurrmann, N., and Brigelius-Flohe, R. (2003) *Biol. Chem.* **384**, 609–617
44. Shrivastava, A., and Aggarwal, B. B. (1999) *Antioxid. Redox. Signal* **1**, 181–191
45. Kamata, H., Honda, S., Maeda, S., Chang, L., Hirata, H., and Karin, M. (2005) *Cell* **120**, 649–661
46. Gu, Y., Xu, Y. C., Wu, R. F., Nwariaku, F. E., Souza, R. F., Flores, S. C., and Terada, L. S. (2003) *J. Biol. Chem.* **278**, 17210–17217
47. Jefferies, C., Bowie, A., Brady, G., Cooke, E. L., Li, X., and O'Neill, L. A. (2001) *Mol. Cell. Biol.* **21**, 4544–4552
48. Sanlioglu, S., Williams, C. M., Samavati, L., Butler, N. S., Wang, G., McCray, P. B., Jr., Ritchie, T. C., Hunninghake, G. W., Zandi, E., and Engelhardt, J. F. (2001) *J. Biol. Chem.* **276**, 30188–30198
49. Hatano, E., Bradham, C. A., Stark, A., Iimuro, Y., Lemasters, J. J., and Brenner, D. A. (2000) *J. Biol. Chem.* **275**, 11814–11823
50. Schwabe, R. F., Schnabl, B., Kweon, Y. O., and Brenner, D. A. (2001) *J. Immunol.* **166**, 6812–6819
51. Fan, C., Yang, J., and Engelhardt, J. F. (2002) *J. Cell Sci.* **115**, 4843–4853
52. Iimuro, Y., Nishiura, T., Hellerbrand, C., Behrns, K. E., Schoonhoven, R., Grisham, J. W., and Brenner, D. A. (1998) *J. Clin. Invest.* **101**, 802–811
53. Anasagasti, M. J., Alvarez, A., Avivi, C., and Vidal-Vanaclocha, F. (1996) *J. Cell. Physiol.* **167**, 314–323
54. Nian, M., Lee, P., Khaper, N., and Liu, P. (2004) *Circ. Res.* **94**, 1543–1553
55. Mendes, A. F., Caramona, M. M., Carvalho, A. P., and Lopes, M. C. (2003) *Cell Biol. Toxicol.* **19**, 203–214
56. Schreck, R., Rieber, P., and Baeuerle, P. A. (1991) *EMBO J.* **10**, 2247–2258
57. Marangolo, M., McGee, M. M., Tipton, K. F., Williams, D. C., and Zisterer, D. M. (2001) *Neurotox. Res.* **3**, 397–409
58. Valacchi, G., Pagnin, E., Phung, A., Nardini, M., Schock, B. C., Cross, C. E., and van der Vliet, A. (2005) *Antioxid. Redox. Signal* **7**, 25–31
59. Je, J. H., Lee, J. Y., Jung, K. J., Sung, B., Go, E. K., Yu, B. P., and Chung, H. Y. (2004) *FEBS Lett.* **566**, 183–189
60. Xiong, S., She, H., Sung, C. K., and Tsukamoto, H. (2003) *Alcohol* **30**, 107–113
61. Xiong, S., She, H., Takeuchi, H., Han, B., Engelhardt, J. F., Barton, C. H., Zandi, E., Giulivi, C., and Tsukamoto, H. (2003) *J. Biol. Chem.* **278**, 17646–17654
62. Zhang, J., Johnston, G., Stebler, B., and Keller, E. T. (2001) *Antioxid. Redox. Signal* **3**, 493–504
63. Choi, M. H., Lee, I. K., Kim, G. W., Kim, B. U., Han, Y. H., Yu, D. Y., Park, H. S., Kim, K. Y., Lee, J. S., Choi, C., Bae, Y. S., Lee, B. I., Rhee, S. G., and Kang, S. W. (2005) *Nature* **435**, 347–353
64. Wu, H., and Arron, J. R. (2003) *BioEssays* **25**, 1096–1105
65. Mendes, A. F., Carvalho, A. P., Caramona, M. M., and Lopes, M. C. (2001) *Mediators Inflamm.* **10**, 209–215
66. Lo, Y. Y., Conquer, J. A., Grinstein, S., and Cruz, T. F. (1998) *J. Cell. Biochem.* **69**, 19–29
67. Lambeth, J. D. (2004) *Nat. Rev. Immunol.* **4**, 181–189

EXHIBIT D

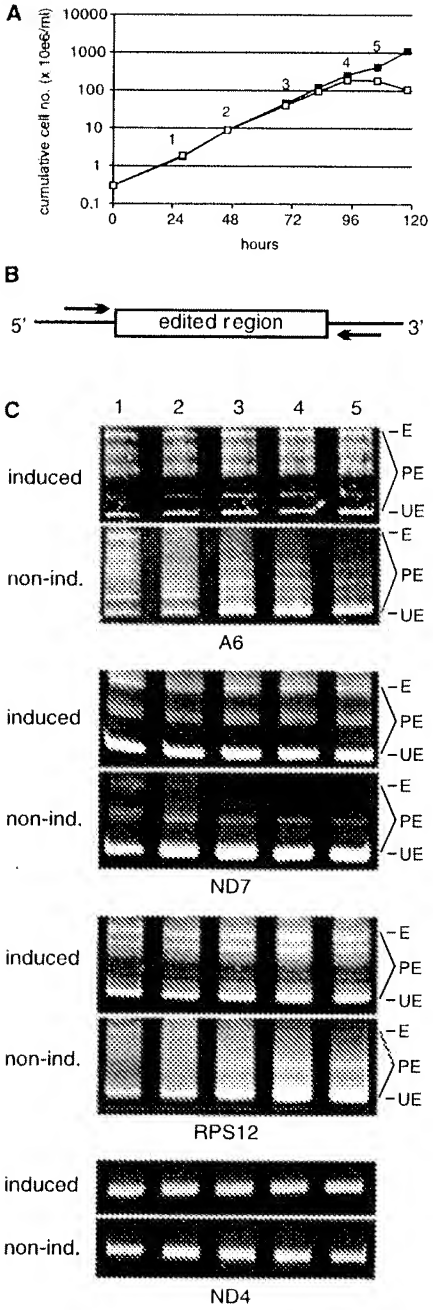

Fig. 4. Loss of TbMP52 blocks RNA editing. (**A**) Growth of induced (black squares) and non-induced (white squares) parasites. Total RNA was prepared from samples taken at the time points indicated (*16*). (**B**) Diagram showing RT-PCR primer locations relative to the edited region. (**C**) Polyacrylamide gel analysis of RT-PCR products from RNAs that are normally edited in bloodforms (A6, ND7, and RPS12) and ND4 RNA, which does not get edited (*16*). Fully edited (E), partially edited (PE), and unedited (UE) molecules were identified by cloning and sequencing.

Table 1. Growth in mice of *T. brucei* with induced or non-induced TbMP52. C57 BL/6 mice were infected by intraperitoneal inoculation with 10^5 cultured bloodstream-form *T. brucei* clones 1B3 or 1-5 (the parental clone with one endogenous allele plus the ectopic allele). Dox (200 μg/ml) and/or 5% sucrose was added to the drinking water beginning 1 week before infection for induction. Parasites were counted with a hemocytometer.

Genotype	dox	Parasites ($\times 10^6$ per milliliter of blood)			
		66 hours	81 hours	105 hours	128 hours
1B3	–	3	1	0	0
	–	16	41	0	0
	+	10	232	*	
	+	0	4	78	955*
1-5	–	26	395	*	
	–	14	239	*	
	+	4	266	*	

*These mice died of the infection or were killed because of high parasitemia.

References and Notes

1. S. L. Hajduk *et al.*, *Nucleic Acids Symp. Ser.* **36**, 15 (1997).
2. K. Stuart *et al.*, *Microbiol. Mol. Biol. Rev.* **61**, 105 (1997).
3. A. M. Estévez, L. Simpson, *Gene* **240**, 247 (1999).
4. A. K. Panigrahi *et al.*, *Mol. Cell. Biol.* **21**, 380 (2001).
5. Searches were done at www.ncbi.nlm.nih.gov/Structure/cdd/cdd.shtml.
6. S. Shuman, B. Schwer, *Mol. Microbiol.* **17**, 405 (1995).
7. Single-letter abbreviations for the amino acid residues are as follows: A, Ala; C, Cys; D, Asp; E, Glu; F, Phe; G, Gly; H, His; I, Ile; K, Lys; L, Leu; M, Met; N, Asn; P, Pro; Q, Gln; R, Arg; S, Ser; T, Thr; V, Val; W, Trp; Y, Tyr; X, any amino acid.
8. A. E. Tomkinson *et al.*, *Proc. Natl. Acad. Sci. U.S.A.* **88**, 400 (1991).
9. R. Sabatini, S. L. Hajduk, *J. Biol. Chem.* **270**, 7233 (1995).
10. M. Peris *et al.*, *Mol. Biochem. Parasitol.* **85**, 9 (1997).
11. L. N. Rusché *et al.*, *EMBO J.* **16**, 4069 (1997).
12. Using published methods (*13*, *14*), one endogenous allele was eliminated in cultured bloodforms, using construct pTbMP52-KO1, but several attempts to knock out the second allele using construct pTbMP52-KO2 failed. An "ectopic" allele with a tet-inducible promoter was inserted using construct pTbMP52-ect to get clone 1-5, and then the second endogenous allele was replaced with construct pTbMP52-KO2 to get clone 1B3, which was chosen at random for analysis. See (*16*) for details.
13. E. Wirtz *et al.*, *Mol. Biochem. Parasitol.* **99**, 89 (1999).
14. C. M. Ochatt *et al.*, *Mol. Biochem. Parasitol.* **103**, 35 (1999).
15. A. K. Panigrahi, unpublished data.
16. Supplemental Web material is available on *Science* Online at www.sciencemag.org/cgi/content/full/1058955/DC1.
17. M. J. Moore, P. D. Sharp, *Science* **256**, 992 (1992).
18. A. Missel *et al.*, *Mol. Cell. Biol.* **17**, 4895 (1997).
19. J. W. Priest, S. L. Hajduk, *J. Bioenerg. Biomembr.* **26**, 179 (1994).
20. K. D. Stuart, *J. Cell. Biol.* **49**, 189 (1971).
21. D. S. Beattie, M. M. Howton, *Eur. J. Biochem.* **241**, 888 (1996).
22. J. Feagin, K. Stuart, *Mol. Cell. Biol.* **8**, 1259 (1988).
23. D. J. Koslowsky *et al.*, *Cell* **62**, 901 (1990).
24. rTbMP52 was expressed in vitro from the coding sequence in pSG1 vector, using the TNT quick coupled transcription/translation system (Promega) with either [^{35}S]-labeled or cold methionine. Control reactions used pSG1 vector alone. Translation products were immunoprecipitated from the TNT mix with mAb P3C1-G2 (*4*).
25. R. P. Igo Jr. *et al.*, *Mol. Cell. Biol.* **20**, 8447 (2000).

26. We thank N. Carmean for technical assistance; T. White and H. Interthal for comments on the manuscript; the George Cross laboratory for the knockout plasmids; E. Vassella for helpful suggestions; M. Parsons for antiserum to phosphoglycerate kinase (PGK); V. Kumar for the pSG1 plasmid; and the Stuart laboratory for helpful discussions. Support was from NIH grants GM42188 and AI14102 and Human Frontier Science Program Organization grant RG/97.

24 October 2000; accepted 2 February 2001
Published online 15 February 2001;
10.1126/science.1058655
Include this information when citing this paper.

Defective Lymphotoxin-β Receptor–Induced NF-κB Transcriptional Activity in NIK-Deficient Mice

Li Yin,[1] Lin Wu,[2] Holger Wesche,[2] Cora D. Arthur,[1] J. Michael White,[1] David V. Goeddel,[2] Robert D. Schreiber[1]*

The role of NF-κB–inducing kinase (NIK) in cytokine signaling remains controversial. To identify the physiologic functions of NIK, we disrupted the NIK locus by gene targeting. Although NIK$^{-/-}$ mice displayed abnormalities in both lymphoid tissue development and antibody responses, NIK$^{-/-}$ cells manifested normal NF-κB DNA binding activity when treated with a variety of cytokines, including tumor necrosis factor (TNF), interleukin-1 (IL-1), and lymphotoxin-β (LTβ). However, NIK was selectively required for gene transcription induced through ligation of LTβ receptor but not TNF receptors. These results reveal that NIK regulates the transcriptional activity of NF-κB in a receptor-restricted manner.

apeutic targets for kinetoplastid pathogens, which employ RNA editing (such as African and American trypanosomes and *Leishmania*).

The transcription factor NF-κB is activated by a variety of cell surface receptors (*1*). Although different receptors often use distinct combinations of intracellular proteins to initiate NF-κB activation, the signals converge downstream into a common pathway

that leads to activation of the IκB kinase (IKK) complex and the phosphorylation and degradation of IκB (inhibitor of NF-κB) (*2–8*). The upstream kinases that activate the IKK complex are not defined (*1, 9*). However, the serine-threonine kinase NIK has been suggested to fulfill this role (*10, 11*). NIK was identified by its interaction with TRAF2, an adapter protein that interacts with TNF receptors (*10*). NIK was thought to be an integral component of the NF-κB signaling pathway because, when overexpressed in cells, wild-type NIK interacted with the IKK subunits IKKα and IKKβ, enhanced IKK complex kinase activity (*5*), and caused ligand-independent activation of NF-κB (*10, 11*). Moreover, kinase-inactive NIK inhibited NF-κB activation in cells treated with a variety of ligands (*10, 11*). Recent studies of alymphoplasia (*aly/aly*) mice, which have defective lymphorganogenesis and express a point mutant form of NIK that retains catalytic potential, suggest that NIK may function in NF-κB activation in a cell- or receptor-specific manner (*12–15*). However, the presence of the catalytically active mutant NIK protein in the *aly/aly* mouse makes it difficult to draw firm conclusions about the precise functional role of this protein.

To determine whether NIK plays an obligatory role in signal-induced NF-κB activation, we generated $NIK^{-/-}$ mice by gene targeting (*16*). Disruption of the NIK gene was verified by Southern and Western blot analyses. Although $NIK^{-/-}$ mice were born in Mendelian proportions and were grossly normal, they displayed abnormal lymphorganogenesis similar to that observed in *aly/aly* mice and mice lacking the LTβ receptor (LTβR) (*12, 17*). Specifically, they lacked all lymph nodes (including cervical, inguinal, mesenteric, popliteal, and axillary lymph nodes) and did not develop Peyer's patches (*18*). In addition, they showed an abnormal architecture of spleen and thymus, and formed only poor antibody responses upon immunization (*18*).

To assess whether NIK was required for TNF or IL-1 signaling, we treated $NIK^{-/-}$ or wild-type mouse embryonic fibroblasts (MEFs) with each ligand and assessed NF-κB DNA binding activity by electrophoretic mobility-shift assay (EMSA). No substantial differences were observed between the two cell types, even when different durations of stimulation or different doses of cytokine were used (Fig. 1, A and B). Moreover, activation of the IKK complex and c-Jun NH_2-terminal kinase (JNK) enzymes, which are known to be stimulated by these ligands, occurred equivalently in $NIK^{-/-}$ and wild-type MEFs (Fig. 1C). TNF and IL-1 also induced comparable biologic responses in $NIK^{-/-}$ and wild-type cells, including apoptosis (Fig. 1D) and production of IL-6 (Fig. 1E) or nitric oxide (Fig. 1F). Thus, NIK does not play an obligate role in either TNF or IL-1 signaling in fibroblasts. This conclusion was generalizable to other cell types from the $NIK^{-/-}$ mouse, such as bone marrow–derived macrophages (BMMs) and T cells, which developed wild-type levels of NF-κB DNA binding activity after TNF stimulation (Fig. 2A).

We also considered the possibility that NIK functioned to induce NF-κB DNA binding activity in a receptor-specific manner. As shown by EMSA, MEFs and BMMs from $NIK^{-/-}$ and wild-type mice formed equivalent amounts of DNA binding complexes after treatment with a variety of known NF-

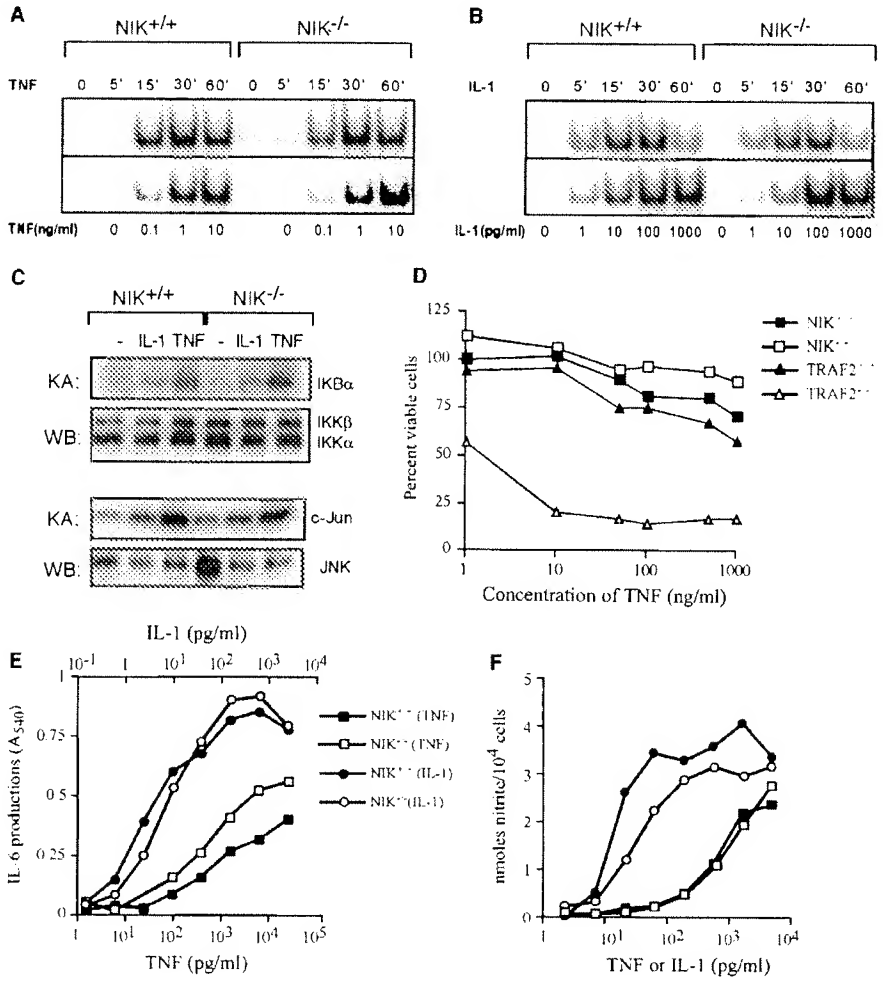

Fig. 1. $NIK^{-/-}$ MEFs display unimpaired signaling and biologic responsiveness to murine TNF and IL-1β. (**A** and **B**) Comparable activation of NF-κB DNA binding activity in $NIK^{-/-}$ or wild-type MEFs treated with TNF (A) or IL-1 (B) (10 ng/ml each) for the indicated numbers of minutes (top panel), or treated with the indicated doses of cytokines for 30 min (bottom panel). EMSA was performed as described using a probe derived from the immunoglobulin κ promoter (*21*). (**C**) In vitro kinase assays showing comparable activation of the kinase activity (KA) of the IKK complex and JNK in $NIK^{-/-}$ or wild-type MEFs incubated for 5 min with either IL-1 (50 ng/ml) or TNF (100 ng/ml). The IKK complex and JNK were immunoprecipitated, and kinase activities in the immunoprecipitates were determined using recombinant IκB or c-Jun proteins as substrates. IKKα, IKKβ, and JNK protein levels were assessed by Western blotting (WB). (**D**) $NIK^{-/-}$ and wild-type MEFs are similar in their sensitivity to TNF-dependent cytotoxicity. This assay was performed on cycloheximide-treated MEFs as described (*22*). $TRAF2^{-/-}$ MEFs were used as a pathway control. (**E**) Unimpaired cytokine-induced IL-6 production in $NIK^{-/-}$ cells. $NIK^{-/-}$ or wild-type MEFs were stimulated with various amounts of TNF or IL-1 for 24 hours, and IL-6 levels in culture supernatants were determined using the IL-6–dependent T1165 cell line. (**F**) Normal TNF- or IL-1–induced nitric oxide production by $NIK^{-/-}$ cells. MEFs were cultured with various amounts of TNF or IL-1 in the presence of murine interferon-γ (250 ng/ml), and the level of nitrite in the supernatants was determined as described (*23*).

[1]Center for Immunology, Department of Pathology and Immunology, Washington University School of Medicine, St. Louis, MO 63110, USA. [2]Tularik Inc., 2 Corporate Drive, South San Francisco, CA 94080, USA.

*To whom correspondence should be addressed. E-mail: schreiber@immunology.wustl.edu

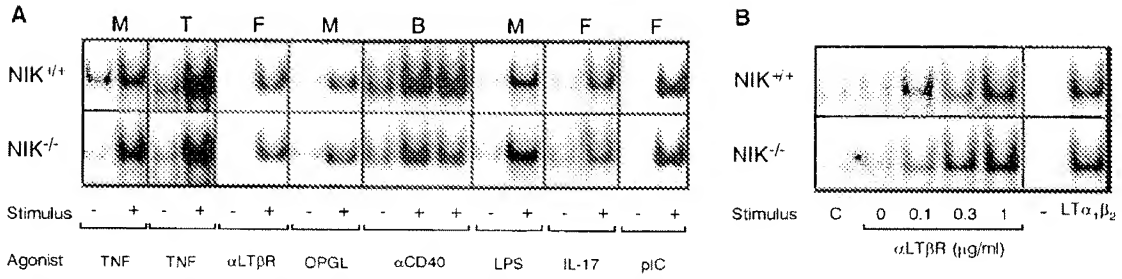

Fig. 2. Induction of NF-κB DNA binding activity in $NIK^{-/-}$ cells after stimulation with different agonists. (**A**) $NIK^{-/-}$ or wild-type BMMs (M), T lymphocytes (T), fibroblasts (F), or B lymphocytes (B) were stimulated with TNF (10 ng/ml, 30 min), LTβR mAb (*24*) (αLTβR; 1 μg/ml, 1 hour), osteoprotegerin ligand (OPGL; 100 ng/ml, 15 min), antibody to CD40 (αCD40; 10 μg/ml, 1 and 4 hours), lipopolysaccharide (LPS; 10 μg/ml, 1 hour), IL-17 (100 ng/ml, 30 min), or polyinosinic-polycytidylic acid (pIC; 100 μg/ml, 2 hours). NF-κB DNA binding activity was then assessed by EMSA. (**B**) $NIK^{-/-}$ or wild-type MEFs were stimulated with the indicated doses of LTβR mAb, irrelevant mAb (C, 1 μg/ml), or $LT\alpha_1\beta_2$ (Sigma; 100 ng/ml) for 1 hour and assayed by EMSA.

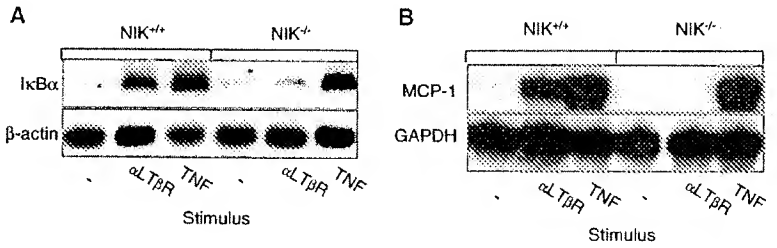

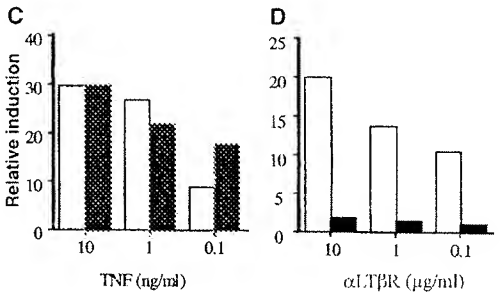

Fig. 3. Failure of $NIK^{-/-}$ cells to transcribe NF-κB–regulated genes after LTβR stimulation. (**A**) IκBα or β-actin gene expression was determined by Northern blotting for $NIK^{-/-}$ or wild-type MEFs treated for 8 hours with buffer, LTβR mAb (αLTβR, 1 μg/ml), or TNF (10 ng/ml). (**B**) RNA samples prepared as in (A) were assayed for gene expression using the RiboQuant multiprobe ribonuclease protection assay system and mCK-5 template (Pharmingen). In wild-type cells, the gene encoding MCP-1 was the only gene induced among those represented in the mCK-5 template upon LTβR mAb treatment. (**C** and **D**) Immortalized MEFs were transiently transfected using SuperFect reagent (Qiagen) with 1 μg of an $(NF\text{-}\kappa B)_2$-Luc reporter construct (*25*) together with 1 μg of pRL-TK (Promega) for transfection normalization. The transfected wild-type cells (open bars) or $NIK^{-/-}$ cells (filled bars) were stimulated with TNF (10 ng/ml) (C) or LTβR mAb (1 μg/ml) (D) for 6 to 8 hours, and luciferase activity was determined and normalized. Data are presented as relative induction of luciferase activity over the unstimulated control.

κB-activating stimuli (Fig. 2A). In contrast, $NIK^{-/-}$ B cells developed normal levels of NF-κB DNA binding activity after 1 hour of treatment with antibody to CD40 but showed reduced levels (relative to wild-type cells) 4 hours after stimulation. However, because B cells in $NIK^{-/-}$ mice are abnormal, it is not possible to determine whether this defect is attributable to an abnormality in signaling or cellular development. Because mice lacking NIK displayed a phenotype that was similar to LTβR-deficient mice, we studied LTβR signaling in the former in more detail. $NIK^{-/-}$ MEFs produced wild-type levels of NF-κB DNA binding activity after treatment with different doses of LTβR monoclonal antibody (mAb) or with the natural ligand for the LTβR (i.e., the $LT\alpha_1\beta_2$ complex) (Fig. 2B). Thus, NIK is not required for promoting NF-κB DNA binding activity by a variety of receptors on different cells.

We next examined whether NIK regulates the transcriptional activity of the activated NF-κB complex. To test this hypothesis, we monitored the capacity of TNF or LTβR mAb to induce expression of representative NF-κB–responsive genes in wild-type and $NIK^{-/-}$ cells. In wild-type MEFs, both LTβR mAb and TNF induced the genes encoding IκBα (Fig. 3A) and monocyte chemoattractant protein-1 (MCP-1, Fig. 3B). These genes were also induced by TNF in $NIK^{-/-}$ cells. In contrast, neither gene was induced in $NIK^{-/-}$ MEFs after LTβR mAb stimulation. Further experiments tested whether this unresponsiveness was due to a defect in the transcriptional activity of the NF-κB complex. Using a luciferase reporter gene construct driven by an NF-κB responsive element, we found that TNF induced comparable levels of luciferase in wild-type and $NIK^{-/-}$ MEFs (Fig. 3C). Reporter gene activation was also consistently observed in wild-type MEFs treated with LTβR mAb (Fig. 3D). In contrast, no reporter activity was observed in $NIK^{-/-}$ MEFs treated with a wide range of doses of LTβR mAb (Fig. 3D). Thus, even though engagement of LTβR induces normal DNA binding activity of NF-κB in $NIK^{-/-}$ cells, the activated NF-κB in these cells cannot transactivate (at least some) NF-κB–regulated genes.

These results show that NIK is not the common upstream kinase that activates IKKs in the NF-κB signaling pathway, as previously proposed (*10*, *11*). Rather, NIK acts in a receptor-selective manner, and its function is limited in the case of the LTβR to promoting the transcriptional action of the NF-κB complex. Hence, the function of NIK in LTβR signaling may be similar to that of glycogen synthase kinase–3β or the T2K/TBK1/NAK kinase, which function in TNF and IL-1 signaling to induce NF-κB transcriptional activity without altering IκB degradation or NF-κB nuclear translocation (*19*, *20*). Thus, different receptors that signal through NF-κB may use distinct serine kinases to regulate the transcriptional activity of the activated NF-κB complex. In this manner, the NF-κB signal emanating from each type of receptor may be slightly different and thereby effect distinctive cellular response patterns after receptor stimulation.

References and Notes

1. S. Ghosh, M. J. May, E. B. Kopp, *Annu. Rev. Immunol.* **16**, 225 (1998).
2. C. H. Regnier *et al.*, *Cell* **90**, 373 (1997).
3. J. A. DiDonato, M. Hayakawa, D. M. Rothwarf, E. Zandi, M. Karin, *Nature* **388**, 548 (1997).
4. F. Mercurio *et al.*, *Science* **278**, 860 (1997).
5. J. D. Woronicz, X. Gao, Z. Cao, M. Rothe, D. V. Goeddel, *Science* **278**, 866 (1997).
6. E. Zandi, D. M. Rothwarf, M. Delhase, M. Hayakawa, M. Karin, *Cell* **91**, 243 (1997).
7. S. Yamaoka *et al.*, *Cell* **93**, 1231 (1998).
8. D. M. Rothwarf, E. Zandi, G. Natoli, M. Karin, *Nature* **395**, 297 (1998).
9. M. Karin, *J. Biol. Chem.* **274**, 27339 (1999).
10. N. L. Malinin, M. P. Boldin, A. V. Kovalenko, D. Wallach, *Nature* **385**, 540 (1997).
11. H. Y. Song, C. H. Regnier, C. J. Kirschning, D. V.

Goeddel, M. Rothe, *Proc. Natl. Acad. Sci. U.S.A.* **94**, 9792 (1997).
12. S. Miyawaki *et al.*, *Eur. J. Immunol.* **24**, 429 (1994).
13. R. Shinkura *et al.*, *Nature Genet.* **22**, 74 (1999).
14. N. Garceau *et al.*, *J. Exp. Med.* **191**, 381 (2000).
15. S. Fagarasan *et al.*, *J. Exp. Med.* **191**, 1477 (2000).
16. The NIK gene was targeted in GS-1 embryonic stem cells by replacing 1.3 kb of DNA containing the first 120 base pairs of exon 1 with a neomycin resistance gene (*18*). $NIK^{-/-}$ mice were maintained on either 129/SvEv or 129/SvEv × C57BL/6 backgrounds. $NIK^{-/-}$ mice were more susceptible to bacterial eye infections but showed no gross abnormalities in growth, behavior, or capacities to reproduce or nurse.
17. A. Futterer, K. Mink, A. Luz, M. H. Kosco-Vilbois, K. Pfeffer, *Immunity* **9**, 59 (1998).
18. See *Science* Online (www.sciencemag.org/cgi/content/full/291/5511/2162/DC1).
19. K. P. Hoeflich *et al.*, *Nature* **406**, 86 (2000).
20. M. Bonnard *et al.*, *EMBO J.* **19**, 4976 (2000).
21. T. L. Murphy, M. G. Cleveland, P. Kulesza, J. Magram, K. M. Murphy, *Mol. Cell. Biol.* **15**, 5258 (1995).
22. M. Tanaka *et al.*, *Immunity* **10**, 421 (1999).
23. M. A. Meraz *et al.*, *Cell* **84**, 431 (1996).
24. J. L. Browning *et al.*, *J. Immunol.* **159**, 3288 (1997).
25. H. C. Liou, W. C. Sha, M. L. Scott, D. Baltimore, *Mol. Cell. Biol.* **14**, 5349 (1994).
26. We thank J. Browning for LTβR mAb; D. Novack, S. Teitelbaun, and Y. Choi for osteoprotegerin ligand; and W. Sha for the $(NF\text{-}\kappa B)_2$-Luc reporter construct. Supported by grants from NIH and Tularik Inc. L.Y. is a Postdoctoral Fellow of the Cancer Research Institute.

20 December 2000; accepted 1 February 2001

Dyslexia: Cultural Diversity and Biological Unity

E. Paulesu,[1,2]* J.-F. Démonet,[3] F. Fazio,[2,4] E. McCrory,[5] V. Chanoine,[3] N. Brunswick,[6] S. F. Cappa,[7] G. Cossu,[8] M. Habib,[9] C. D. Frith,[6] U. Frith[5]

The recognition of dyslexia as a neurodevelopmental disorder has been hampered by the belief that it is not a specific diagnostic entity because it has variable and culture-specific manifestations. In line with this belief, we found that Italian dyslexics, using a shallow orthography which facilitates reading, performed better on reading tasks than did English and French dyslexics. However, all dyslexics were equally impaired relative to their controls on reading and phonological tasks. Positron emission tomography scans during explicit and implicit reading showed the same reduced activity in a region of the left hemisphere in dyslexics from all three countries, with the maximum peak in the middle temporal gyrus and additional peaks in the inferior and superior temporal gyri and middle occipital gyrus. We conclude that there is a universal neurocognitive basis for dyslexia and that differences in reading performance among dyslexics of different countries are due to different orthographies.

Developmental dyslexia is increasingly acknowledged to be a disorder of genetic origin with a basis in the brain (*1*). However, there continues to be doubt about the universality and specificity of the syndrome because behavioral studies have shown that the nature and prevalence of dyslexia differs across languages (*2*). The prevalence estimates of dyslexia in different countries seem to be related to the shallowness of the orthography. For instance, using one of the most respected behavioral definitions of dyslexia (word recognition accuracy in relation to IQ), the prevalence of dyslexia in Italy was half that in the United States (*3*).

Current theories of dyslexia favor a neurocognitive explanation with the implicit assumption of a universal application. There is considerable agreement that a causal link between brain abnormality and reading difficulties involves phonological processing deficits (*4, 5*). The cause of these deficits is, however, less clear. Recently, more general perceptual problems have been postulated, either auditory (*6*) or visual deficits associated with dysfunction of the magnocellular system of the brain (*7*). At a neurological level, it has been shown that dyslexics have microscopic cortical abnormalities, particularly in the perisylvian language areas in the form of cortical ectopias and dyslamination of cortical layers (*8*). These diffuse neurological abnormalities may reduce corticocortical connectivity, as suggested by recent positron emission tomography (PET) and magnetic resonance imaging (MRI) studies (*9, 10*). Until now, most of the biological studies used English-speaking subjects; none have directly compared dyslexics across different orthographies.

In languages with transparent or shallow orthography (e.g., Italian), the letters of the alphabet, alone or in combination, are in most instances uniquely mapped to each of the speech sounds occurring in the language (*11*). Learning to read in such languages is easier than in languages with deep orthography (e.g., English and French), where the mapping between letters, speech sounds, and whole-word sounds is often highly ambiguous (*12, 13*). Adult skilled readers show a speed advantage in shallow orthographies (*14, 15*). Differences have also been demonstrated at the physiological level (*15*).

Our aim was to contrast dyslexic and normal adult readers in deep (English and French) and shallow (Italian) orthographies in order to explore similarities and differences at both the behavioral and neurophysiological level. If dyslexia has a universal basis, then substantial similarities should be found, either at the cognitive or the brain level, or both. We investigated single-word reading at explicit and automatic levels, because differential response to the written word is the most widely agreed defining behavioral feature of dyslexia. Given that stimuli differ between different orthographies, and given that orthographic depth affects reading difficulty, any commonality found in underlying physiological responses in dyslexics would be strong evidence for a unitary biological basis.

Normal controls and subjects with dyslex-

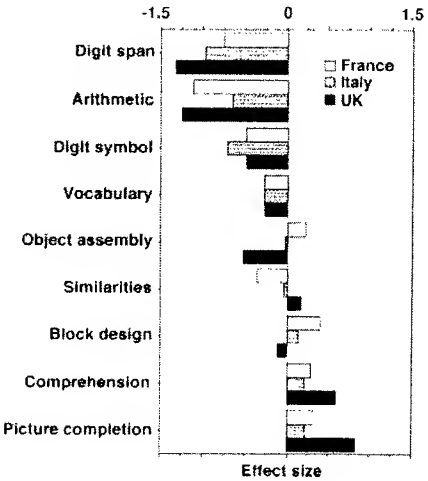

Fig. 1. Effect size (Z-scores) of the differences between dyslexic and normal readers in each country on Wechsler scale subtests. Z-scores were derived from the group differences expressed in standard deviation (SD) units using pooled SDs. Negative Z-scores represent impaired performance. The dyslexics were only impaired on subtests involving phonological short-term memory.

[1]Psychology Department, University of Milan Bicocca, Milan, Italy. [2]INB-CNR, Scientific Institute H San Raffaele, Milan, Italy. [3]INSERM U455, Hôpital Purpan, Toulouse, France. [4]Neuroscience and Biomedical Technologies Department, University of Milan Bicocca, Milan, Italy. [5]Institute of Cognitive Neuroscience, University College London, London, UK. [6]Wellcome Department of Cognitive Neurology, Institute of Neurology, London, UK. [7]Psychology Department, University "Vita e Salute H San Raffaele", Milan, Italy. [8]Institute of Human Physiology, University of Parma, Parma, Italy. [9]Centre de Recherche Institut Universitaire de Gériatrie, Montréal, Quebec, Canada.

*To whom correspondence should be addressed at University of Milan Bicocca. E-mail: eraldo.paulesu@unimib.it

EXHIBIT E

Oncogene (2003) 22, 4348–4355

www.nature.com/onc

NIK is a component of the EGF/heregulin receptor signaling complexes

Danying Chen[1], Liang-Guo Xu[2], Lei Chen[1], Lixia Li[1], Zhonghe Zhai[1], Hong-Bing Shu*[,1,2]

[1]*Department of Cell Biology and Genetics, College of Life Sciences, Peking University, Beijing 100871, China;* [2]*Department of Immunology, National Jewish Medical and Research Center, University of Colorado Health Sciences Center, 1400 Jackson Street, k516c, Denver, CO 80206, USA*

Nuclear factor κB-inducing kinase (NIK) is a member of the MAP kinase kinase kinase family that was first identified as a component of the TNF-R1-induced NF-κB activation pathway (TNF, tumor necrosis factor; nuclear factor kappaB, NF-κB). Gene knockout study, however, suggests that NIK is dispensable for TNF-R1- but required for lymphotoxin-β receptor-induced NF-κB activation. A NIK kinase inactive mutant is a potent inhibitor of NF-κB activation triggered by various stimuli, suggesting that NIK is involved in a broad range of NF-κB activation pathways. To unambiguously identify signaling pathways that NIK participates in, we screened antibody arrays for proteins that are associated with NIK. This effort identified ErbB4, one of the EGF/heregulin receptors, and Grb7, an adapter protein associated with ErbB4 (ErbB, epidermal growth factor receptor family protein; EGF, epidermal growth factor; Grb, growth factor receptor bound). Coimmunoprecipitation experiments demonstrated that NIK interacted with Grb7, as well as Grb10 and Grb14, but not Grb2. Domain mapping experiments indicated that the central GM domain of Grb7 was sufficient for its interaction with NIK. Coimmunoprecipitation experiments also indicated that Grb7 and NIK could be simultaneously recruited into signaling complexes of all known EGF/heregulin receptors, including EGFR, ErbB2, ErbB3, and ErbB4. In reporter gene assays, NIK could potentiate Grb7, ErbB2/ErbB4, and EGF-induced NF-κB activation. A NIK kinase inactive mutant could block ErbB2/ErbB4 and EGF-induced NF-κB activation. Moreover, EGF/heregulin receptors activated NF-κB in wild-type, but not NIK−/− embryonic fibroblasts. Our findings suggest that NIK is a component of the EGF/heregulin receptor signaling complexes and involved in NF-κB activation triggered by these receptors.
Oncogene (2003) **22,** 4348–4355. doi:10.1038/sj.onc.1206532

Keywords: NIK; EGF; Grb7; NF-κB; signaling

*Correspondence: Hong-Bing Shu, Department of Immunology, National Jewish Medical and Research Center, University of Colorado Health Sciences Center, 1400 Jackson Street, k516c, Denver, CO 80206, USA; E-mail: shuh@njc.org
Received 3 January 2003; revised 20 February 2003; accepted 26 February 2003

Introduction

Nuclear factor κB-inducing kinase (NIK) is a serine/threonine protein kinase belonging to the MAP kinase kinase kinase family, which also includes MEKK1-4, ASK1, and Raf, among others (Malinin *et al.*, 1997). NIK was first identified as a TRAF2-interacting protein by yeast two-hybrid screening and was shown to be involved in the TNF-R1-induced NF-κB activation pathway (Malinin *et al.*, 1997) (TNF, tumor necrosis factor; nuclear factor kappaB, NF-κB). Subsequently, it has been suggested that NIK interacts with various TRAFs and can activate IKK, a kinase complex that is critically involved in NF-κB activation triggered by divergent stimuli (Lin *et al.*, 1998a, b). However, gene knockout experiments indicate that NIK is essential for lymphotoxin-β- but not TNF-R-induced NF-κB activation (Matsushima *et al.*, 2001; Yin *et al.*, 2001). Furthermore, it is suggested that NIK functions at a nuclear rather than a cytoplasmic step in the lymphotoxin-β-induced NF-κB activation pathway (Yin *et al.*, 2001). Since a kinase inactive mutant of NIK can block NF-κB activation by various stimuli, such as TNF, IL1, and LPS, this suggests that NIK may be involved in a broad range of NF-κB activation pathways.

Previously, it has been shown that epidermal growth factor (EGF) can activate NF-κB through undefined pathways (Obata *et al.*, 1996; Sun and Carpenter, 1998; Biswas *et al.*, 2000; Habib *et al.*, 2001). EGF family members interact with receptors belonging to the EGF receptor family, including epidermal growth factor receptor (EGFR), epidermal growth factor receptor family protein (ErbB)2, ErbB3, and ErbB4 (Pawson, 1995). The cytoplasmic domains of the EGF receptor family members, except for ErbB2, have intrinsic tyrosine kinase activity. Ligand stimulation leads to homo- or heterodimerization of the EGF receptor family members and their autophosphorylation. This process creates docking sites for downstream signaling molecules that contain the SH2 domain (Pawson, 1995). Interaction of these signaling molecules with the receptors initiates intracellular signaling cascades that lead to activation of a number of transcription factors such as AP-1 and STATS (Hill and Treisman, 1995). Previous studies also suggest that EGF can activate NF-κB in several types of cells, including smooth muscle, A431, fibroblasts, and EGF receptor-overexpressing

breast cancer cells (Obata *et al.*, 1996; Sun and Carpenter, 1998; Biswas *et al.*, 2000; Habib *et al.*, 2001).

The growth factor receptor bound (Grb)7 family members are some of the adapter molecules that interact with activated receptor tyrosine kinases, including the EGF receptor family members. The Grb7 family consists of Grb7, Grb10, and Grb14, which do not have intrinsic enzymatic activity and signal through their interaction with downstream proteins (Daly, 1998; Han *et al.*, 2001). Unlike Grb2, which contains an SH2 domain flanked by two SH3 domains, the Grb7 family members contain an N-terminal proline-rich (PR) region, a central GM region that is homologous with the *C. elegans* protein Mig10, and a C-terminal SH2 domain (Daly, 1998; Han *et al.*, 2001). The SH2 domain of the Grb7 family is responsible for interaction with the majority of identified Grb7-interacting proteins, such as the EGF receptor family members, Shc, Raf, Tek/Tie2, and FAK, among others (Han *et al.*, 2001). It has been shown that the PR domain of Grb7 family members interacts with c-Abl and Tankyrase (Frantz *et al.*, 1997; Han *et al.*, 2001; Lyons *et al.*, 2001). Proteins that interact with the large central GM domain of the Grb7 family members are not known.

In addition to their roles in EGF receptor signaling, the Grb7 family members play divergent roles in various signaling pathways and pathophysiological processes. Grb7 is overexpressed in some human primary cancers and tumor cell lines, suggesting a possible role in tumorigenesis (Stein *et al.*, 1994). Various studies have also suggested a role for Grb7 in the regulation of cell migration (Tanaka *et al.*, 1998; Han and Guan, 1999; Han *et al.*, 2000; Lee *et al.*, 2000; Vaysssiere *et al.*, 2000). Grb10 has been found to be associated with mitochondria, where it interacts with Raf1 and is likely to be involved in the regulation of apoptosis (Nantel *et al.*, 1998, 1999). It was also reported that Grb10 is recruited to the c-Kit receptor in the course of SCF-mediated activation of c-Kit and forms a complex with Akt (Jahn *et al.*, 2002). Grb14 was recently shown to be a specific inhibitor of insulin receptor catalytic activity (Berezia *et al.*, 2002).

To unambiguously identify the signaling pathways that NIK participates in, we searched NIK-associated proteins by screening antibody arrays. This effort identified ErbB4 and Grb7 as two proteins that are associated with NIK. Our findings suggest that NIK is a component of the EGF/heregulin receptor signaling complexes and involved in NF-κB activation by these receptors.

Results

Identification of NIK-associated proteins by screening of antibody arrays

To search for potential NIK-associated proteins, we used the Signal Transduction Antibody ArrayTM system (Hypromatrix, Inc.). Each Antibody ArrayTM membrane contains 400 antibodies against well-studied proteins. The antibodies are immobilized on a nitrocellulose membrane, each at a predetermined position, and they retain their capabilities of recognizing and capturing antigens as well as antigen-associated proteins. We transfected 293 cells with an expression plasmid for Flag-NIK and the cell lysate was used to incubate with the antibody array membrane. Using anti-Flag antibody, we detected that 21 antibodies could recruit Flag-NIK, probably directly or indirectly through their antigens. These include antibodies against NBK, Mad-1, p38, CD3-ε, eNOS, HSP-70, ANT, DAXX, SODD, thyroid receptor α1, Sp1, ErbB4, TNF-R1, B7-1, DMBT1, GATA-1, IRF2, TRADD, BOK, caspase-2, and Grb7. Results for part of the membrane are shown in Figure 1. Previously, it was shown that Grb7 is associated with EGF receptor family members, including EGFR, ErbB2, ErbB3, and ErbB4 (Margolis *et al.*, 1992; Stein *et al.*, 1994; Janes *et al.*, 1997; Daly, 1998; Fiddes *et al.*, 1998; Han *et al.*, 2001). Thus, recruitment of NIK to two independent antibodies against ErbB4 and Grb7, respectively, suggests a high possibility that NIK is a true component of the ErbB4/Grb7 signaling complex.

NIK interacts with Grb7, Grb10, and Grb14, but not Grb2

To determine whether NIK interacts with Grb7, we transfected 293 cells with expression plasmids for HA-tagged NIK and Flag-tagged Grb7 and performed immunoprecipitation experiments. These experiments suggest that NIK interacts with Grb7 in 293 cells (Figure 2). The Grb7 adapter family contains three members, including Grb7, Grb10, and Grb14 (Daly, 1998; Han *et al.*, 2001). Coimmunoprecipitation experiments indicate that NIK also interacts with Grb10 and Grb14 (Figure 2). These interactions are specific because Grb2, an adapter protein not belonging to the Grb7 family, does not interact with NIK under the same condition (Figure 2).

Domain mapping of interaction between Grb7 and NIK

It has been shown that the SH2 domain of Grb7 family members is responsible for interaction with most

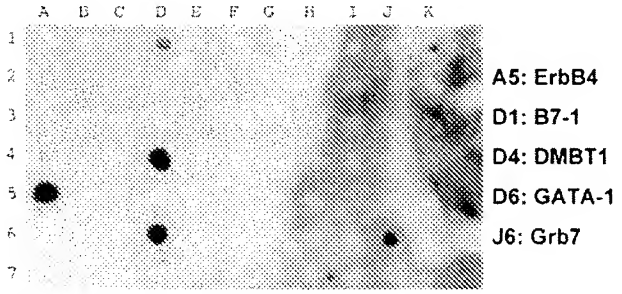

Figure 1 Identification of NIK-associated proteins by screening of antibody arrays. The antibody array membranes were incubated with cell lysate containing Flag-NIK, probed with anti-Flag antibody, and then detected by ECL. The positive signals correspond to: ErbB4 (A5), B7-1 (D1), DMBT1 (D4), GATA-1 (D6), Grb7 (J6)

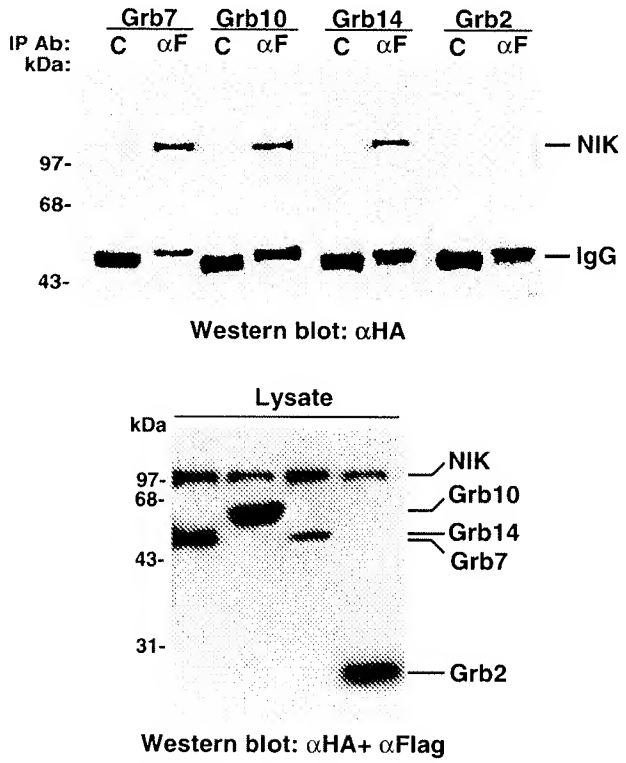

Figure 2 NIK interacts with Grb7, Grb10, and Grb14, but not Grb2. 293 cells ($\sim 5 \times 10^6$) were transfected with 10 μg of an expression plasmid for HA-tagged NIK, together with 10 μg of an expression plasmid for Flag-tagged Grb7, Grb10, Grb14, or Grb2. Coimmunoprecipitation was performed with anti-Flag antibody (αF) or control IgG (C), and Western blot analysis was performed with anti-HA antibody (upper panel). Expression levels of NIK, Grb7, Grb10, Grb14, and Grb2 were confirmed by Western blot analysis of the lysates with anti-Flag and anti-HA antibodies (lower panel)

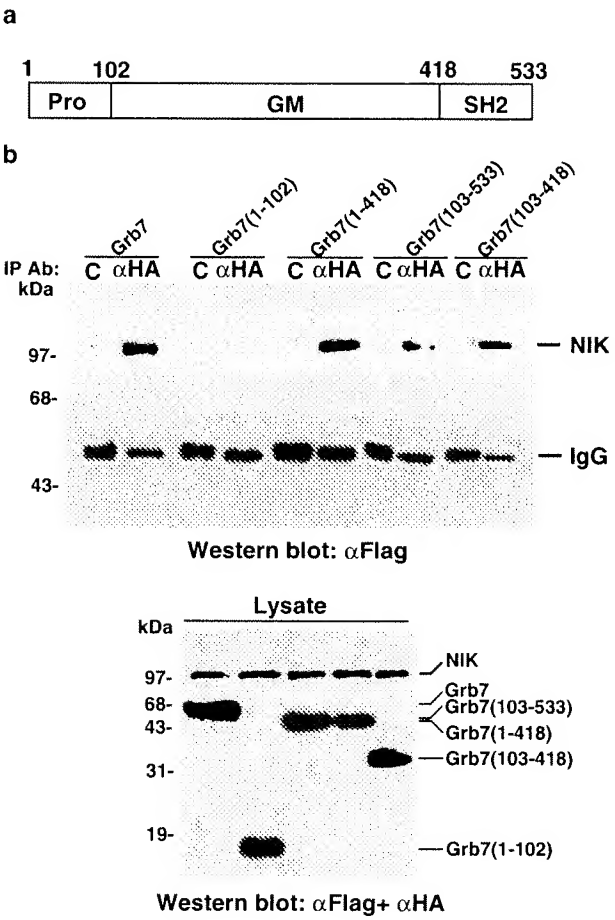

Figure 3 Domain mapping of Grb7 interaction with NIK. (**a**) Schematic presentation of Grb7 deletion mutants. (**b**) Coimmunoprecipitations between Grb7 mutants and NIK. 293 cells ($\sim 5 \times 10^6$) were transfected with 10 μg of an expression plasmid for Flag-tagged NIK, together with 10 μg of an expression plasmid for HA-tagged Grb7 or its various mutants. Coimmunoprecipitation was performed with anti-HA antibody (αHA) or control IgG (C), and Western blot analysis was performed with anti-Flag antibody (upper panel). Expression levels of NIK, Grb7, and its mutants were confirmed by Western blot analysis of the lysates with anti-Flag and anti-HA antibodies (lower panel)

identified binding partners (Daly, 1998; Han *et al.*, 2001). To determine which domain of Grb7 interacts with NIK, we constructed a series of HA epitope-tagged deletion mutants of Grb7, including Grb7(1–102) (the PR domain), Grb7(1–418) (the PR and GM domains), Grb7(103–533) (the GM and SH2 domains), and Grb7(103–418) (the GM domain). We cotransfected these deletion mutants with Flag-tagged NIK into 293 cells and performed coimmunoprecipitation experiments. These experiments suggest that the central GM domain of Grb7, aa103–418, is sufficient for its interaction with NIK (Figure 3).

NIK is recruited to EGF/heregulin receptor signaling complexes

To determine whether NIK is recruited to EGF/heregulin receptor signaling complexes, we transfected 293 cells with expression plasmids for HA-tagged Grb7 and NIK, together with Flag-tagged ErbBs, and performed coimmunoprecipitation experiments. The results suggest that Grb7 and NIK can be simultaneously recruited to all EGF/heregulin receptors, including EGFR, ErbB2, ErbB3, and ErbB4 (Figure 4a). We also found that EGFR/ErbB2 could form a complex with Grb7, Grb10, Grb14, and NIK, respectively (Figure 4b).

We next determined whether NIK is associated with Grb7 and the EGF receptors in untransfected cells. Previously, it was shown that Grb7 is coamplified, overexpressed, and in a tight complex with ErbB2 (Stein *et al.*, 1994; Akiyama *et al.*, 1997; Tanaka *et al.*, 1997). Therefore, we have used a breast cancer cell line, MCF7, for endogenous coimmunoprecipitation experiments. The results suggest that NIK is constitutively associated with Grb7 and the EGFR/ErbB2 complex (Figure 4b). It is possible that the EGFR/ErbB2 complex is constitutive active in MCF7 cells and thus results in a constitutive recruitment of NIK to the complex.

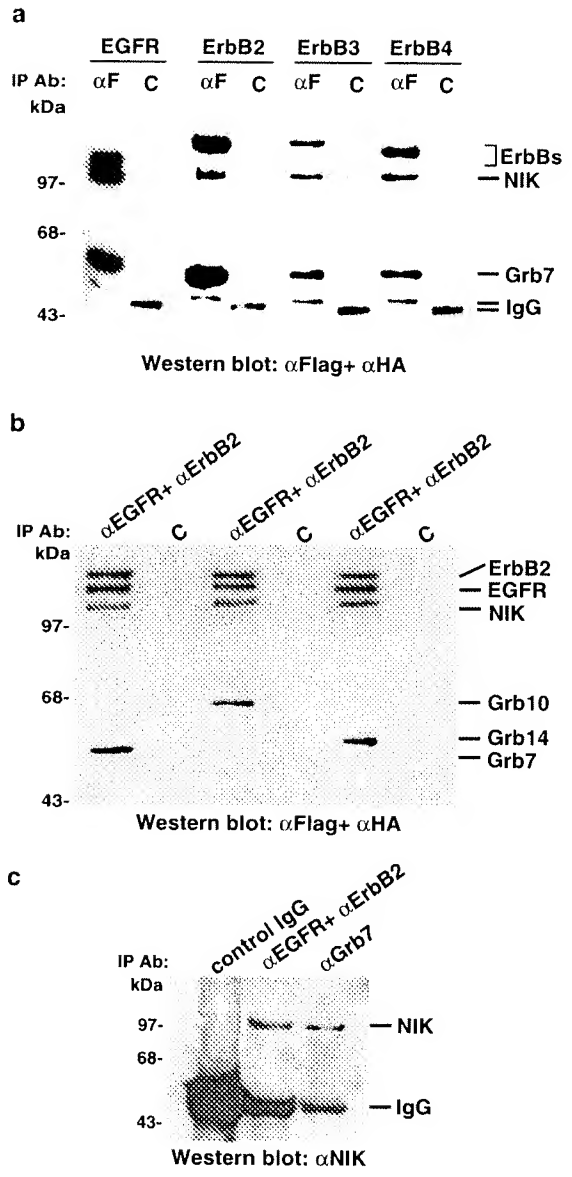

Figure 4 NIK is recruited to EGF/heregulin receptor signaling complexes. (**a**) NIK and Grb7 are associated with ErbBs. 293 cells ($\sim 5 \times 10^6$) were transfected with an expression plasmid for Flag-tagged EGFR, ErbB2, ErbB3, or ErbB4 (10 μg), together with expression plasmids for HA-tagged Grb7 and NIK (each 10 μg). Coimmunoprecipitation was performed with anti-Flag antibody (αF) or control IgG (C), and Western blot analysis was performed with anti-HA and anti-Flag antibodies. (**b**) NIK and Grb7, Grb10, or Grb14 are recruited to EGFR/ErbB2 complex. 293 cells ($\sim 5 \times 10^6$) were transfected with expression plasmids for Flag-tagged EGFR and ErbB2 (each 10 μg), together with expression plasmids for HA-tagged NIK and Flag-tagged Grb7, Grb10, or Grb14 (each 10 μg). Coimmunoprecipitation was performed with anti-EGFR and anti-ErbB2 antibodies (αEGFR + αErbB2) or control IgG (C), and Western blot was performed with anti-HA and anti-Flag antibody mixture. (**c**) NIK is associated with Grb7 and EGF receptors in untransfected cells. MCF7 cells ($\sim 2 \times 10^7$) were lysed and the lysate was immunoprecipitated with a mixture of rabbit anti-EGFR (1 μg) + anti-ErbB2 (1 μg) antibodies, rabbit anti-Grb7 antibody (2 μg), or rabbit control IgG (2 μg). Western blot analysis was performed with rabbit anti-NIK antibody

Grb7 collaborates with NIK to activate NF-κB

It has been shown that NIK is involved in NF-κB activation (Malinin *et al*., 1997; Lin *et al*., 1998a, b; Yin *et al*., 2001). To determine whether Grb7 has a similar function, we performed NF-κB luciferase reporter gene assays. These experiments indicated that overexpression of Grb7 could weakly activate NF-κB in a dose-dependent manner (Figure 5a). In addition, Grb7 could collaborate with NIK to activate NF-κB (Figure 5a). To exclude the possibility that Grb7 affects NIK expression but not NIK signaling, we examined NIK levels in all transfections by Western blot analysis. As shown in Figure 5a, NIK levels were not significantly changed with the increased expression of Grb7.

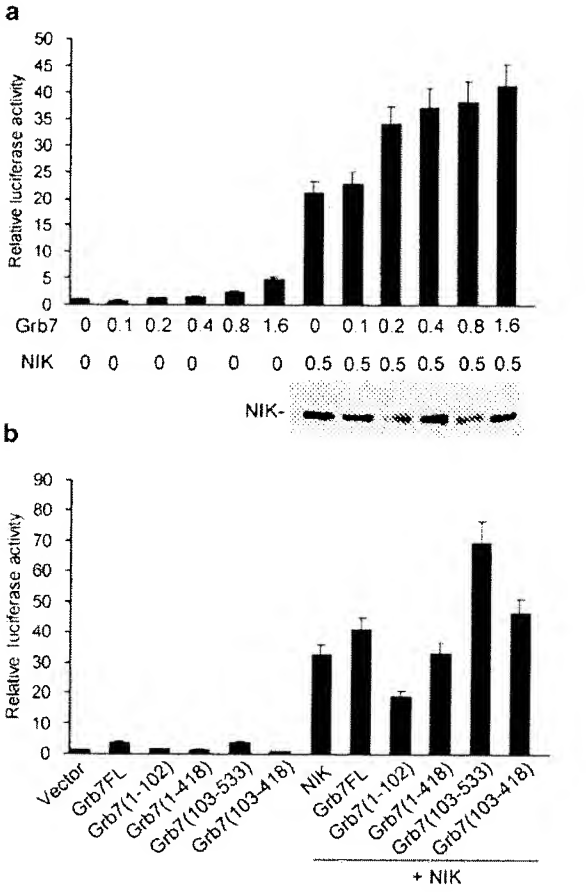

Figure 5 Interaction of Grb7 with NIK in NF-κB activation. (**a**) Grb7 collaborates with NIK to activate NF-κB. 293 cells ($\sim 1 \times 10^5$) were transfected with 0.2 kg of NF-κB-luciferase reporter plasmid, 0.2 μg of pRL-TK *Renilla* luciferase reporter plasmid, and the indicated amounts (μg) of expression plasmids. At 16 h after transfection, luciferase activities were measured and normalized based on *Renilla* luciferase levels. The levels of NIK expression in the transfected cells are shown under the graph. (**b**) Effects of Grb7 mutants on NIK-induced NF-κB activation. 293 cells ($\sim 1 \times 10^5$) were transfected with reporter plasmids and the indicated expression plasmids, and luciferase assays were performed as above. Data shown are averages and standard deviations of relative luciferase activities from three independent experiments (transfection was performed in triplicate in each experiment)

We also determined the effects of different Grb7 domains on NIK-induced NF-κB activation. These experiments suggest that the N-terminal PR domain (aa1–102) can inhibit NIK-induced NF-κB activation, while the central GM domain is sufficient for collaboration with NIK to activate NF-κB (Figure 5b). Moreover, the SH2 domain of Grb7 can enhance its collaborative ability in NIK-induced NF-κB activation (Figure 5b).

NIK is involved in NF-κB activation mediated by EGF/heregulin receptors

To determine the role of Grb7 in the NF-κB activation pathways mediated by ErbBs, we performed NF-κB luciferase reporter gene assays. The results indicated that overexpression of ErbB2/ErbB4 could activate NF-κB and this was enhanced by EGF stimulation (Figure 6a). In these assays, NIK could collaborate

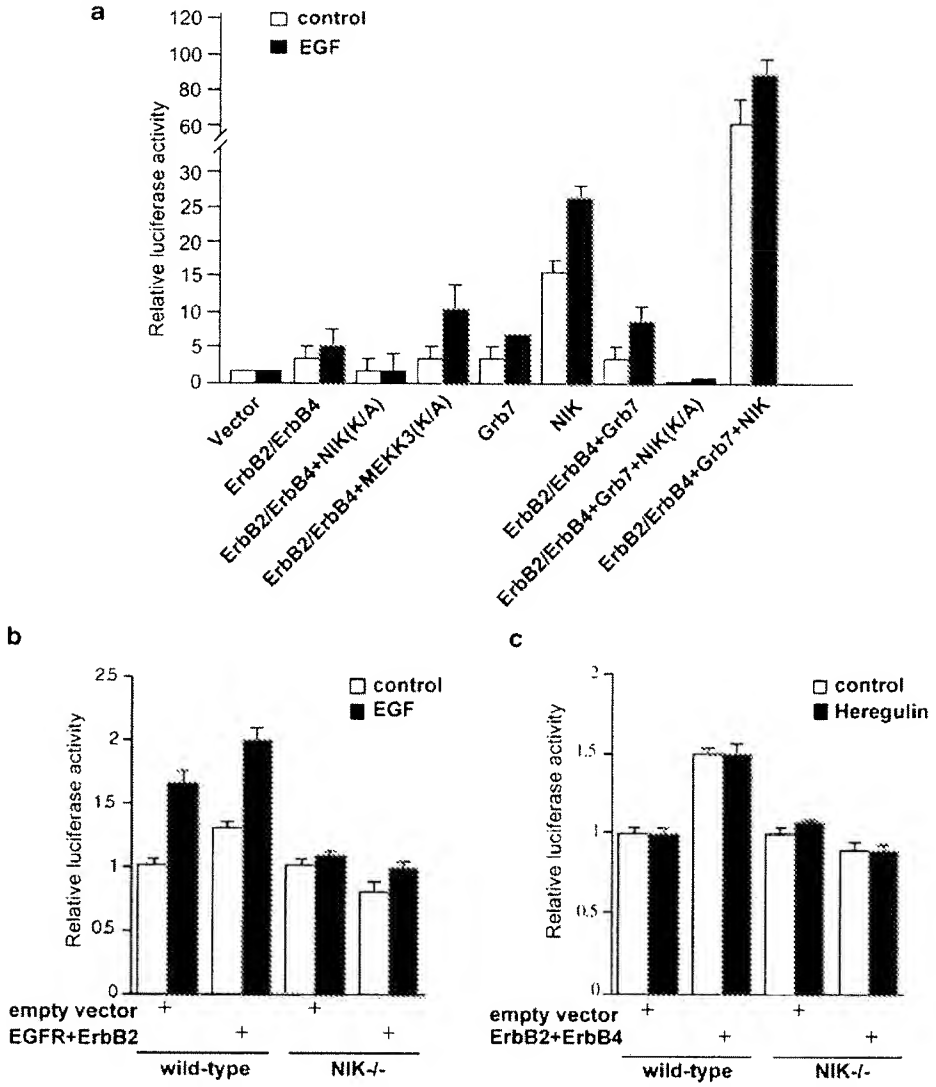

Figure 6 NIK is required for NF-κB activation mediated by EGF/heregulin receptors. (**a**) Effects of NIK and its kinase inactive mutant on ErbB2/ErbB4- and Grb7-mediated NF-κB activation. 293 cells (~1 × 10^5) were transfacted with 0.3 μg of NF-κB-luciferase reporter plasmid, 0.3 μg of RSV-β-galactosidase plasmid, and the indicated expression plasmids (each 1 μg). At 16 h after transfection, luciferase activities were measured and normalized based on β-galactosidase levels. Data shown are averages and standard deviations of relative luciferase activities from one representative experiment in which each transfection was performed in triplicate. (**b**) EGFR/ErbB2-mediated NF-κB activation in wild-type and NIK−/− embryonic fibroblasts. Wild-type or NIK−/− embryonic fibroblasts (~1 × 10^5) were transfected with expression plasmids for EGFR (1 μg) and ErbB2 (1 μg) or empty control plasmid (2 μg), together with NF-κB-luciferase (0.5 μg) and RSV-β-galactosidase reporter plasmids. At 8 h after transfection, cells were treated with EGF (10 ng/ml) or left untreated for 6 h. Reporter gene assays were performed as in (**a**). (**c**) ErbB2/ErbB4-mediated NF-κB activation in wild-type and NIK−/− embryonic fibroblasts. Wild-type or NIK−/− embryonic fibroblasts (~1 × 10^5) were transfected with expression plasmids for ErbB2 (1 μg) and ErbB4 (1 μg) or empty control plasmid (2 μg), together with NF-κB-luciferase (0.5 μg) and RSV-β-galactosidase reporter plasmids. At 8 h after transfection, cells were treated with heregulin (10 ng/ml) or left untreated for 6 h. Reporter gene assays were performed as in (**a**)

with ErbB2/ErbB4 and Grb7 to activate NF-κB. On the other hand, a kinase inactive mutant of NIK, but not that of MEKK3, inhibited ErbB2/ErbB4-mediated NF-κB activation (Figure 6a).

To determine whether NIK is involved in EGF/heregulin receptor-induced NF-κB activation under physiological conditions, we examined whether EGF/heregulin receptors can activate NF-κB in NIK-deficient embryonic fibroblasts by reporter gene assays. As shown in Figure 6b, c, we found that EGF/heregulin receptors could activate NF-κB in wild-type, but not NIK-deficient cells. Taken together, these data suggest that NIK is a component of EGF/heregulin receptor-mediated NF-κB activation pathways.

Discussion

NIK is a serine/threonine protein kinase that has been implicated in NF-κB activation pathways. In this study, we found that NIK interacts with Grb7 family members and is a component of the EGF/heregulin receptor-mediated NF-κB activation pathways. Our studies support previous reports that EGF/heregulin can activate the transcriptional factor NF-κB (Obata *et al*., 1996; Sun and Carpenter, 1998; Biswas *et al*., 2000; Habib *et al*., 2001) and further provide a mechanistic explanation for this observation.

Grb7 was initially identified as an EGF receptor binding protein (Margolis *et al*., 1992); thereafter many other binding partners have been reported for Grb7. These include HER2/Shc, SHPTP2, PDGFR, ErbB2, ErbB3, ErbB4, c-Kit, FAK, Tek/Tie2, c-Kit/SCFR, Rnd1, IR, and caveolin (Han *et al*., 2001). Most of these binding partners are upstream regulators of Grb7 family proteins. Little is known about potential downstream effectors of the Grb7 family proteins. Previous studies have shown that the PR domain of Grb10 interacts with c-Abl *in vitro* (Frantz *et al*., 1997). It has also been suggested that the PR domain of Grb14 interacts with Tankyrase in the mammalian overexpression system and this interaction is involved in vesicle trafficking (Lyons *et al*., 2001). However, it is unknown whether these proteins are associated with the Grb7 family members in untransfected cells.

In this study, we identified NIK as a protein interacting with the GM domain of Grb7. NIK also interacts with Grb10 and Grb14, two other members of the Grb7 family. As far as we know, NIK is the first protein that has been shown to interact with the large central GM domain of the Grb7 family members. Endogenous coimmunoprecipitation experiments have suggested that NIK is associated with Grb7 and is a component of the EGF receptor signaling complex. A kinase inactive mutant of NIK, but not that of MEKK3, inhibits Grb7 and ErbB2/ErbB4-mediated NF-κB activation. Moreover, experiments with NIK-deficient embryonic fibroblasts indicate that NIK is required for EGF/heregulin receptor-mediated NF-κB activation. Therefore, we propose that NIK is a downstream effecter of EGF/heregulin receptor-mediated NF-κB activation pathways.

Previously, it has been shown that the Grb7 family members are phosphorylated on serine and threonine residues (Stein *et al*., 1994; Ooi *et al*., 1995; Daly *et al*., 1996; Dong *et al*., 1997; Reilly *et al*., 2000). The phosphorylation is either constitutive or can be induced by stimulation with growth factors, such as EGF, heregulin, and PDGF. Since NIK is a serine/threonine protein kinase, it would be interesting to examine whether NIK is responsible for the serine/threonine phosphorylation of the Grb7 family members. It is also possible that NIK functions as a kinase for other downstream signaling proteins, for example, c-Abl and Tankyrase, two proteins that are associated with the PR domain of the Grb7 family members.

Grb7 has been shown to be amplified and overexpressed in concert with ErbB2 in several breast cancer cell lines and other cancer cell types (Margolis *et al*., 1992; Akiyama *et al*., 1997; Tanaka *et al*., 1997). It has also been shown recently that EGF-induced NF-κB activation was a major pathway of cell-cycle progression in estrogen-receptor negative breast cancer cells (Biswas *et al*., 2000). In addition, human tumor cell lines resistant to TNF express high levels of EGFR, ErbB2, or ErbB3 (Hoffmann *et al*., 1998). Since NF-κB activation can prevent cells from apoptosis induced by divergent stimuli (Van Antwerp *et al*., 1996; Beg and Baltimore, 1996; Liu *et al*., 1996; Wang *et al*., 1998), it is possible that NF-κB activation is involved in cell proliferation and malignancy triggered by overexpression of EGF receptor family members. The identification of NIK as a component of EGF/heregulin receptor-mediated NF-κB activation pathways may therefore provide a molecular target for drug development against cancers caused by overexpression of EGF/heregulin receptor family members.

Materials and methods

Reagents

Recombinant EGF and heregulin (R&D Systems), monoclonal antibodies against FLAG and the HA (Sigma) epitopes, rabbit polyclonal antibodies against EGFR, ErbB2, Grb7 and NIK (Santa Cruz Biotechnology), and 293 cells (ATCC) were purchased from the indicated resources. Wild-type and NIK-deficient mouse embryonic fibroblasts (Dr Robert Schreiber, Washington University at St Louis), and MCF7 cells (Dr Gary Johnson, University of Colorado Health Sciences Center) were provided by the indicated investigators.

Constructs

NF-κB luciferase reporter construct (Dr Gary Johnson, University of Colorado Health Sciences Center), mammalian expression plasmids for Flag-NIK (Dr David Goeddel, Tularik Inc.), EGFR, ErbB2-4 (Dr Gibbes Johnson, Center for Biologics Evaluation and Research) were provided by the indicated investigators. Mammalian expression plasmids for HA-NIK, HA- or FLAG-tagged Grb2, Grb10, Grb14, Grb7 and its deletion mutants were constructed by PCR amplifica-

tion of the corresponding cDNA fragments and subsequently cloning into a CMV promoter-based vector containing a 5′ or 3′ HA or FLAG tag.

Antibody array screening

The antibody arrays that contain 400 antibodies were purchased from Hypromatrix, Inc. To screen for NIK-associated proteins, 293 cells (5×10^6) were transfected with 10 μg of expression plasmid for Flag-NIK. At 24 h after transfection, cells were lysed in 1 ml of Triton Extraction Solution (15 mM Tris, pH 7.5, 120 mM NaCl, 1% Triton, 25 mM KCl, 2 mM EGTA, 2 mM EDTA, 0.1 mM DTT, 0.5% Triton X-100, 10 μg/ml leupeptin, 0.5 mM phenylmethylsulfonyl fluoride). The cell lysate was collected and applied to preblocked Antibody ArrayTM membranes for 2 h. The membranes were then washed with TBS-T buffer (150 mM NaCl, 25 mM Tris, 0.05% Tween-20, pH 7.5) and incubated with HRP-conjugated anti-Flag antibody for 2 h at room temperature. The membranes were washed again and the signals were detected by ECL.

Cell transfection and reporter gene assays

293 cells (1×10^5) were seeded in 12-well dishes and transfected the following day by the standard calcium phosphate precipitation (Sambrook *et al*., 1989). Mouse embryonic fibroblasts (1×10^5) were seeded in 12-well dishes and transfected the following day with Lipofectamine 2000 reagent (Invitrogen) by following procedures suggested by the manufacturer. Within the same experiment, each transfection was performed in triplicate and, where necessary, empty control plasmid was added to ensure that each transfection receives the same amount of total DNA. To normalize for transfection efficiency, 0.1 μg of pRL-TK *Renilla* luciferase or RSV-β-galactosidase reporter plasmid was added to each transfection. Luciferase and β-galactosidase assays were performed as previously described (Chen *et al*., 2002). Luciferase activities were normalized on the basis of *Renilla* luciferase or β-galactosidase expression levels.

Coimmunoprecipitation and Western blot analysis

For transient transfection and coimmunoprecipitation experiments, transfected 293 cells from each 100-mm dish were lysed in 1 ml of lysis buffer (15 mM Tris, 120 mM NaCl, 1% Triton, 25 mM KCl, 2 mM EGTA, 2 mM EDTA, 0.1 mM DTT, 0.5% Triton X-100, 10 μg/ml leupeptin, 0.5 mM phenylmethylsulfonyl fluoride, pH 7.5). For each immunoprecipitation, a 0.4-ml aliquot of lysate was incubated with 0.5 μg of the indicated monoclonal antibody or control mouse IgG and 25 μl of 1 : 1 slurry of GammaBind A Plus-Sepharose (Amersham Pharmacia) for at least 2 h. The sepharose beads were washed three times with 1 ml of lysis buffer. The precipitates were fractionated on SDS–PAGE and subsequent Western blot analysis was performed as described (Chen *et al*., 2002).

For endogenous coimmunoprecipitation, MCF cells ($\sim 6 \times 10^7$) were lysed in 3 ml of lysis buffer. A 1 ml aliquot of lysate was incubated with a mixture of rabbit anti-EGFR (1 μg) and anti-ErbB2 (1 μg) antibodies, a rabbit anti-Grb7 antibody (2 μg), or control rabbit IgG (2 μg). The subsequent immunoprecipitation and Western blot (with a rabbit anti-NIK antibody) experiments were performed as described above.

All immunoprecipitation experiments were performed at least two times and similar results were obtained.

Abbreviations

NIK, nuclear factor κB-inducing kinase; Grb, growth factor receptor bound; EGFR, epidermal growth factor receptor; ErbB, epidermal growth factor receptor family protein; EGF, epidermal growth factor; TRADD, tumor necrosis factor associated death domain protein; RIP, receptor interacting protein; TNF, tumor necrosis factor; NF-κB, nuclear factor kappaB; STAT, signal transducers and activators of transcription.

Acknowledgements

We thank Xiaoyan Li for technical resistance, Dr Robert Schreiber for NIK-/- EF cells, and members of the Shu laboratories for discussion. This work was supported in part by the National Natural Science Foundation of China (39925016 and 30100097), the Chinese High-Technology program (2001AA221281), the Special Funds for Major State Basic Research of China (G19990539), the Ellison Medical Foundation, and the NIH (R01 AI49992-01).

References

Akiyama N, Sasaki H, Ishizuka T, Kishi T, Sakamoto H, Onda M, Hirai H, Yazaki Y, Sugimura T and Terada M. (1997). *Cancer Res.*, **57**, 3548–3553.

Antwerp DJ, Martin SJ, Kafri T, Green DR and Verma IM. (1996). *Science*, **274**, 787–789.

Beg AA and Baltimore D. (1996). *Science*, **274**, 782–784.

Berezia V, Kasus-Jacobi A, Perdereau D, Cariou B, Girard J and Burnol AF. (2002). *J. Biol. Chem.*, **277**, 4845–4852.

Biswas DK, Cruz AP, Gansberger E and Pardee AB. (2000). *Proc. Natl. Acad. Sci. USA*, **97**, 8542–8547.

Chen D, Li X, Zhai Z and Shu HB. (2002). *J. Biol. Chem.*, **277**, 15985–15991.

Daly RJ. (1998). *Cell. Signal.*, **10**, 613–618.

Daly RJ, Sanderson GM, Janes PW and Sutherland RL. (1996). *J. Biol. Chem.*, **271**, 12502–12510.

Dong LQ, Du H, Porter SG, Kolakowski Jr LF, Lee AV, Mandarino LJ, Fan J, Yee D, Liu F and Mandarino J. (1997). *J. Biol. Chem.*, **272**, 29104–29112.

Fiddes RJ, Campbell DH, Janes PW, Sivertsen SP, Sasaki H, Wallasch C and Daly RJ. (1998). *J. Biol. Chem.*, **273**, 7717–7724.

Frantz JD, Giorgetti-Peraldi S, Ottinger EA and Shoelson SE. (1997). *J. Biol. Chem.*, **272**, 2659–2667.

Habib AA, Chatterjee S, Park SK, Ratan RR, Lefebvre S and Vartanian T. (2001). *J. Biol. Chem.*, **276**, 8865–8874.

Han DC and Guan JL. (1999). *J. Biol. Chem.*, **274**, 24425–24430.

Han DC, Shen TL and Guan JL. (2000). *J. Biol. Chem.*, **275**, 28911–28917.

Han DC, Shen TL and Guan JL. (2001). *Oncogene*, **20**, 6315–6321.

Hill CS and Treisman K. (1995). *Cell*, **80**, 199–211.

Hoffmann M, Schmidt M and Wels W. (1998). *Cancer Immunol. Immunother.*, **47**, 167–175.

Jahn T, Seipel P, Urschel S, Peschel C and Duyster J. (2002). *Mol. Cell. Biol.*, **22**, 979–991.

Janes PW, Lackmann M, Church WB, Sanderson GM, Sutherland RL and Daly RJ. (1997). *J. Biol. Chem.*, **274**, 30896–30905.

Lee H, Volonte D, Galbiati F, Lyengar P, Lublin DM, Bregman DB, Milson MT, Campos-Gonzalez R, Bouzahzah B, Pestell RG, Scherer PE and Lisanti MP. (2000). *Mol. Endocrinol.*, **14**, 1750–1755.

Lin L, Cao Z and Goeddel DV. (1998a). *Proc. Natl. Acad. Sci. USA*, **95**, 3792–3379.

Lin X, Mu Y, Cunningham ET, Marcu KB, Geleziunas R and Greene WC. (1998b). *Mol. Cell. Biol.*, **18**, 5899–5907.

Liu Z, Hsu H, Goeddel DV and Karin M. (1996). *Cell*, **87**, 565–576.

Lyons RJ, Deane R, Lynch DK, Ye ZS, Sanderson GM, Eyre HJ, Sutherland GR and Daly RJ. (2001). *J. Biol. Chem.*, **276**, 17172–17180.

Malinin NL, Boldin MP, Kovalenko AV and Wallach D. (1997). *Nature*, **385**, 540–544.

Margolis B, Silvennoinen O, Comoglio F, Roonprapunt C, Skolnik E, Ullrich A and Schlessinger J. (1992). *Proc. Natl. Acad. Sci. USA*, **89**, 8894–8898.

Matsushima A, Kaisho T, Rennert PD, Nakano H, Kurosawa K, Uchida D, Takeda K, Akira S and Matsumoto M. (2001). *J. Exp. Med.*, **193**, 631–636.

Nantel A, Huber M and Thomas DY. (1999). *J. Biol. Chem.*, **274**, 35719–35724.

Nantel A, Mohammad-Ali K, Sherk J, Posner BI and Thomas DY. (1998). *J. Biol. Chem.*, **273**, 10475–10484.

Obata H, Biro S, Arima N, Kaieda T, Eto H, Miyata M and Tanaka H. (1996). *Biochem. Biophys. Res. Commun.*, **224**, 27–32.

Ooi J, Yajnik V, Immanuel D, Gordon M, Moskow JJ, Buchberg AM and Margolis B. (1995). *Oncogene*, **10**, 1621–1630.

Pawson T. (1995). *Nature*, **373**, 573–580.

Reilly JF, Mickey G and Maher PA. (2000). *J. Biol. Chem.*, **275**, 7771–7778.

Sambrook J, Fritch EF and Maniatis T. (1989). *Molecular Cloning: A Laboratory Manual*. 2nd edn. Cold Spring Harbor Laboratory Press: Cold Spring Harbor, NY.

Stein D, Wu J, Fuqua S, Roonprapunt C, Yajnik V, D'Eustachio P, Moskow J, Buchberg A, Osborne C and Margolis B. (1994). *EMBO J.*, **13**, 1331–1340.

Sun L and Carpenter G. (1998). *Oncogene*, **16**, 2095–2102.

Tanaka S, Mori M, Akiyoshi T, Tanaka Y, Mafune K, Wands J and Sugimachi K. (1997). *Cancer Res.*, **57**, 28–31.

Tanaka S, Mori M, Akiyoshi T, Tanaka Y, Mafune KI, Wants JR and Sugimachi K. (1998). *J. Clin. Invest.*, **102**, 821–827.

Vaysssiere B, Zalcman G, Mache Y, Mirey G, Ligensa T, Weidner KM, Chardin P and Camonis J. (2000). *FEBS Lett.*, **467**, 91–96.

Wang CY, Mayo MW, Korneluk RG, Goeddel DV and Baldwin Jr AS. (1998). *Science*, **281**, 1680–1683.

Yin L, Wu L, Wesche H, Arthur CD, White JM, Goeddel DV and Schreiber RD. (2001). *Science*, **291**, 2162–2165.

EXHIBIT F

Cell Research (2007) 17:520-530.

www.nature.com/cr

ORIGINAL ARTICLE

Hsp90 regulates processing of NF-κB2 p100 involving protection of NF-κB-inducing kinase (NIK) from autophagy-mediated degradation

Guoliang Qing[1], Pengrong Yan[1], Zhaoxia Qu[1], Hudan Liu[1], Gutian Xiao[1]

[1]*Department of Cell Biology and Neuroscience, Rutgers, The State University of New Jersey, Piscataway, NJ 08854, USA*

NF-κB-inducing kinase (NIK) is required for NF-κB activation based on the processing of NF-κB2 p100. Here we report a novel mechanism of NIK regulation involving the chaperone 90 kDa heat shock protein (Hsp90) and autophagy. Functional inhibition of Hsp90 by the anti-tumor agent geldanamycin (GA) efficiently disrupts its interaction with NIK, resulting in NIK degradation and subsequent blockage of p100 processing. Surprisingly, GA-induced NIK degradation is mediated by autophagy, but largely independent of the ubiquitin-proteasome system. Hsp90 seems to be specifically involved in the folding/stabilization of NIK protein, because GA inhibition does not affect NIK mRNA transcription and translation. Furthermore, Hsp90 is not required for NIK-mediated recruitment of the α subunit of IκB kinase to p100, a key step in induction of p100 processing. These findings define an alternative mechanism for Hsp90 client degradation and identify a novel function of autophagy in NF-κB regulation. These findings also suggest a new therapeutic strategy for diseases associated with p100 processing.

Keywords: autophagy, geldanamycin, Hsp90; NF-κB2, NIK, proteasome-independent degradation

Cell Research (2007) **17**:520-530. doi: 10.1038/cr.2007.47; published online 12 June 2007

Introduction

The non-canonical NF-κB pathway, based on processing of the *nf-kb2* gene product p100 to generate p52, plays an important role in the function and development of the secondary lymphoid tissues, as well as in autoimmune disease progression and tumorigenesis [1-3]. Whereas the precursor protein p100 serves as a potent inhibitor of NF-κB, the processed product p52 is an important functional member of NF-κB [4]. Thus, the functions of p100 processing are two-fold: one is to relieve p100-mediated inhibition and liberate specific NF-κB dimers, and the other is to generate functional p52 NF-κB.

Correspondence: Gutian Xiao
Tel: +1-732-445-2839; Fax: +1-732-445-5870
E-mail: xiao@biology.rutgers.edu
Received 26 April 2007; revised 28 April 2007; accepted 29 April 2007; published online 12 June 2007

Abbreviations: 5-aminoimidazole-4-carboxamide 1-b-D-ribofuranoside (AICAR); B-cell activating factor (BAFF); CD40 ligand (CD40L); geldanamycin (GA); 90 kDa heat shock protein (Hsp90); IκB kinase (IKK); α subunit of IκB kinase (IKKα); lymphotoxin beta (LTβ); NF-κB-inducing kinase (NIK); tumor necrosis factor receptor-associated factor 3 (TRAF3)

The processing of p100 is a tightly regulated event. Induction of this process strictly depends on NF-κB-inducing kinase (NIK) and its downstream kinase IKKα (α subunit of IκB kinase, also named IKK1) [5, 6], and is mediated only by a limited number of stimuli, such as lymphotoxin beta (LTβ), B-cell activating factor (BAFF) and CD40 ligand (CD40L) [2, 6-10]. One important function of these stimuli is to prevent basally translated NIK protein from undergoing degradation mediated by the tumor necrosis factor receptor-associated factor 3 (TRAF3) [11-13]. Stabilized NIK in turn specifically activates and recruits IKKα into the p100 complex via serines 866 and 870 of p100 [14]. After recruitment into the p100 complex, activated IKKα phosphorylates serines 99, 108, 115, 123 and 872 of p100 [14]. The phosphorylation of these specific serines results in ubiquitination and subsequent processing of p100 mediated by the β-TrCP ubiquitin ligase and 26S proteasome, respectively [6, 15, 16].

By controlling the stability of various signaling regulatory proteins, the proteasome regulates various signaling pathways in addition to p100 processing. For example, almost all the known clients of the molecular chaperone

Hsp90 (90 kDa heat-shock protein), including many important kinases and transcription factors, are found to be degraded by the proteasome when Hsp90 is inactivated by its specific inhibitor geldanamycin (GA), an anti-tumor drug [17-19]. On the other hand, the role of macroautophagy (simply referred to as autophagy hereafter) in the regulation of Hsp90 clients and specific signaling pathways remains largely unknown, although this mode of lysosome-dependent degradation is well-known to be the primary mechanism other than the proteasome employed for protein degradation within eukaryotes [19]. Additionally, whether Hsp90 is involved in p100 processing has not been determined yet.

Here, we find that NIK is a novel client of Hsp90, which interacts with Hsp90 through its C-terminal regulatory domain. GA inhibition of Hsp90 disrupts NIK/Hsp90 interaction and leads to NIK degradation and inhibition of p100 processing. Notably, the GA-induced NIK degradation is independent of both ubiquitination and proteasome but is mediated by autophagy. However, Hsp90 is not required for the transcription/translation of NIK mRNA. Furthermore, Hsp90 is not required for NIK-mediated IKKα recruitment into the p100 complex either. Thus, Hsp90 regulates p100 processing indirectly via controlling stability of NIK protein. These findings establish a link among autophagy, Hsp90 and non-canonical NF-κB signaling for the first time, and also suggest a therapeutic strategy for diseases associated with p100 processing.

Materials and Methods

Expression vectors and reagents

Expression vectors encoding p100 and NIK have been described previously [6, 20]. The anti-NIK (H248), anti-Hsp90 (F-8) and anti-p53 (FL-393) antibodies were from Santa Cruz Biotechnology, Inc. The antibody used for detecting mouse NIK protein (#4994) was from Cell Signaling Tech. The anti-actin (AAN01) and anti-HA (12CA5) antibodies were from Cytoskeleton Inc. and Roche Molecular Biochemicals, respectively. The antibody recognizing the N-terminus of p100 (anti-p100N) was described previously [16]. The monoclonal antibodies for human CD40 and Myc were prepared from hybridomas G28-5 and 9E10, respectively [12]. 5-aminoimidazole-4-carboxamide 1-b-D-ribofuranoside (AICAR) and MG132 were from Biomol and Calbiochem, respectively [21].

Cell culture and transfection

Human B-cell line Ramos RG69, mouse M12.4.1 B cell stably infected with pCLXSN-NIK-HA, mouse fibroblasts ts20, Atg5 knockout mouse embryonic fibroblasts (MEFs) and TRAF3 knockout MEFs were gifts from Drs L Covey, SC Sun, HL Ozer, N Mizushima and G Cheng, respectively. Human kidney 293 cells were described previously [22]. 293, ts20 and MEF cells were cultured in Dulbecco's modified Eagle's medium supplemented with 10% fetal bovine serum and 2 mM L-glutamine. Ramos RG69 and M12.4.1 cells were cultured in RPMI supplemented with 10% fetal bovine serum, 2 mM L-glutamine and 10 mM 2-mercaptoethanol [11, 12]. ts20 cells were usually maintained at 35 °C instead of 37 °C. To inactivate E1 in the ts20 cells, the culture temperature was shifted to 39 °C. 293, ts20 and MEF cells were transfected with DEAE-Dextran and LipofectAMINE 2000 (Invitrogen), respectively [23].

Immunoblotting and immunoprecipitation

Whole-cell lysates were prepared by lysing the cells in radioimmuoprecipitation assay buffer (RIPA buffer) (50 mM Tris-HCl pH 7.4, 150 mM NaCl, 1 mM EDTA, 0.25% Na-deoxycholate, 1% NP-40, 1 mM dithiothreitol, 1 mM phenylmethylsulfonyl fluoride (PMSF). For immunoblotting (IB) assays, the whole-cell lysates (~30 μg) were fractionated by SDS-PAGE, transferred to nitrocellulose membranes and subjected to IB using the indicated antibodies. To detect MG132-induced recovery of Akt from GA-mediated degradation, the whole-cell lysates were made by the RIPA buffer containing 1% SDS [24]. For immunoprecipitation (IP) assays, the whole-cell lysates (~1 000 μg) were diluted to 1 ml using RIPA buffer, incubated for 30 min at 4 °C in the presence or absence of GA, followed by incubating with the indicated antibodies for 1 h and with 30 μl protein-A-agarose for another 2 h at 4 °C. The agarose beads were washed three times with RIPA buffer, and the bound proteins were eluted by 2×SDS loading buffer and subjected to SDS-PAGE and IB analysis [25].

Polysome and RNA isolation

Ramos RG69 cells were treated for 2 h with anti-CD40 antibody (10 μg/ml) or GA (2 μM) or left untreated. Twenty percent of treated or untreated cells (2×10^7 cells/each group) were pelleted and employed as a source for total RNA using Trizol reagent (Invitrogen). The remaining cells were incubated with cycloheximide (100 μg/ml) for 15 min, followed by cytoplasm extraction. The cytoplasmic extract was then loaded onto a linear 10-45% (w/w) sucrose gradient and centrifuged for 2 h 30 min at 36 000 r.p.m. with a Beckman SW-41 rotor. After centrifugation, the gradient was fractionated and its absorbance at 254 nm was determined continuously by an Isco UA-5 monitor as described before [12, 21]. The polysome-containing fractions were pooled and subjected to phenol extraction. RNA was precipitated with ethanol and dissolved in DEPC-treated water.

Real-time reverse transcription -PCR analysis

Two micrograms of total RNA or RNA isolated from polysomes were reverse-transcribed for real-time reverse transcription (RT)-PCR using the following primers:

NIK, forward 5'-CCCACCTTTTCAGAAGCATT, reverse 5'-CATTTTGCCCTCTGTAGCATGG;
p100, forward 5'-TGCCATTGTGTTCCGGACA, reverse 5'-TGTTTGGAATCAGACACGTCCC;
GAPDH, forward 5'-GCAAATTCCATGGCACCGT, reverse 5'-TCGCCCCACTTGATTTTGG.

Real-time PCR assays were performed with an ABI Prism 7900HT sequence detection system using the SYBR Green PCR Core Reagent (Applied Biosystems, Foster City, CA, USA) [12, 21].

Results

Hsp90 is required for both NIK protein stabilization and p100 processing

Since GA, a specific inhibitor of Hsp90, has been used for tumor treatment in phase II clinical trials [18, 26], we investigated whether GA inhibition of Hsp90 blocks p100 processing, a signaling pathway that has recently been linked to tumorigenesis [2, 3]. As shown in Figure 1A, addition of GA efficiently prevented p100 processing induced by non-canonical NF-κB inducing stimuli (BAFF or anti-CD40 antibody) at a concentration as low as 2 μM. Moreover, GA inhibition of Hsp90 also suppressed p100 processing induced by overexpression of NIK, a kinase downstream of ligation of these receptors, in a dose-dependent manner (Figure 1B). Interestingly, GA inhibition of p100 processing was associated with decreased levels of NIK protein (Figure 1B, lower panel). This result is consistent with the molecular chaperone function of Hsp90 in protein folding and stabilization [17], suggesting that Hsp90 regulates p100 processing possibly by stabilizing the NIK protein.

NIK is a novel bona fide client of Hsp90

The results shown above also suggested that NIK is a

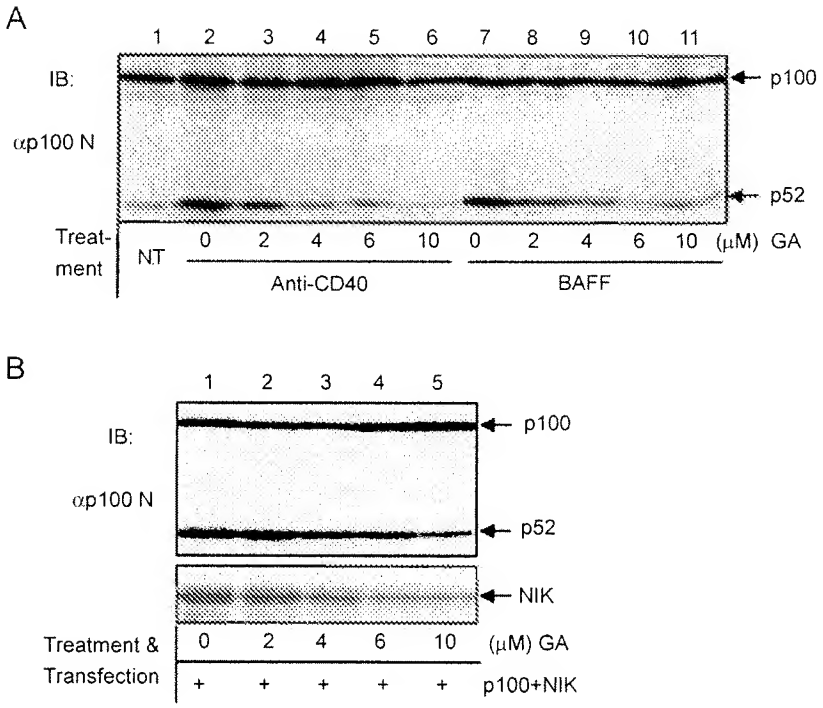

Figure 1 GA inhibition of Hsp90 efficiently prevents p100 processing, which is correlated with decreased levels of NIK protein. **(A)** GA inhibition of p100 processing triggered by receptor ligation. Ramos B cells were treated with BAFF (0.25 μg/ml) or anti-CD40 (10 μg/ml) in the presence of increased amounts of GA for 10 h, followed by IB assays using anti-p100N antibody. Equal amounts of proteins (30 μg) were loaded for each lane. **(B)** GA inhibition of p100 processing induced by overexpression of NIK. 293 cells were transfected with p100 and NIK. Twenty-four hours after transfection, the cells were incubated with the indicated amount of GA for 20 h, followed by IB assays using anti-p100N antibody (upper panel) or anti-NIK antibody (lower panel).

previously unidentified client of Hsp90. To test this possibility, we examined whether NIK forms a complex with Hsp90 by performing co-IP (co-IP) assays. As expected, NIK stably bound to Hsp90 (Figure 2A, lane 2). We also examined whether GA disrupts the NIK/Hsp90 interaction. To do so, we added GA into the cell lysate immediately

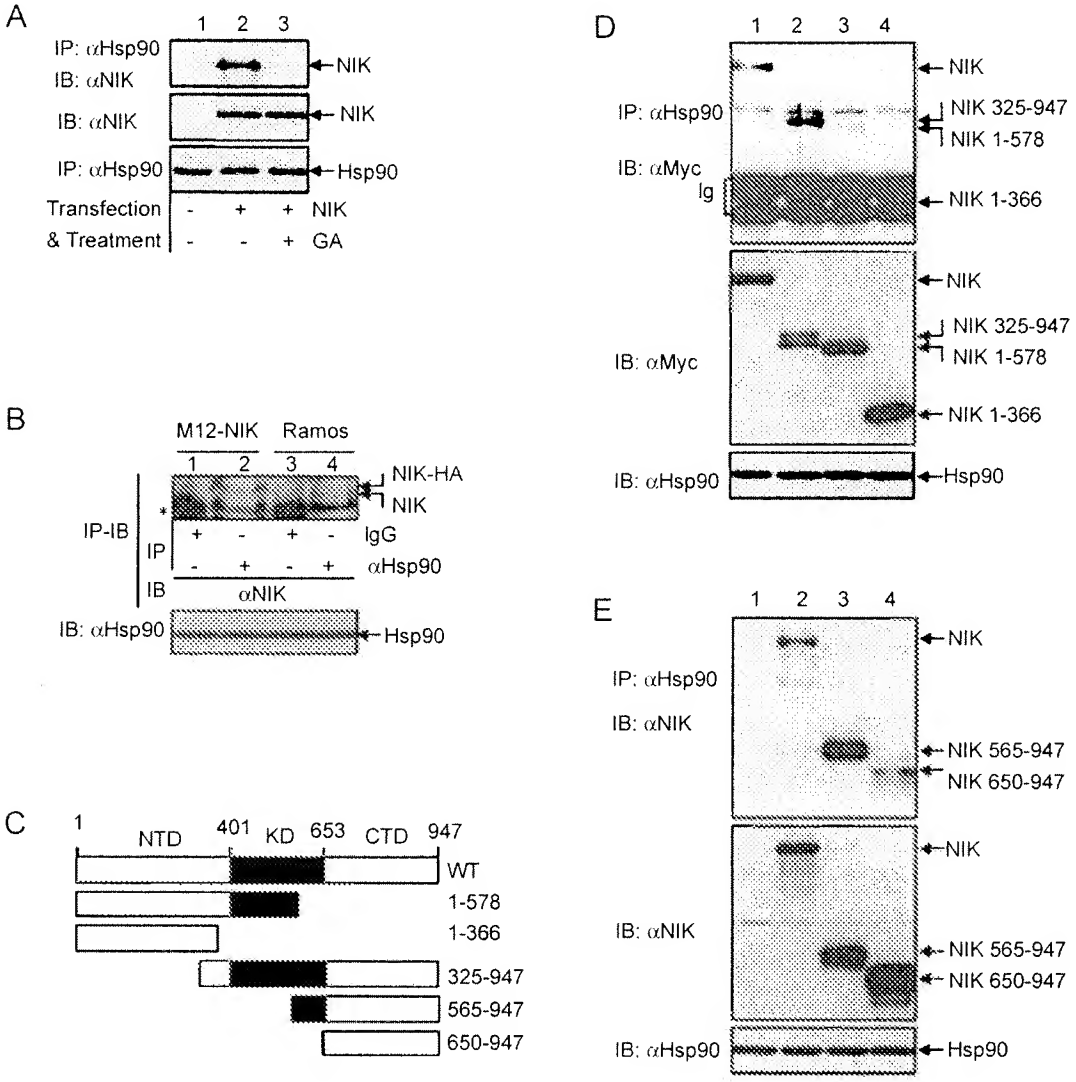

Figure 2 NIK physically interacts with Hsp90, which is sensitive to GA. **(A)** GA inhibition of NIK/Hsp90 interaction. Cell lysates from 293 cells transfected with NIK were immunoprecipitated with anti-Hsp90 antibody in the presence or absence of 10 μM GA, followed by IB using anti-NIK antibody (top panel). Some of the cell lysates were directly subjected to IB for the expression levels of NIK (middle panel) and Hsp90 (bottom panel). **(B)** Interaction between endogenous NIK and Hsp90. Cell lysates from M12.4.1 B cells stably infected with pCLXSN-NIK-HA (labeled as M12-NIK) and CD40L-treated Ramos cells (labeled as Ramos) were immunoprecipitated with anti-Hsp90 antibody (lanes 2 and 4) or control IgG (lanes 1 and 3), followed by IB using anti-NIK antibody (upper panel). Some of the cell lysates were directly subjected to IB for the expression level of Hsp90 (lower panel). The non-specific band was indicated as asterisk (*). Note the CD40L treatment is to prevent NIK from the proteasomal degradation largely mediated by TRAF3 (see Figure 7C for details). **(C)** Schematic picture of NIK and its mutants, showing the N-terminal domain (NTD), the kinase domain (KD), and the C-terminal domain (CTD). **(D and E)** Mapping of domains within NIK responsible for binding to Hsp90. 293 cells were transfected with the indicated NIK mutants, followed by IP using anti-Hsp90 antibody and IB using anti-Myc antibody **(D)** or anti-NIK C-terminal antibody **(E)** to detect the co-immunoprecipitated NIK and NIK mutants (top panel). The expression levels of Hsp90, NIK or NIK mutants were also detected by IB (lower panels). The multiple bands detected for NIK mutants were due to constitutive phosphorylation at their C-terminal region (20).

before co-IP assay, because GA efficiently triggers NIK protein degradation *in vivo* (Figure 1B). Importantly, GA efficiently blocked the interaction between NIK and Hsp90 (Figure 2A, lane 3). To confirm the NIK/Hsp90 interaction under more physiological conditions, we repeated the co-IP assays using NIK protein from mouse B cells stably expressing a low level of HA-tagged NIK or using endogenous NIK protein from human B cells [11, 12]. Consistently, both stably expressed and endogenous NIK form a complex with endogenous Hsp90 (Figure 2B, lanes 2 and 4, respectively). Taken together, these results clearly indicated that NIK is a novel client of Hsp90.

To identify the region within NIK protein responsible for the interaction with Hsp90, we repeated the co-IP assay using various NIK C- or N-terminal deletion mutants (Figure 2C). Deletion of 368 amino acids from the C-terminal end of NIK largely prevented its interaction with Hsp90 (Figure 2D, lane 3). Further deletion from this end completely disrupted the interaction between NIK and Hsp90 (Figure 2D, lane 4). In contrast, deletion of up to 324 amino acids from the N-terminal end of NIK had no effect on the NIK/Hsp90 interaction (Figure 2D, lane 2). These results suggested that the C-terminal regulatory domain (CTD) of NIK is required for its interaction with Hsp90, while the N-terminal regulatory domain and the middle kinase domain are largely dispensable for this association. In further support, the CTD alone was sufficient to bind to Hsp90 (Figure 2E, lane 4). Thus, the C-terminal regulatory domain of NIK is involved in its association with Hsp90.

NIK degradation induced by GA is independent of the ubiquitination and proteasome system

Since it has been reported so far that GA-induced degradation of Hsp90 clients is mediated by the ubiquitin-proteasome pathway [17-19], we first investigated the role of ubiquitination in GA-mediated degradation of NIK. To achieve this goal, we utilized the temperature-sensitive (ts) mutant cell line (ts20) expressing a heat-labile ubiquitin-activating enzyme (E1) and thus defective in the ubiquitin pathway upon heat shock [27]. Surprisingly, heat shock failed to prevent GA-induced NIK degradation in these mutant cells (Figure 3A, lane 4). This was not due to inefficient inactivation of E1 by heat shock, because it completely blocked p53 degradation (lane 6). It is worth to note that the heat-shock condition we used did not cause NIK dissociation from Hsp90 (Figure 3B), suggesting NIK was not denatured under this condition. These results demonstrated that the ubiquitin system is not required for GA-induced NIK degradation.

These results also suggested that NIK degradation by GA might be independent of the proteasome, although the proteasome can mediate either ubiquitin-dependent or

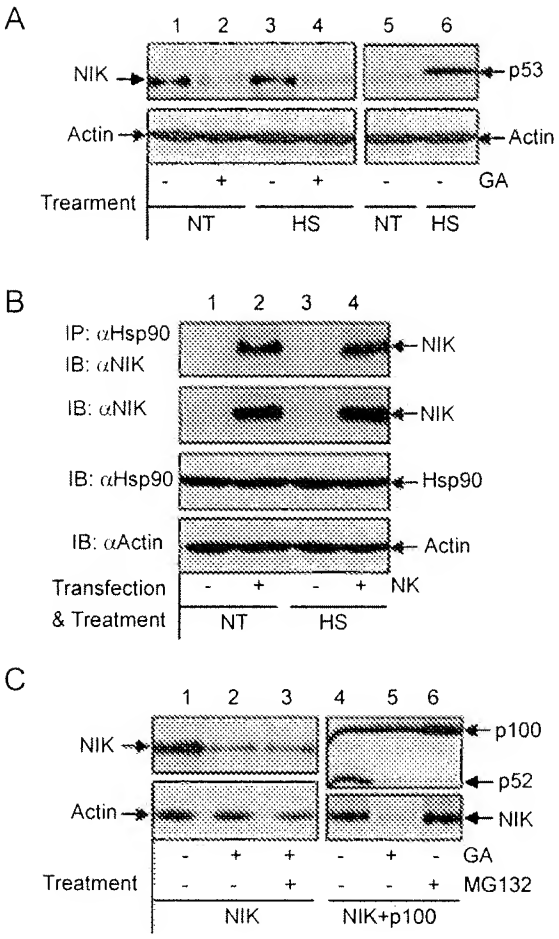

Figure 3 GA-induced NIK degradation does not involve the ubiquitin-proteasome system. **(A)** Ubiquitination system is dispensable for GA-induced NIK degradation. NIK or mock transfected ts20 cells were incubated at 35 °C (labeled as NT) or 39 °C (labeled as HS) in the presence of 10 μM GA (+) or DMSO (−) for 20 h, followed by IB using NIK antibody (lanes 1-4) or anti-p53 antibody (lanes 5-6). **(B)** Heat shock fails to block the NIK/Hsp90 interaction. Cell lysates from normal or heat shocked cells transfected with NIK-expressing or empty vector were immunoprecipitated with anti-Hsp90 antibody, followed by IB using anti-NIK antibody (top panel). Some of the cell lysates were directly subjected to IB for the expression levels of NIK (middle panel) and Hsp90 (bottom panel). **(C)** The proteasome is dispensable for GA-induced NIK degradation. 293 cells transfected with NIK alone (lanes 1-3) or both NIK and p100 (lanes 4-6) were incubated with 10 μM GA (+) or DMSO (−) in the presence or absence of 25 μM MG132 for 20 h, followed by IB using the indicated antibodies.

-independent proteolysis [28]. To address this important issue, we inhibited the proteolytic activity of the proteasome using MG132, a specific inhibitor of the proteasome. Consistent with the essential role of the proteasome in p100

processing, addition of MG132 efficiently inhibited processing of p100 (Figure 3C, lane 6). However, the addition of MG132 failed to block GA-induced NIK degradation (lane 3). Of note, the mechanisms mediating inhibition of p100 processing by GA and MG132 are different, as evidenced by that NIK expression was suppressed by GA (upper panel, lane 3) while MG132 alone failed to do so (lower panel, lane 6). As a matter of fact, MG132 treatment alone actually increased NIK protein levels (clearer in short exposure, data not shown; also see Figure 7). Collectively, these studies clearly demonstrated that NIK degradation in the absence of Hsp90 function is independent of both ubiquitination and proteasome, further suggesting that an unidentified mechanism is responsible for the degradation of this new Hsp90 client.

GA-mediated NIK degradation is largely mediated by autophagy

To define the novel mechanism by which NIK is degraded in the absence of Hsp90 function, we examined the possible role of autophagy, since autophagy is the other major system responsible for protein degradation in addition to the proteasome [19, 21]. As shown in Figure 4A, AICAR, an inhibitor of autophagy [21, 29], efficiently prevented NIK degradation induced by GA (top panel, lane 3). The role of AICAR is specific, because it failed to protect Akt, a well-known client of Hsp90, from GA-mediated degradation (middle panel, lane 3). Consistent with previous studies showing that Akt degradation induced by GA depends on the proteasome [24], proteasome inhibition by MG132 rescued Akt from GA-induced degradation (middle panel, lane 4). These studies suggested that autophagy may be responsible for the GA-mediated degradation of NIK.

To validate these biochemical studies, we utilized the Atg5-deficient cells. Atg5 is essential for autophagosome formation, and knockout of Atg5 blocks autophagy [30]. Consistent with the results shown above, knockout of Atg5 also significantly inhibited GA-triggered degradation of NIK (Figure 4B, top panel, lane 4). In sharp contrast, Atg5 is not required for GA-induced Akt degradation, because Akt was still degraded in the Atg5 null cells (Figure 4B, middle panel, lane 4). Thus, NIK degradation in the absence of Hsp90 is mediated by autophagy. This evidence also indicated that autophagy may function as an alternative mechanism for Hsp90 client degradation when Hsp90 function is lost.

Hsp90 is not required for NIK transcription or translation

Although our biochemical and genetic data clearly demonstrated that GA treatment induces autophagy-mediated degradation of NIK protein, we also examined any potential effects of GA on NIK mRNA transcription and translation by performing the real-time RT-PCR and polysome fractionation analysis. As a control, the transcription and translation of p100 mRNA was also examined. In agreement with the fact that CD40L can activate canonical NF-kB to induce p100 expression, we found that CD40 antibody treatment dramatically enhanced p100 mRNA transcription and subsequent protein translation (Figure 5, column 4). However, GA treatment hardly influenced NIK mRNA transcription and translation (column 2). Taken together, these studies strongly suggested that Hsp90 regulation of NIK biosynthesis is largely, if not completely, at the protein level.

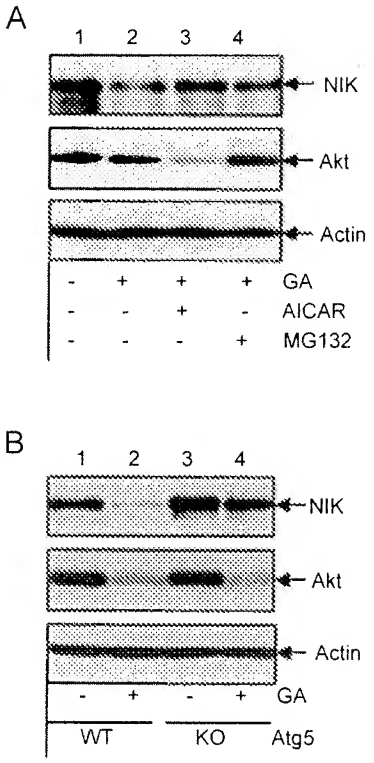

Figure 4 NIK protein degradation induced by GA is largely mediated by autophagy. **(A)** AICAR, an inhibitor of autophagy, blocks GA-induced NIK degradation. 293 cells transfected with NIK or Akt were incubated with 10 μM GA (+) or DMSO (−) in the presence of AICAR (1 mM), or MG132 (25 μM) for 20 h, followed by IB to detect protein levels of NIK (top panel) or Akt (middle panel). The protein level of actin (bottom panel) was detected as a loading control. **(B)** GA-induced degradation of NIK is blocked in Atg5 deficient cells. Atg5 wild type or null cells transfected with NIK or Akt were incubated with 5 μM GA (+) or DMSO (−) for 20 h, followed by IB as described in **(A)**.

Hsp90 is dispensable for NIK-mediated IKKα recruitment to p100

In addition to its function in protein stabilization, Hsp90 may also play other important roles in cell signaling. For example, Hsp90 has been found to be involved in signaling complex assembly [31]. We thus also examined whether Hsp90 is required for the formation of NIK/IKKα/p100 complex, a step serving as a molecular switch for p100 processing [12, 14]. Since NIK nucleates the signaling complex by functioning as an adaptor to bind to both IKKα and p100 [14], we first checked the effect of GA on the NIK/IKKα and NIK/p100 interactions. Although it could efficiently disrupt the interaction between NIK and Hsp90 (Figure 2A), GA had no effect on NIK binding to IKKα or p100 (Figure 6A and 6B, lanes 3). Not surprisingly, NIK recruitment of IKKα to p100 was also resistant to GA treatment (Figure 6C, lane 3).

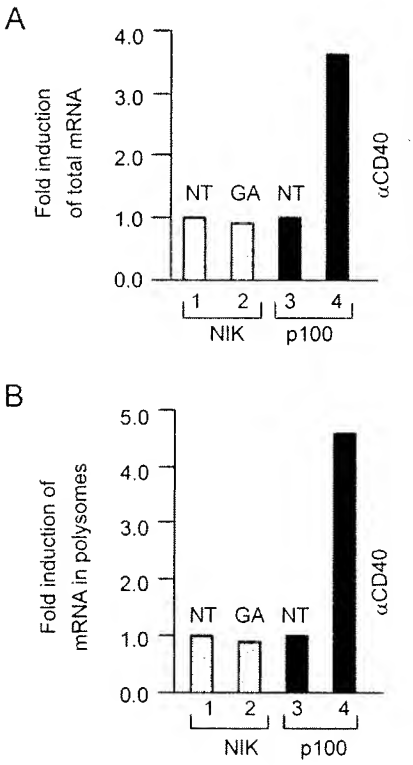

Figure 5 GA treatment does not change the transcription or translation of NIK mRNA. **(A)** GA addition has no obvious effect on NIK RNA transcription. Ramos B cells were either untreated or treated for 10 h with DMSO, GA (2 μM) or anti-CD40 (10 μg/ml), followed by RNA extraction. NIK and p100 mRNAs were quantitated by real-time RT-PCR. The amount of NIK and p100 mRNA was normalized to the level of GAPDH mRNA. The values represented fold change in mRNA abundance relative to the DMSO-treated sample (arbitrarily set as one-fold) and were averages of three independent experiments. **(B)** GA addition has no obvious effect on NIK protein translation. Polysomes were isolated from the Ramos B cells treated as in **(A)**, followed by RNA extraction. The mRNA levels of NIK and p100 in the polysomes were quantitated by real-time RT-PCR as described in **(A)**.

Hsp90-mediated maturation is upstream of TRAF3-mediated proteasomal degradation of NIK protein

In resting cells, NIK protein is usually undetectable (Figure 7A, lane 1), at least partially due to TRAF3-mediated proteasomal degradation [11-13]. Hence, it seems that NIK is regulated by both autophagic and proteasomal degradation. However, the potential link between these two degradation mechanisms is unknown. To address this important issue, we investigated the effect of GA on NIK in both TRAF3 wild type and knockout cells in the presence or absence of MG132. Consistent with previous findings [11-13], MG132 treatment or TRAF3 deficiency could stabilize NIK in the absence of GA (Figure 7A, lane 3 and 7B, lane 1, respectively). However, GA addition could diminish the effect of MG132 treatment or TRAF3 knockout (Figure 7A and 7B, lanes 4 and 2, respectively). Of note, the constitutive processing of p100 caused by TRAF3 deficiency was also blocked by GA (Figure 7B, lane 2). These results suggested that Hsp90-mediated maturation of NIK protein precedes the TRAF3-midated proteasomal degradation.

Discussion

The proteasome and autophagy are two highly conserved mechanisms that are primarily employed for protein degradation within eukaryotes. It is generally believed that autophagy is in principle a non-selective, bulk degradation system of long-lived proteins and organelles through the lysosome; while the proteasome specifically degrades short-lived proteins, including regulatory proteins and misfolded proteins caused by the absence of Hsp90 function. Our recent studies showed that Hsp90 inhibition leads to autophagic but not proteasomal degradation of IKK [21]. The data presented in the current study demonstrate that NIK, a novel client of Hsp90, is also degraded by autophagy when Hsp90 function is inhibited. This study thus provides the second piece of evidence showing that Hsp90 clients may be targeted for degradation by a mechanism different from the proteasome with autophagy serving as the alternative mechanism.

Previous studies have clearly demonstrated that newly synthesized NIK protein is rapidly eliminated by TRAF3-mediated proteasomal degradation [11-13]. It seems that proteins other than TRAF3 may also contribute to the proteasomal degradation of NIK protein, since inhibition

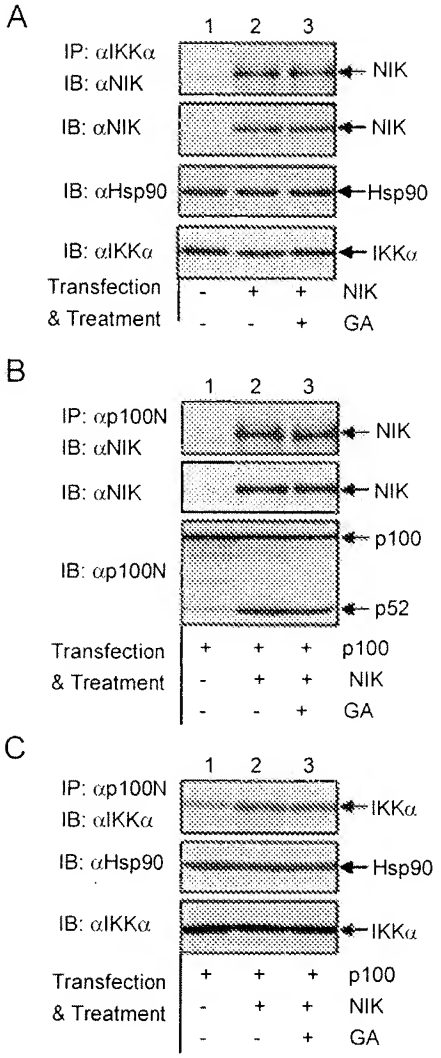

Figure 6 GA disruption of NIK/Hsp90 interaction has no effect on NIK-mediated recruitment of IKKα to p100. **(A)** GA inhibition of Hsp90 does not affect the NIK/IKKα interaction. 293 cells were transfected with an empty vector or the vector expressing NIK, followed by IP using anti-IKKα antibody in the presence or absence of GA (10 μM) and IB using anti-NIK (top panel). Direct IB was also performed to check the expression levels of transfected NIK (2nd panel from the top), endogenous Hsp90 (3rd panel) and IKKα (bottom panel). **(B)** GA inhibition of Hsp90 does not affect the NIK/p100 interaction. 293 cells were transfected with the indicated constructs, followed by IP using anti-p100 antibody in the presence or absence of GA (10 μM) and IB using anti-NIK (top panel). Direct IB was also performed to check the expression levels of NIK (middle panel) and p100 (bottom panel). **(C)** GA inhibition of Hsp90 does not affect NIK-mediated IKKα recruitment to p100. 293 cells were transfected with the indicated constructs, followed by IP using anti-p100N antibody in the presence or absence of GA (10 μM) and IB using anti-IKKα (top panel). The expression levels of Hsp90 (middle panel) and IKKα (bottom panel) were also examined by direct IB. The NIK and p100 expression levels were similar to those shown in **(B)**.

of the proteasome by MG132 could further significantly increase NIK protein levels in TRAF3 knockout cells (Figure 7B). But more importantly, Hsp90-mediated folding and maturation of nascent NIK protein is prior to the TRAF3-mediated proteasomal degradation, or in other words, the NIK protein degraded by the TRAF3-activated proteasome is already maturated (Figure 7). Based on these findings, a model of NIK regulation is presented in Figure 7C. In brief, Hsp90 binds to newly synthesized NIK protein, which promotes the correct folding, maturation and/or conformation maintenance of NIK. When Hsp90 function is absent, such as upon inhibition by GA, the nascent NIK protein cannot be folded correctly and/or the mature NIK protein cannot maintain the correct conformation, resulting in its degradation via the autophagy pathway. In resting cells, however, the mature NIK protein associated with Hsp90 is still rapidly degraded by the proteasome, which is mediated by TRAF3 and possibly also by other proteins such as TRAF2. The non-canonical NF-κB stimuli, such as BAFF, LTβ and CD40L, somehow lead to TRAF3 degradation and/or its dissociation from NIK, thereby protecting NIK from proteasomal degradation. The NIK protein that has escaped from both autophagic and proteasomal degradation then functions as the molecular switch for p100 processing.

Like the proteasomal proteolysis, autophagic degradation has also been linked to the pathogenesis of various disorders, particularly tumorigenesis [19, 32-34]. Current models suggest that autophagy generally contributes to tumor suppression, and defects in autophagy facilitate or even lead to oncogenesis. The responsible mechanisms, however, remain unclear. As over-activation of the non-canonical NF-κB signaling has been found in various tumors [1-3], our study provides one possible explanation for the tumor suppression function of autophagy: by specifically targeting signaling regulatory proteins (such as NIK and IKK) for degradation, autophagy negatively regulates signaling pathways (such as NF-κB pathways) that contribute to tumorigenesis.

Another important aspect of these data is the identification of Hsp90 as an essential component for the non-canonical NF-κB signaling. In addition to IKK regulation [21], another important function of Hsp90 is to regulate NIK, whose expression functions as a molecular switch in p100 processing and ultimate activation of the alternative NF-κB signaling [12, 14]. Although it is not required for NIK mRNA transcription and translation (Figure 5), Hsp90 is necessary for NIK expression and subsequent p100 processing (Figure 1). Thus, the role of Hsp90 in controlling NIK expression is to protect NIK protein from autophagic degradation by facilitating its correct folding and maturation.

Although this is the first demonstration of a link of Hsp90

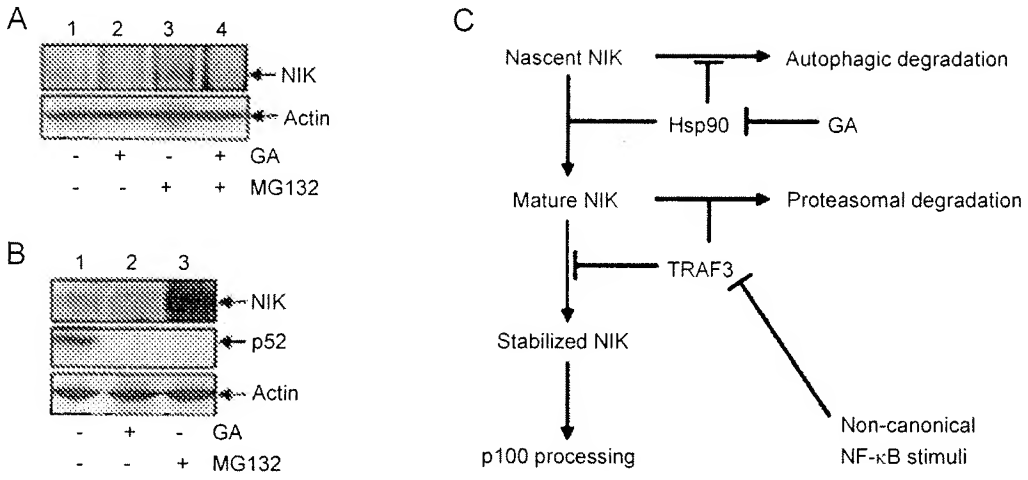

Figure 7 Hsp90 function is required for the increase of NIK protein mediated by the proteasome inhibition or TRAF3 deficiency. **(A)** GA inhibition of Hsp90 prevents the MG132-induced increase of NIK protein. Wild-type MEFs were treated with the indicated drugs for 20 h, followed by IP-IB using anti-NIK antibody (upper panel) for endogenous NIK expression. Some of the cell lysates were directly subjected to IB for the expression level of actin (lower panel). **(B)** GA inhibition of Hsp90 prevents NIK protein increase and p100 processing caused by TRAF3 deficiency. TRAF3 null MEFs were treated with GA (10 μM), MG132 (25 μM), or DMSO for 20 h, followed by IB to detect the expression levels of endogenous NIK (top panel), p52 (middle panel) and actin (bottom panel). **(C)** Dual regulation of NIK by autophagic and proteasomal degradation. In resting cells, newly synthesized NIK proteins bind to Hsp90 for their maturation and/or conformation maintenance, with any free NIK being degraded via autopagy-lysosome pathway due to failure of correct folding and/or conformation maintenance. However, the mature NIK proteins, which are still associated with Hsp90, are rapidly captured by TRAF3 and quickly degraded by the proteasome. In response to the non-canonical NF-κB stimuli, NIK proteins are somehow freed from TRAF3 and therefore being stabilized. The stabilized NIK proteins then induce p100 processing for the activation of the non-canonical NF-κB signaling (see text for details).

to the non-canonical NF-κB signaling, the importance of Hsp90 for activation of the canonical NF-κB pathway has already been suggested [35, 36]. Mechanistic studies showed that RIP and IKK, two important components for NF-κB activation, are Hsp90 clients. Like most Hsp90 clients, RIP is degraded by the proteasome when its interaction with Hsp90 is disrupted by GA [36]. Similarly, GA treatment also leads to IKK degradation. However, the GA-induced IKK degradation is not through the proteasome but rather mediated by autophagy [21], which resembles the NIK degradation induced by GA. Interestingly, disruption of Hsp90/IKK association abolishes the recruitment of IKK to the tumor necrosis factor (TNF) receptor I (TNFR-I) and subsequent activation of IKK induced by TNF, a prototypic stimulator of the canonical NF-κB signaling [31]. Surprisingly, disruption of the Hsp90/NIK interaction does not affect NIK binding to its downstream factors IKKα or p100 and subsequent recruitment of IKKα to p100, essential steps for p100 processing (Figures 2 and 6). Moreover, NIK degradation induced by GA is mediated by autophagy but not by the proteasome (Figures 3 and 4). It therefore seems that different mechanisms are applied by Hsp90 to regulate the canonical and non-canonical NF-κB pathways.

In addition to NF-κB pathways, Hsp90 function is also required for activation of several other signaling pathways that have been linked to tumorigenesis [17]. Due to its significance, Hsp90 is a therapeutic target of tumor treatment. As a matter of fact, Hsp90 has been identified as a specific target of the novel anti-tumor drug GA [18]. Thus, inhibition of the non-canonical NF-κB activation pathway by GA may be a critical component of the anti-tumor activity of this drug, at least for some tumors. Reasonably, GA may be therapeutically effective for those tumors and autoimmune diseases associated with deregulated p100 processing.

Acknowledgments

We thank Genhong Cheng (University of California Los Angeles) for TRAF3 null MEFs, Lori Covey (Rutgers, The State University of New Jersey) for Ramos cells, Noboru Mizushima (Tokyo Medical and Dental University Graduate School and Faculty of Medicine) for Atg5 null MEFs, Harvey L Ozer (University of Medicine and Dentistry of New Jersey) for ts20 cells, Shao-Cong Sun (Pennsylva-

nia State Univerisity School of Medicine) for M12-NIK cells, and Warner C Greene (University of California San Francisco) for p100 construct. We also thank Arnold B Rabson (University of Medicine and Dentistry of New Jersey) for helpful suggestions and critical reading of the manuscript. This study was assisted partially by research grants from the New Jersey Commission on Cancer Research, Fifth District AHEPA Cancer Research Foundation, American Cancer Society RSG-06-066-01-MGO and USA National Institutes of Health/National Cancer Institute R01 CA116616 to G.X.

References

1 Sun SC, Xiao G. Deregulation of NF-κB and its upstream kinases in cancer. Cancer Metastasis Rev 2003; **22**:405-422.
2 Xiao G, Rabson A, Young W, Qing G, Qu Z. Alternative pathways of NF-κB activation: a double-edged sword in health and disease. Cytokine Growth Factor Rev 2006; **17**:281-293.
3 Qing G, Qu Z, Xiao G. Endoproteolytic processing of C-terminally truncated NF-κB2 precursors at κB-containing promoters. Proc Natl Acad Sci USA 2007; **104**:5324-5329.
4 Mercurio F, DiDonato JA, Rosette C, Karin M. p105 and p98 precursor proteins play an active role in NF-κB-mediated signal transduction. Genes Dev 1993; **8**:705-718.
5 Senftleben U, Cao Y, Xiao G, *et al.* Activation by IKKα of a second, evolutionary conserved, NF-κB signaling pathway. Science 2001; **293**:1495-1499.
6 Xiao G, Harhaj EW, Sun SC. NF-κB-inducing kinase regulates the processing of NF-κB2 p100. Mol Cell 2001; **8**:401-409.
7 Claudio E, Brown K, Park S, Wang H, Siebenlist U. BAFF-induced NEMO-independent processing of NF-κB2 in maturing B cells. Nat Immunol 2002; **3**:958-965.
8 Coope HJ, Atkinson PG, Huhse B, *et al.* CD40 regulates the processing of NF-κB2 p100 to p52. EMBO J 2002; **21**:5375-5385.
9 Dejardin E, Droin NM, Delhase M, *et al.* The lymphotoxin-β receptor induces different patterns of gene expression via two NF-κB pathways. Immunity 2002; **17**:525-535.
10 Kayagaki N, Yan M, Seshasayee D, *et al.* BAFF/BLyS receptor 3 binds the B cell survival factor BAFF ligand through a discrete surface loop and promotes processing of NF-κB2. Immunity 2002; **17**:515-524.
11 Liao G, Zhang M, Harhaj EW, Sun SC. Regulation of the NF-κB-inducing kinase by tumor necrosis factor receptor-associated factor 3-induced degradation. J Biol Chem 2004; **279**:26243-26250.
12 Qing G, Qu Z, Xiao G. Stabilization of basally translated NF-κB-inducing kinase (NIK) protein functions as a molecular switch of processing of NF-κB2 p100. J Biol Chem 2005; **280**:40578-40582.
13 He JQ, Zarnegar B, Oganesyan G, *et al.* Rescue of TRAF3-null mice by p100 NF-κB deficiency. J Exp Med 2006; **203**:2413-2418.
14 Xiao G, Fong A, Sun SC. Induction of p100 processing by NF-κB-inducing kinase involves docking IκB kinase alpha (IKKα) to p100 and IKKα-mediated phosphorylation. J Biol Chem 2004; **279**: 30099-30105.
15 Fong A, Sun SC. Genetic evidence for the essential role of β-transducin repeat-containing protein in the inducible processing of NF-κB2/p100. J Biol Chem 2002; **277**:22111-22114.
16 Qu Z, Qing G, Rabson A, Xiao G. Tax deregulation of NF-κB2 p100 processing involves both β-TrCP-dependent and -independent mechanisms. J Biol Chem 2004; **279**:44563-44572.
17 Zhang H, Burrows F. Targeting multiple signal transduction pathways through inhibition of Hsp90. J Mol Med 2004; **82**:488-499.
18 Dai C, Whitesell L. HSP90: a rising star on the horizon of anticancer targets. Future Oncol 2005; **1**:529-540.
19 Xiao G. Autophagy and NF-κB: Fight for fate. Cytokine Growth Factor Rev 2007 May 6; [Epub ahead of print]
20 Xiao G, Sun SC. Negative regulation of the nuclear factor κB-inducing kinase by a cis-acting domain. J Biol Chem 2000; **275**:21081-21085.
21 Qing G, Yan P, Xiao G. Hsp90 inhibition results in autophagy-mediated proteasome-independent degradation of IκB kinase (IKK). Cell Res 2006; **16**:895-901.
22 Xiao G, Sun SC. Activation of IKKα and IKKβ through their fusion with HTLV-I tax protein. Oncogene 2000; **19**:5198-5203.
23 Qing G, Xiao G. Essential role of IκB kinase a in the constitutive processing of NF-κB2 p100. J Biol Chem 2005; **280**:9765-9768.
24 Basso AD, Solit DB, Chiosis G, Giri B, Tsichlis P, Rosen N. Akt forms an intracellular complex with heat shock protein 90 (Hsp90) and Cdc37 and is destabilized by inhibitors of Hsp90 function. J Biol Chem 2002; **277**:39858-39866.
25 Qing G, Qu Z, Xiao G. Regulation of NF-κB2 p100 processing by its cis-acting domain. J Biol Chem 2005; **280**:18-27.
26 Whitesell L, Mimnaugh EG, De Costa B, Myers CE, Neckers LM. Inhibition of heat shock protein HSP90-pp60v-src heteroprotein complex formation by benzoquinone ansamycins: essential role for stress proteins in oncogenic transformation. Proc Natl Acad Sci USA 1994; **91**:8324-8328.
27 Chowdary DR, Dermody JJ, Jha KK, Ozer HL. Accumulation of p53 in a mutant cell line defective in the ubiquitin pathway. Mol Cell Biol 1994; **14**:1997-2003.
28 Orlowski M, Wilk S. Ubiquitin-independent proteolytic functions of the proteasome. Arch Biochem Biophys 2003;**415**:1-5.
29 Samari HR, Seglen PO. Inhibition of hepatocytic autophagy by adenosine, aminoimidazole-4-carboxamide riboside, and *N*6-mercaptopurine riboside. Evidence for involvement of amp-activated protein kinase. J Biol Chem 1998; **273**:23758-23763.
30 Kuma A, Hatano M, Matsui M, *et al.* The role of autophagy during the early neonatal starvation period. Nature 2004; **432**:1032-1036.
31 Chen G, Cao P, Goeddel DV. TNF-induced recruitment and activation of the IKK complex require Cdc37 and Hsp90. Mol Cell 2002; **9**:401-410.
32 Edinger AL, Thompson CB. Defective autophagy leads to cancer. Cancer Cell 2003; **4**:442-424.
33 Kondo Y, Kanzawa T, Sawaya R, Kondo S. The role of autophagy in cancer development and response to therapy. Nat Rev Cancer 2005; **5**:726-734.
34 Levine B, Yuan J. Autophagy in cell death: an innocent convict? J Clin Invest 2005; **115**:2679-2688.
35 Sugita T, Tanaka S, Murakami T, Miyoshi H, Ohnuki T. Immunosuppressive effects of the heat shock protein 90-binding

antibiotic geldanamycin. Biochem Mol Biol Int 1999; **47**:587-595.

36 Lewis J, Devin A, Miller A, *et al*. Disruption of hsp90 function results in degradation of the death domain kinase, receptor-interacting protein (RIP), and blockage of tumor necrosis factor-induced nuclear factor-κB activation. J Biol Chem 2000; **275**:10519-10526.

EXHIBIT G

Proc. Natl. Acad. Sci. USA
Vol. 95, pp. 9067–9069, August 1998

Commentary

JNK or IKK, AP-1 or NF-κB, which are the targets for MEK kinase 1 action?

Michael Karin and Mireille Delhase*

Laboratory of Gene Regulation and Signal Transduction, Department of Pharmacology, University of California, San Diego, 9500 Gilman Drive, La Jolla, CA 92093-0636

MEKK1 (MEK kinase 1) is a mammalian serine/threonine kinase in the mitogen-activated protein kinase (MAPK) kinase kinase (MAPKKK) group (1). Being the first mammalian homolog of STE11, a MAPKKK that activates the pheromone responsive MAPK cascade of budding yeast, MEKK1 as its name indicates was thought to be an activator of the MAPK kinase (MAPKK) MEK1/2 and thus an activator of the ERK MAPK cascade. It therefore was rather surprising that titration experiments (2) or analysis of cells engineered to express MEKK1 from an inducible promoter (3) revealed that it is a far more potent activator of the JNK MAPK cascade. These observations made by using either the catalytic domain of MEKK1 (MEKK1Δ) or a 672-aa C-terminal fragment recently were confirmed by using full-length human MEKK1 (Y. Xia, Z. Wu, B. Su, B. Murray, and M.K., unpublished work). Most importantly, when different mammalian MAPKKs were examined *in vitro* or *in vivo* for phosphorylation and activation by MEKK1, a MAPKK called JNKK1 (MKK4 or SEK1), whose function is JNK (and p38 MAPK) activation (4) was found to be the preferred MEKK1 substrate (Y. Xia, Z. Wu, B. Su, B. Murray, and M.K., unpublished work). Based on specificity constants, MEKK1 phosphorylates JNKK1 45-fold more efficiently than it phosphorylates MEK1/2 (Y. Xia, Z. Wu, B. Su, B. Murray, and M.K., unpublished work), thus providing a clear biochemical explanation for the marked pro-JNK bias of MEKK1. Targets for JNK include transcription factors c-Jun and ATF2, which are components of the AP-1 dimer that are involved in induction of the *c-jun* protooncogene (5). JNK-mediated phosphorylation enhances the transcriptional activity of both c-Jun and ATF2 (6, 7). Correspondingly, MEKK1 expression plasmids are potent activators of a chimeric c-Jun-GAL4 transcription factor, in which the c-Jun activation domain is fused to the GAL4 DNA binding domain (8). Overexpression of a catalytically inactive MEKK1(KM) mutant inhibits JNK activation by either epidermal growth factor (EGF) or tumor necrosis factor (TNF) (refs. 8 and 9 and Y. Xia, Z. Wu, B. Su, B. Murray, and M.K., unpublished work). This mutant was used to show that signals generated by occupancy of TNF type I receptor (TNF-RI) diverge downstream to the signaling proteins TRAF2 and RIP, which are recruited to TNF-RI, such that one pathway leads to JNK (and p38 MAPK) activation followed by stimulation of AP-1 activity and the other mediates NF-κB activation (10, 11) (Fig. 1). These experiments also demonstrated that NF-κB activation protects cells against TNF-induced apoptosis, whereas JNK (and p38) activation does not affect programmed cell death either positively or negatively. Similar results were obtained by analysis of mice and cells deficient in the RelA(p65) subunit of NF-κB (12, 13).

In light of these findings, it was somewhat surprising that under different circumstances overexpression of MEKK1 was found to stimulate NF-κB activity (14, 15). NF-κB is a dimeric transcription factor composed of Rel proteins whose activity is regulated through interaction with specific inhibitors, the IκBs (16–18). In response to cell stimulation the IκBs are rapidly phosphorylated and then undergo ubiquitin-mediated proteolysis, resulting in the release of active NF-κB dimers that translocate to the nucleus. Initially, the demonstration that MEKK1 overexpression leads to NF-κB activation was based solely on the use of an NF-κB transcriptional reporter. As there are ample examples for transcriptional synergy between AP-1 and NF-κB (19, 20), such results should be interpreted with caution. It is expected that a signaling pathway that enhances only AP-1 activity still may stimulate an NF-κB-dependent promoter, even in the absence of overt AP-1 binding sites. Likewise, an AP-1-dependent promoter may respond to NF-κB even in the absence of recognizable NF-κB binding sites. In light of these limitations, a bigger surprise were the results of Lee *et al.* (21) who reported that addition of recombinant MEKK1Δ to a partially enriched fraction of nonstimulated HeLa cells stimulated a protein kinase activity that phosphorylated IκBα at serines (S) 32 and 36, sites that previously were shown to be phosphorylated in response to cell stimulation with TNF or interleukin 1 (IL-1). Phosphorylation at S32 and S36 results in polyubiquitination and degradation of IκBα (22, 23). Homologous phosphoacceptor sites are essential for the induced degradation of other IκB proteins (23). As activation of an IκB kinase by MEKK1Δ was demonstrated by using a rather crude fraction whose polypeptide composition was not described, the identity of this activity remained a mystery. In the meantime, two other groups working independently have succeeded in purifying an inducible IκB kinase activity from extracts of TNF-stimulated HeLa or Jurkat cells (24, 25). Extensive purification of that activity, named IKK, which elutes from gel filtration columns as a large complex with an apparent molecular mass of 700–900 kDa, revealed the presence of two polypeptides with molecular masses of 85 and 87 kDa that precisely coeluted with IκB kinase activity. Microsequencing and molecular cloning revealed that these polypeptides are closely related protein kinases named IKKα (or IKK1) and IKKβ (or IKK2), respectively (24–26). IKKα and IKKβ also were identified through a different approach, based on yeast two-hybrid screens, as proteins that interact with a MAPKKK called NIK (NF-κB-inducing kinase) (27, 28). NIK originally was identified as a TRAF2-interacting kinase whose overexpression results in potent NF-κB activation (29) without any considerable effect on MAPKs, including JNK (30). Therefore the observed interaction between NIK and the IKKs immediately suggested that NIK may be an upstream activator of IKK (Fig. 1). Although the IKK complex is similar in size to the MEKK1Δ-responsive activity, the relationships between the two remained nebulous, and various attempts to stimulate IKK activity with modest amounts of MEKK1Δ expression vector, that are sufficient for JNK activation, have failed (24) (D. Goeddel, personal communication). In addition, several reports indicating that NF-κB transcriptional reporters are not stimulated by low to modest doses of MEKK1 (which are sufficient for JNK activation), while being highly responsive to co-

The companion to this commentary is published on pages 9319–9324.

*To whom reprint requests should be addressed. e-mail: karinoffice@ucsd.edu.

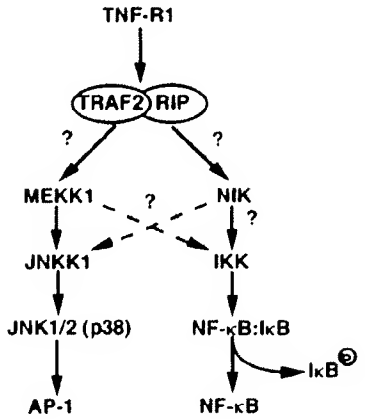

FIG. 1. Signal transduction from TNF receptor type I (TNF-R1) to transcription factors AP-1 and NF-κB. Activation of TNF-RI results in recruitment of several signaling proteins including TRAF2 and RIP. By yet unidentified mechanisms these proteins lead to activation and/or recruitment of MAPKKKs, such as MEKK1 and NIK. MEKK1 is responsible for direct activation of JNKK1, a MAPKK that directly activates JNK1/2 and p38 MAPK, thereby leading to stimulation of transcription factor AP-1. MEKK1 also may be involved in NF-κB activation. NIK or a closely related family member leads to activation of the IKK complex, which leads to phosphorylation of IκBs, thereby triggering their degradation. This results in activation of NF-κB.

transfected NIK, have appeared (30, 31). However, in new work published in this issue of the *Proceedings*, Lee *et al.* (32) present evidence that the MEKK1Δ-responsive activity they previously identified is none other than the cytokine-responsive IKK. Furthermore, they suggest that MEKK1 may be a direct activator of IKKα and IKKβ.

That IKK activity is regulated through phosphorylation of some of its subunits previously was demonstrated by the use of protein phosphatase 2A (PP2A) catalytic subunit, whose incubation with purified IKK resulted in loss of IκB kinase activity (24). Furthermore, coexpression with NIK stimulates the kinase activity of transiently expressed IKKα, which is also efficiently phosphorylated *in vitro* by NIK immunoprecipitates (33). Although no specificity constants were determined, IKKβ appears to be a relatively poor NIK substrate (33). Analysis of the IKKα and IKKβ protein sequences reveals several potential phosphoacceptor sites in a region conserved in all protein kinases, the T (or activation) loop, that resemble those that are used by MAPKKKs to activate MAPKKs (25). Indirect evidence that these sites may be used to activate IKKα and IKKβ was provided by site-directed mutagenesis (25, 33), but so far these sites were not shown to be phosphorylated in TNF or IL-1 stimulated cells or be involved in cytokine-mediated IKK activation. Substitution of S176 in IKKα with alanine was found to decrease its phosphorylation and activation by NIK (33), whereas a dual substitution of S177 and S181 of IKKβ with glutamic acid was reported to increase its catalytic activity (25). The current work (32) shows that recombinant MEKK1Δ can phosphorylate a synthetic peptide corresponding to the T loop of IKKβ and that substitution of S177 and S181 with alanines reduces the extent of ^{32}P incorporation (32). It also is shown that incubation of a partially purified preparation with MEKK1Δ results in phosphorylation of two polypeptides whose sizes match those of IKKα and IKKβ (32). However, as these and similar experiments conducted with NIK have not been performed with fully purified proteins the results fall short of a conclusive demonstration that MEKK1 or NIK can directly phosphorylate and activate native IKKα and IKKβ. Nevertheless, the simplest interpretation of past and present results is that either of these MAPKKKs can activate IKK.

An important question, however, that is yet to be answered is which MAPKKKs are physiologically involved in IKK and NF-κB activation and whether different NF-κB-activating stimuli use the same MAPKKKs. It is also to be resolved whether MEKK1 acts exclusively on the JNK (and p38) to AP-1 pathway or whether it also is involved in IKK and NF-κB activation. In this respect, it would be useful to compare whether the specificity constants for IKKα or IKKβ phosphorylation by MEKK1 match the one for JNKK1, the most efficient and relevant MEKK1 substrate identified so far. Most groups who cotransfected varying amounts of truncated MEKK1 expression vectors with either a JNK reporter plasmid or an NF-κB transcriptional reporter find that JNK activity is potently stimulated at low input levels whereas NF-κB transcriptional activity is stimulated only by very high doses of MEKK1 (10, 30–32). High doses of MEKK1 are known to have nonspecific effects (2). Activation of a GAL4 transcriptional reporter by the c-Jun-GAL4 chimera and cotransfected MEKK1 parallels the stimulation of JNK activity (8, 34), but a different AP-1 reporter containing multiple c-Jun:ATF2 binding sites is stimulated only by very high doses of MEKK1, similar to those required for stimulation of the NF-κB reporter (32). Although all groups seem to agree that cotransfection of a NIK expression vector has no effect on JNK activity, some find that it nevertheless can enhance AP-1 activity, albeit less efficiently than MEKK1 (31). Currently it is hard to reconcile all of these results even if one invokes transcriptional synergy between AP-1 and NF-κB. More puzzling differences are found when the abilities of MEKK1Δ and NIK to activate NF-κB and IKK are compared. All groups agree that MEKK1 is a much poorer activator of the NF-κB transcriptional reporter than NIK is (30–32). However, some find that MEKK1 and NIK expression plasmids have similar effects on the activity of transiently expressed IKKα (32), and others find that NIK is a much more potent activator of IKKα than MEKK is, whereas IKKβ is slightly more responsive to MEKK1 than to NIK (35). A major difference between measuring the response of an NF-κB transcriptional reporter to MEKK1 vs. activation of a transiently expressed epitope tagged IKKα or IKKβ is that in the former case NF-κB activation depends on stimulation of endogenous (physiological) IKK activity, whereas in the latter case the transiently overexpressed IKK subunit probably is not incorporated into the physiological IKK complex. In fact, protein purification and immunoprecipitation experiments strongly suggest that most of the IKK complexes are IKKα:IKKβ heterodimers plus additional subunits and that very little IKKα or IKKβ homodimeric complexes exist (E. Zandi, D. Rothwarf, and M.K., unpublished results). It is important to express only small amounts of exogenous IKKα or IKKβ to ensure their incorporation into the physiological 900-kDa IKK complex (26). It is therefore safer to compare the abilities of NIK and MEKK1 to activate the endogenous IKK complex rather than the artificial IKKα or IKKβ homodimers generated by transient overexpression. When such a comparison is performed, transient transfection of a NIK vector into 293 cells results in preferential activation of endogenous IKK whereas transfection of a full-length MEKK1 vector results in preferential JNK activation (Fig. 2*A*). However overexpression of NIK can lead to JNK activation whereas overexpression of MEKK1 can lead to IKK activation (Fig. 2*B*). These results are in complete agreement with all published comparisons of the effect of these MAPKKKs on NF-κB and AP-1 transcriptional reporters. Nevertheless, it should be realized that these results do not rule out the possibility that, although weak, MEKK1 may contribute to IKK activation nor do they prove that, although potent, NIK is a physiological NF-κB activator. In addition these experiments highlight the potential pitfalls associated with overexpression of signaling proteins.

In addition to proinflammatory cytokines IKK activity is potently stimulated by the Tax transactivator protein of human T cell leukemia virus (HTLV) (36, 37). This response leading to NF-κB activation is likely to play a major role in the leukemogenic

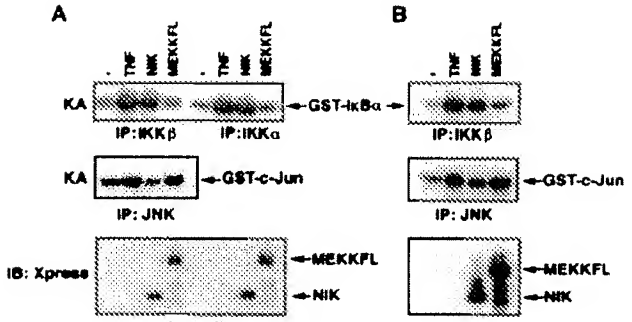

FIG. 2. Stimulation of endogenous IKK activity by NIK and MEKK1. 293 cells were transiently transfected with either Xpress-tagged NIK or Xpress-tagged MEKK1 full-length expression vectors (1 μg DNA in A or 2 μg DNA in B/60-mm plate). After 24 hr, cells were treated or not with TNF (20 ng/ml for 10 min) and then lysed. Cell lysates were immunoprecipitated (IP) with either anti-IKKα or anti-IKKβ or anti-JNK antibodies. The IKK activity (KA) was determined by using glutathione *S*-transferase (GST)-IκBα (1–54) as a substrate. The JNK activity (KA) was determined by using GST-cJun (1–79) as a substrate.

function of this virus. Like proinflammatory cytokines Tax was proposed to act either via MEKK1 (37) or NIK (36). Although the strongest evidence in favor of MEKK1 as a target is based on its ability to physically interact with Tax (37), the pro-NIK evidence is based on genetic arguments (36). Uhlik *et al.* (36) isolated variants of the Jurkat T cell line that fail to activate NF-κB in response to Tax. Although the basis for this defect currently is unknown, it can be complemented by transient expression of NIK but not by MEKK1 overexpression (36).

A major problem in sorting out the exact physiological functions of these and other MAPKKKs is the difficulty in detecting considerable changes in their enzymatic activity in response to cell stimulation by using conventional immunoprecipitation experiments. This deficiency can be overcome by genetic experiments similar to those that established the function of the yeast MAPKKK STE11 in three distinct MAPK cascades (38, 39). Although we will have to await the results of gene knockout experiments in which the activities of NIK and MEKK1 are selectively abolished, similar experiments conducted with components of the TNF-RI response pathway clearly support the earlier conclusion (10) that the pathways leading from this receptor to either JNK and AP-1 or IKK and NF-κB diverge at the level of TRAF2 and RIP (Fig. 1). Cells established from TRAF2 knockout embryos are defective in JNK activation in response to TNF, while exhibiting only a slightly retarded NF-κB activation response (40). In contrast, cells derived from RIP knockout embryos are defective in NF-κB activation, while exhibiting a normal JNK activation response (41). As MAPKKKs, like MEKK1 and NIK, are thought to act downstream to TRAF2 and RIP rather than upstream to them, it is unlikely that they play equal roles in transducing signals generated by TNF-RI activation to transcription factors. It is also possible that neither MEKK1 nor NIK are involved in TNF signaling. After all, the MAPKKK family contains many other members in addition to these two usual suspects.

We thank Dr. D. Goeddel for his comments. Research in our laboratory is supported by the National Institutes of Health (R01 AI43477). M.D. was supported by a postdoctoral fellowship from the D. Collen Research Foundation vzw.

1. Lange-Carter, C. A., Pleiman, C., Gardner, A., Blumer, K. & Johnson, G. (1993) *Science* **260,** 315–319.
2. Minden, A., Lin, A., McMahon, M., Lange-Carter, C., Dérijard, B., Davis, R. J., Johnson, G. L. & Karin, M. (1994) *Science* **266,** 1719–1723.
3. Yan, M., Dai, T., Deak, J. C., Kyriakis, J. M., Zon, L. I., Woodgett, J. R. & Templeton, D. J. (1994) *Nature (London)* **372,** 798–800.
4. Lin, A., Minden, A., Martinetto, H., Claret, F. X., Lange-Carter, C., Mercurio, F., Johnson, G. L. & Karin, M. (1995) *Science* **268,** 286–290.
5. Karin, M. (1995) *J. Biol. Chem.* **270,** 16483–16486.
6. Smeal, T., Binétruy, B., Mercola, D., Birrer, M. & Karin, M. (1991) *Nature (London)* **354,** 494–496.
7. Gupta, S., Campbell, D., Dérijard, B. & Davis, R. J. (1995) *Science* **267,** 389–393.
8. Minden, A., Lin, A., Claret, F. X., Abo, A. & Karin, M. (1995) *Cell* **81,** 1147–1157.
9. Coso, O. A., Chiariello, M., Yu, J. C., Teramoto, H., Crespo, P., Xu, N., Miki, T. & Gutkind, J. S. (1995) *Cell* **81,** 1137–1146.
10. Liu, Z.-G., Hu, H., Goeddel, D. V. & Karin, M. (1996) *Cell* **87,** 565–576.
11. Natoli, G., Costanzo, A., Ianni, A., Templeton, D. J., Woodgett, J. R., Balsano, C. & Levrero, M. (1997) *Science* **275,** 200–203.
12. Beg, A. A. & Baltimore, D. (1996) *Science* **274,** 782–784.
13. Van Antwerp, D. J., Martin, S. J., Kafri, T., Green, D. R. & Verma, I. M. (1996) *Science* **274,** 787–789.
14. Hirano, M., Osada, S., Aoki, T., Hirai, S., Hosaka, M., Inoue, J. & Ohno, S. (1996) *J. Biol. Chem.* **271,** 13234–13248.
15. Meyer, C. F., Wang, X., Chang, C., Templeton, D. & Tan, T. H. (1996) *J. Biol. Chem.* **271,** 8971–8976.
16. Baeuerle, P. A. & Baltimore, D. (1996) *Cell* **87,** 13–20.
17. Baldwin, A. S. (1996) *Annu. Rev. Immunol.* **14,** 649–681.
18. Verma, I. M., Stevenson, J. K., Schwarz, E. M., Van Antwerp, D. & Miyamoto, S. (1995) *Genes Dev.* **9,** 2723–2735.
19. Stein, B., Baldwin, A. S., Jr., Ballard, D. W., Green, W. C., Angel, P. & Herrlich, P. (1993) *EMBO J.* **12,** 3879–3891.
20. Yasumoto, K., Okamoto, S., Mukaida, N., Murakami, S., Mai, M. & Matsushima, K. (1992) *J. Biol. Chem.* **267,** 22506–22511.
21. Lee, F. S., Hagler, J., Chen, Z. J. & Maniatis, T. (1997) *Cell* **88,** 213–222.
22. Brown, K., Gerstberger, S., Carlson, L., Franzoso, G. & Siebenlist, U. (1995) *Science* **267,** 1485–1491.
23. DiDonato, J. A., Mercurio, F., Rosette, C., Wu-li, J., Suyang, H., Ghosh, S. & Karin, M. (1996) *Mol. Cell. Biol.* **16,** 1295–1304.
24. DiDonato, J. A., Hayakawa, M., Rothwarf, D. M., Zandi, E. & Karin, M. (1997) *Nature (London)* **388,** 548–554.
25. Mercurio, F., Zhu, H., Murray, B. W., Shevchenko, A., Bennett, B. L., Li, J., Young, D. B., Barbosa, M., Mann, M., Manning, A. & Rao, A. (1997) *Science* **278,** 860–866.
26. Zandi, E., Rothwarf, D., Delhase, M., Hayakawa, M. & Karin, M. (1997) *Cell* **91,** 243–252.
27. Régnier, C. H., Yeong Song, H., Gao, X., Goeddel, D. V., Cao, Z. & Rothe, M. (1997) *Cell* **90,** 373–383.
28. Woronicz, J. D., Gao, X., Cao, Z., Rothe, M. & Goeddel, D. V. (1997) *Science* **278,** 866–869.
29. Malinin, N. L., Boldin, M. P., Kovalenko, A. V. & Wallach, D. (1997) *Nature (London)* **385,** 540–544.
30. Song, H. Y., Régnier, C. H., Kirschning, C. J., Ayres, T. M., Goeddel, D. V. & Rothe, M. (1997) *Proc. Natl. Acad. Sci. USA* **94,** 9792–9796.
31. Natoli, G., Costanzo, A., Moretti, F., Fuleo, M., Balsano, C. & Levrero, M. (1997) *J. Biol. Chem.* **272,** 26079–26082.
32. Lee, F. S., Peters, R. T., Dang, L. C. & Maniatis, T. (1998) *Proc. Natl. Acad. Sci. USA* **95,** 9319–9324.
33. Ling, L., Cao, Z. & Goeddel, D. V. (1998) *Proc. Natl. Acad. Sci. USA* **95,** 2791–2797.
34. Cavigelli, M., Dolfi, F., Claret, F. X. & Karin, M. (1995) *EMBO J.* **14,** 5957–5964.
35. Nakano, H., Shindo, M., Sakon, S., Nishinaka, S., Mihara, M., Yagita, H. & Okumura, K. (1998) *Proc. Natl. Acad. Sci. USA* **95,** 3537–3542.
36. Uhlik, M., Good, L., Xiao, G., Harhaj, E. W., Zandi, E., Karin, M. & Sun, S.-C. (1998) *J. Biol. Chem.*, in press.
37. Yin, M. J., Christerson, L. B., Yamamoto, Y., Kwak, Y.-T., Xu, S., Mercurio, F., Barbosa, M., Cobb, M. H. & Gaynor, R. B. (1998) *Cell* **93,** 875–884.
38. Herskowitz, I. (1995) *Cell* **80,** 187–197.
39. Posas, F. & Saito, H. (1997) *Science* **276,** 1702–1705.
40. Yeh, W. C., Shahinian, A., Speiser, D., Kraunus, J., Billia, F., Wakeham, A., de la Pompa, J. L., Ferrick, D., Hum, B., Iscove, N., *et al.* (1997) *Immunity* **7,** 715–725.
41. Kelliher, M. A., Grimm, S., Ishida, Y., Kuo, F., Stanger, B. Z. & Leder, P. (1998) *Immunity* **8,** 297–303.

EXHIBIT H

THE JOURNAL OF BIOLOGICAL CHEMISTRY Vol. 281, No. 22, pp. 15268–15276, June 2, 2006

Regulation of IκB Kinase (IKK) Complex by IKKγ-dependent Phosphorylation of the T-loop and C Terminus of IKKβ*

Received for publication, December 27, 2005, and in revised form, April 5, 2006 Published, JBC Papers in Press, April 5, 2006, DOI 10.1074/jbc.M513793200

Beth Schomer-Miller[‡1], **Tomoyasu Higashimoto**[‡], **Yung-Kang Lee**[§], **and Ebrahim Zandi**[‡2]

From the [‡]*Department of Molecular Microbiology and Immunology, Keck School of Medicine, Norris Comprehensive Cancer Center, and* [§]*Molecular Pharmacology & Toxicology, School of Pharmacy, University of Southern California, Los Angeles, California 90089-9176*

The mechanistic relationship of phosphorylation of the C terminus of IKKβ with phosphorylation of its T-loop kinase domain within the IKK complex remained unclear. We investigated the regulatory role of the serine cluster residing immediately adjacent to the HLH domain and of the serines in the NEMO/IKKγ-binding domain (NBD/γBD) in the C-terminal portion of IKKβ in MEFs deficient in IKKβ and IKKα and in yeast reconstitution system. We show that phosphorylation events at the C terminus of IKKβ can be divided into autophosphorylation of the serine cluster adjacent to the HLH domain and phosphorylation of the NBD/γBD. Autophosphorylation of the serine cluster occurs immediately after IKK activation and requires IKKγ. In MEFs, this autophosphorylation does not have the down-regulatory function on the IKK complex that was previously described (1). On the other hand, phosphorylation of the NBD/γBD regulates IKKγ-dependent phosphorylation of the T-loop activation domain in IKKβ and, hence, IKK complex activation. Our study suggests that, within the IKK complex, modulation of the NBD/γBD by IKKγ is upstream to the T-loop phosphorylation.

Phosphorylation of inhibitors of κB (IκB)[3] is catalyzed by the 700–900-kDa enzyme complex IκB kinase (IKK) (2–4). IKK is composed of two homologous catalytic subunits IKKα and IKKβ (85 and 87 kDa, respectively), and an unrelated regulatory 52-kDa subunit IKKγ (5) also known as NEMO (NF-κB essential modulator) (6). IKKγ is required for the stimulation of IKK by upstream signals such as TNF, Tax, lipopolysaccharide, and interleukin 1 (5, 6).

IκBs regulate the activity of the NF-κB transcription factors. NF-κBs control the transcription of hundreds of genes involved in immunity, stress, and regulation of apoptosis and cellular proliferation. In resting cells, most NF-κB dimers are bound to inhibitory IκB proteins and sequestered in the cytoplasm (7). Diverse stimuli, including cytokines, bacterial and viral products, oxidants, and mitogens lead to activation of IKK, which phosphorylates two regulatory serine residues on IκBs (8). This phosphorylation leads to recognition by the protein, β-TrCP, and to polyubiquitination by a specific ubiquitin ligase (9, 10). After ubiquitination, the IκB proteins are rapidly degraded by the proteasome. This frees NF-κB, which migrates to the nucleus where it binds to and stimulates the transcription of target genes (7).

IKK complexes are composed of equal numbers of catalytic subunits (IKKα and/or β) and regulatory γ subunits (11). IKKα and IKKβ have similar structures including kinase domains and canonical mitogen-activated protein kinase activation loops (T-loops) toward their N termini (3). In addition, IKKα and IKKβ contain leucine zipper motifs through which the catalytic subunits associate (12) and helix-loop-helix domains toward the C terminus (4). An α-helical region near the N terminus of IKKγ binds to a 6-amino acid region (NEMO/γ-binding domain) at the very C terminus of IKKα and IKKβ, and interfering with this interaction diminishes stimulation of IKK by TNFα (13).

Despite their structural similarities, IKKα and IKKβ differ. IKKβ is essential for the induction of NF-κB by most proinflammatory stimuli whereas IKKα has roles in limb development, skin differentiation, B-cell maturation, and lymphoid organogenesis (14–19). Moreover, IKKβ homodimer has approximately a 30-fold higher activity toward IκBα than the IKKα homodimer (20). Some of these differences may be attributed, in part, to an ubiquitin-like domain present in IKKβ but not IKKα. This domain is located between the kinase domain and leucine zipper of IKKβ, and its mutation or deletion causes loss of activity in IKKβ (21).

Like its substrate IκBα, IKK is regulated by phosphorylation and ubiquitination. TRAF6 (TNF receptor-associated factor 6) is essential for IKK signaling through the IL-1 receptor and Toll-like receptor (22). TRAF6 contains a RING domain that acts as a ubiquitin ligase (23). It undergoes trans-auto-ubiquitination (24), and it also ubiquitinates IKKγ (25). Blocking ubiquitination prevents TRAF6-mediated activation of IKK (26). Moreover, the T cell receptor appears to activate IKK via BCL10 and MALT1, which induce the ubiquitin ligase activity of TRAF6. RNA interference data indicate that TRAF2 and TRAF6 are required for IKK activation after T cell receptor ligation (25). In addition, other signaling pathways that induce IKK activity including NOD2 (which serves as an intracellular signal for bacteria) and genotoxic stress, activate NF-κB by ubiquitination of various lysine residues on IKKγ (23, 27, 28). IKK may be down-regulated by deubiquitinating proteases such as CYLD (the protein mutated in familial cylindromatosis), which associate with IKKγ and deubiquitinate TRAF2 and TRAF6 (29–31).

All three subunits of IKK become phosphorylated within 10 min following treatment of HeLa cells with TNF, with concomitant stimulation of IKK activity (1). IKK is inactivated by protein phosphatase 2a, indicating that it is activated by phosphorylation (2). IKK can also be dephosphorylated by protein phosphatase PP2Cβ, and it has been shown to associate with PP2Cβ with kinetics consistent with a role in down-regulating its activity (32). Phosphopeptide mapping of IKKβ indicates that phosphorylation occurs at serine residues in the T-loop (Ser^{177} and Ser^{181}) and at a cluster of serines located between the HLH domain and the C terminus (1). Mutation of the T-loop serines of IKKβ

* This study was supported in part by National Institutes of Health Grant R01 MG065325 (to E. Z.). The costs of publication of this article were defrayed in part by the payment of page charges. This article must therefore be hereby marked "*advertisement*" in accordance with 18 U.S.C. Section 1734 solely to indicate this fact.

[1] Supported in part by the Training Program in Alcoholic Liver and Pancreatic Diseases (T32 AA07578) funded by the NIAAA, National Institutes of Health.

[2] A 2001 PEW Scholar in Biomedical Sciences. To whom correspondence should be addressed: USC/Norris Comprehensive Cancer Center, 1441 Eastlake Ave., Norris 6429, Los Angeles, CA 90033. Tel.: 323-865-0644; Fax: 323-865-0645; E-mail: Zandi@usc.edu.

[3] The abbreviations used are: IκB, inhibitors of κB; IKK, IκB kinase; TNF, tumor necrosis factor; IL, interleukin; GST, glutathione *S*-transferase; HA, hemagglutinin; Tricine, *N*-[2-hydroxy-1,1-bis(hydroxymethyl)ethyl]glycine; HLH, helix-loop-helix; MEF, mouse embryonic fibroblasts; TRAF, TNF receptor-associated factor.

to alanines prevents IKK activation in mammalian cell lines, whereas conversion of these residues to glutamic acids makes the kinase constitutively active, indicating that the kinase is activated by phosphorylation of the T-loop (1, 3). Phosphorylation of the T-loop of IKKβ, which occurs when IKK is activated, is followed by progressive phosphorylation of the cluster of serines at its C terminus (1). This phosphorylation was suggested to play a role in down-regulating the activity of IKK in HeLa cells (1). A mutation mimicking phosphorylation in the NEMO/γ binding domain (NBD/γBD) of IKKβ diminishes its ability to activate NF-κB, suggesting that phosphorylation of this residue, in particular, may have regulatory significance (33).

In this study, we investigated the regulatory role of the serine cluster residing immediately after the HLH domain and the serines in the NBD/γBD in the C terminus of IKKβ in MEFs deficient in IKKβ and IKKα and in yeast reconstitution system. We show that phosphorylation events at the C terminus of IKKβ can be divided into autophosphorylation of the serine cluster immediately following the HLH domain, and phosphorylation of the NBD/γBD. Autophosphorylation of the serine cluster occurs immediately after IKK activation, and requires IKKγ. In MEFs, this autophosphorylation does not have the previously reported down-regulatory function (1). On the other hand, phosphorylation of the NBD/γBD regulates IKKγ-dependent phosphorylation of the T-loop activation domain in IKKβ and, hence, IKK complex activation. Our study puts regulation of the NBD/γBD through IKKγ upstream of the T-loop phosphorylation and IKK activation.

EXPERIMENTAL PROCEDURES

Cell Culture and Establishing Stable Pools of MEFs—Mouse embryonic fibroblasts (MEFs) deficient in IKKβ (34) or IKKα and IKKβ (35) were grown in Dulbecco's modified Eagle's medium, 10% fetal bovine serum with antibiotics and maintained at 37 °C, 5% CO_2. To establish stable pools of HA-tagged wild type and C-terminal serine to alanine mutants of IKKβ, corresponding plasmids (pRc-β- actin), (1) carrying a neomycin resistance gene were transfected using Lipofectamine Plus™ (Invitrogen). Stable pools of MEFs for each construct were selected by growing cells in 2 mg/ml G418 sulfate (Cellgro, Mediatech, Inc.) for 6 weeks. Stable pools were maintained in 0.25 mg/ml G418 sulfate after the selection period. For experiments, 1.0×10^6 cells were seeded in 60-mm dishes for 24 h, before treating with TNFα (20 ng/ml) or IL-1β (5 ng/ml) for the times indicated in the figures. Cells were harvested and the activities of IKK complexes were determined as described previously (4).

Kinase Assays and Immunoblots—GST-IκBα-(1–54) was used as a substrate for IKKβ because it contains the regulatory serines but lacks other residues that could be phosphorylated nonspecifically. It was expressed in bacteria and purified using glutathione-Sepharose beads (Amersham Biosciences).

Various peptides containing wild-type or mutant versions of the C terminus of IKKβ were also produced so that they could be tested as possible substrates for IKKβ. Some of these peptides contain mutations in which serines were mutated to alanines, and all of these substrates spanned from the helix-loop-helix through the C terminus of IKKβ. DNA was amplified by polymerase chain reaction with full-length IKKβ as template using Pfu Turbo (Stratagene, La Jolla, CA), digested, and inserted into the bacterial expression vector pET-HET-N1, which contains a Myc tag at the 5′-end and a His_6 tag at the 3′-end of the cloning site. DNA sequences of the constructs were verified by automated sequencing (Microchemical Core Facility/USC Norris Cancer Center). Plasmids were transformed into the bacterial strain BL21 and induced with isopropyl-1-thio-β-D-galactopyranoside. The bacterial pellet from 500-ml culture was suspended in 50 ml of phosphate-buffered saline containing 6 M guanidine hydrochloride, sonicated for 3 min, frozen and thawed twice, and brought to a final concentration of 1% Triton X-100 and 5 mM β-mercaptoethanol. The lysate was cleared by centrifugation at 15,000 rpm for 30 min at 4 °C and incubated with 1 ml of pre-equilibrated Ni-NTA superflow agarose (Qiagen) for 1 h at 4 °C. Unbound proteins were washed away, and the bound proteins were renatured with a series of 50-ml buffers containing 4 M, 2 M, 1 M, 0.5 M, and 0 M urea in phosphate-buffered saline with 10 mM imidazole, 1% Triton X-100, and 5 mM β-mercaptoethanol. The IKKβ peptides were eluted with 200 mM imidazole in 1-ml fractions, and the positive fractions were pooled and dialyzed in phosphate-buffered saline with 1 mM dithiothreitol and 10% glycerol.

For most kinase assays, purified human IKKβ from Sf9 cells (12), or gel filtration-purified or immunoprecipitated IKK complex from yeast was incubated for 30 min at 30 °C in a 30-μl reaction mixture containing 20 mM Tris, pH 7.6, 20 mM $MgCl_2$, 20 μM cold ATP, 2 mM dithiothreitol, [γ-^{32}P]ATP (ICN), and 2 μg of protein substrate. The reactions were terminated by the addition of SDS-PAGE sample buffer and heated for 5 min at 97 °C. Proteins were separated by SDS-PAGE and transferred to polyvinylidene difluoride (Bio-Rad), and labeling was detected by PhosphorImager (Molecular Dynamics).

For some experiments, IKK activity was tested using a range of IκBα concentrations (from 4–183 μg/ml). The protocol was the same as above only the substrate concentration was varied, and the incubation time was shortened to 10 min.

Cloning and Expression of IKKs in Yeast—The plasmid pESC-trp-met-HA-IKKβ containing HA-IKKβ under the methionine promoter was described previously (11). To co-express similar levels of IKKγ and IKKβ, HA-IKKγ and its methionine promoter were inserted into the pESC-trp-met-HA-IKKβ plasmid. Various point mutations were generated in IKKβ by PCR using Pfu polymerase (Stratagene). These PCR products were digested and subcloned into the vectors pESC-trp-met-HA-IKKβ and pESC-trp-met-HA-IKKβ met-HA-IKKγ. The mutated regions were verified by sequencing. Plasmids were transformed into *Saccharomyces cerevisiae* strain YPH 499 (Stratagene) using lithium acetate as described (Stratagene pESC Yeast Epitope Tagging Vectors instruction manual).

2 ml of overnight cultures of yeast were grown in selective drop-out medium (Q-Biogene) containing 4 mM methionine (Q-Biogene) to suppress IKK expression and then expanded into 400 ml of selective non-inducing medium. The yeast were grown at 30 °C with shaking at 300 rpm before transfer to inducing medium (without methionine) and induced overnight (at 30 °C with shaking). For harvesting and lysing the yeast, all steps were performed at 4 °C unless otherwise indicated. They were first washed in 400 mM $(NH_4)_2SO_4$, 200 mM Tris-HCl, pH 8.0, 10 mM $MgCl_2$, 10% glycerol, 2 mM *p*-nitrophenyl phosphate containing protease inhibitors (2.5 μg/ml leupeptin, 20 μg/ml aprotinin, 2.5 μg/ml antipain, 2 μg/ml pepstatin, 1 mM phenylmethylsulfonyl fluoride, 0.1 μg/ml chymostatin, and 1.1 μg/ml phosphoramidon). The pellets were resuspended in an equal volume of lysis buffer (20 mM Tris, pH 7.6, 20 mM NaF, 20 mM β-glycerophosphate, 0.5 mM Na_3VO_4, 2.5 mM sodium metabisulfite, 5 mM benzamidine, 1 mM EDTA, 0.5 mM EGTA, 10% glycerol, 300 mM NaCl, 1% Triton X-100, 2 mM dithiothreitol, 2 mM *p*-nitrophenyl phosphate with protease inhibitors), transferred to yeast protein extraction vials (Q-Biogene), and frozen at −80 °C. To lyse the yeast, the vials were thawed on ice, disrupted using a Q-Biogene Fast-Prep apparatus for 20 s on speed 6, and vortexed for 5 min. The vials were spun at 10,000 × *g*, the supernatant was collected, and the pellets were resuspended in 0.67 ml of lysis buffer. The extraction procedure

was repeated an additional three times. The combined supernatants were clarified by centrifugation for 3 min at 3000 × *g* followed by ultracentrifugation for 1.5 h at 65,000 × *g*.

HA-IKK complex was then partially purified by gel filtration. 0.5 ml of extract (2–5 mg total protein) was loaded onto a Superose 6 gel filtration column (Amersham Biosciences) and samples were fractionated at a flow rate of 0.3 ml per minute. The gel filtration buffer contained 20 mM Tris, pH 7.6, 20 mM NaF, 20 mM β-glycerophosphate, 0.5 mM Na_3VO_4, 2.5 mM sodium metabisulfite, 5 mM benzamidine, 1 mM EDTA, 0.5 mM EGTA, 10% glycerol, 300 mM NaCl, and 0.1% Brij 35.

Alkaline Phosphatase Treatment—Approximately 6 μg of yeast extract were immunoprecipitated using 1 μl of anti-HA antibody (USC/Norris core facility) in radioimmune precipitation assay buffer (20 mM Tris, pH 8.0, 1% deoxycholate, 1% Triton X-100, 0.1% SDS, 150 mM NaCl, 2 mM PNPP) followed by binding to protein G-Sepharose beads (Amersham Biosciences). Immune complexes were pelleted and washed once with radioimmune precipitation assay buffer and once with CIP buffer (calf intestinal phosphate buffer from New England BioLabs containing 0.1 mg/ml bovine serum albumin, 2.5 μg/ml leupeptin, 20 μg/ml aprotinin, 2.5 μg/ml antipain, 2 μg/ml pepstatin, 0.1 μg/ml chymostatin, and 1.1 μg/ml phosphoramidon). Pelleted proteins were then incubated for 15 min at 37 °C in a 30-μl reaction containing 10 units of calf intestinal phosphatase in CIP buffer. The alkaline phosphatase treatment was stopped by addition of SDS-PAGE sample buffer and heated for 5 min at 95 °C. For untreated controls, the addition of calf intestinal phosphatase was omitted.

In Vivo Labeling—3.5-ml cultures of yeast were grown in selective medium containing 4 mM methionine to suppress IKK expression until they reached an optical density of 0.7–1.0. Then the yeast were pelleted and resuspended in 1 ml of selective medium without methionine (to induce IKK expression) and containing 1.4 mCi of [^{32}P]orthophosphate. The yeast were radiolabeled and induced for 5 h, then washed with yeast wash buffer containing protease and phosphatase inhibitors, resuspended in 500 μl of yeast lysis buffer containing protease and phosphatase inhibitors, and frozen at −80 °C. The yeast were lysed as described above, and the extract was clarified by microcentrifugation for 1 min at 10,000 × *g* followed by 20 min at 18,000 × *g*.

To remove contaminating nonspecific immune complexes, the extracts were first immunoprecipitated with a nonspecific FLAG antibody (Sigma) and complexed to protein G-agarose (Amersham Biosciences). Then, HA-IKK was immunoprecipitated using monoclonal antibodies directed against HA (USC/Norris core facility) followed by binding to protein G-agarose. The beads were washed repeatedly in radioimmune precipitation assay buffer (20 mM Tris, pH 8.0, 1% deoxycholate, 1% Triton X-100, 0.1% SDS, 150 mM NaCl, 2 mM PNPP) before elution for 5 min at 97 °C in SDS-PAGE loading buffer. The samples were electrophoresed using SDS-PAGE and transferred to polyvinylidene difluoride (Bio-Rad). Radiolabeling was detected by Phosphorimager. Blots were probed with anti-HA antibodies (USC/Norris Core Facility) followed by anti-mouse IgG horseradish peroxidase antibodies (Amersham Biosciences) and then detected by chemiluminescence (Pierce SuperSignal reagent) using a Bio-Rad Fluor-S Max quantification system.

Cyanogen Bromide (CNBr) Digestion—Yeast cells were ^{32}P-labeled and IKK was isolated as described above. For cyanogen bromide digestion, the immunoprecipitated samples were electrophoresed on an 8% SDS-PAGE gel. Autoradiography was used to locate the protein bands which were cut from the gel. The acrylamide slices were transferred to a siliconized tubed, crushed with a pipette, and resuspended in 200 μl of 70% formic acid. Cyanogen bromide was added to a final concentration of 17 mg/ml, the samples were overlaid with argon gas, and digestion was allowed to proceed for 17 h at room temperature in the dark. Samples were microcentrifuged for 5 min, and the supernatants were transferred to siliconized tubes. The acrylamide was rinsed three times with 250 μl of ddH2O, and the rinses were combined with the digested sample. The samples were dried overnight. The peptides were electrophoresed on a 16.5%T 3%C Tris Tricine gel and visualized using a PhosphorImager.

RESULTS

Mutating C-terminal Serine Residues to Alanine in IKKβ Does Not Alter Down-regulation of IKK Complex in MEFs—At least two regions of IKKβ are phosphorylated on serine residues in response to stimulation. Phosphorylation of T-loop serines (177 and 181) in the kinase domain of IKKβ are essential for IKK activation, and phosphorylation of at least ten serines (region spanning amino acid 664 to its end) in its C terminus was shown to play a role in down-regulation of IKK in HeLa cells in the background of endogenous IKKβ (1). However, because a given IKK complex could contain 6 to 9 catalytic subunits (11), expression of mutated forms of IKKα or IKKβ in mammalian cells could result in the formation of heterocomplexes containing endogenous wild-type along with mutated forms. For example, when kinase-defective mutants HA-IKKαKm or HA-IKKβKA were expressed in HeLa or HEK 293 cells, immunoprecipitation of the mutant kinases resulted in precipitation of very active and TNF-inducible IKK complexes (4). This clearly indicates that mutant IKKα or IKKβ were incorporated into the endogenous IKK complexes. Considering this, changes seen in the kinetics of IKK regulation may have been due to the formation of heterocomplexes, when the activity of the C-terminal serine to alanine mutants of IKKβ were tested in HeLa cells in the background of endogenous IKKβ (1). Here we examined the activities of the same mutant IKKβs used in Delhase and co-workers (34), in embryonic fibroblasts derived from IKKβ-deficient mouse (MEFβ$^{-/-}$). We generated stable pools of MEFβ$^{-/-}$ cells expressing either wild-type IKKβ, or M10, L3SA, or M12 mutants. In the M10 construct, 10 serines C-terminal to the helix-loop-helix are mutated to alanines, whereas the last 4 serines remained unchanged, and in the M12 construct, these same 10 serines as well as Ser^{740} and Ser^{750} are mutated to alanines. IKKβL3SA has three serines (Ser^{733}, Ser^{740}, and Ser^{750}) mutated to alanines. The activities of IKK complexes were determined by the immune kinase complex assay in these cells before and after treatment with TNFα for 5, 15, 30, 60, and 120 min. As shown in Fig. 1*A*, there is no obvious difference between the activation and down-regulation kinetics of IKKβ wild type and IKKβM10. The same is true for the IKKβL3SA and IKKβM12 mutants (Fig. 1*A*). In all cases, the reconstituted IKK wild type or mutants show very little activity in untreated cells and reach peak activity at 15 min, similar to native IKK as previously reported (4). The activity of wild type or mutated IKKβ is down-regulated at 30 min and remains low up to 120 min (Fig. 1*A*). The only major difference in IKK activity is that for the M12 and L3SA mutants (which contain mutations in the serines in the γBD) where IKK has faster activation kinetics (Fig. 1*A*). This occurs independently of the mutations of the 10 preceding serines. The L3SA and M12 mutants show reasonably strong TNF-induced activity at 5 min (Fig. 1*A*). These experiments were repeated several times and similar results were obtained (data not shown). Results in Fig. 1*A* indicate that the ten serines preceding the NBD/γBD of IKKβ do not play a role in down-regulating the activity of IKK complex. On the other hand, serines 733, 740, and 750 within and around the γ-binding domain may play a role for IKK regulation (see below).

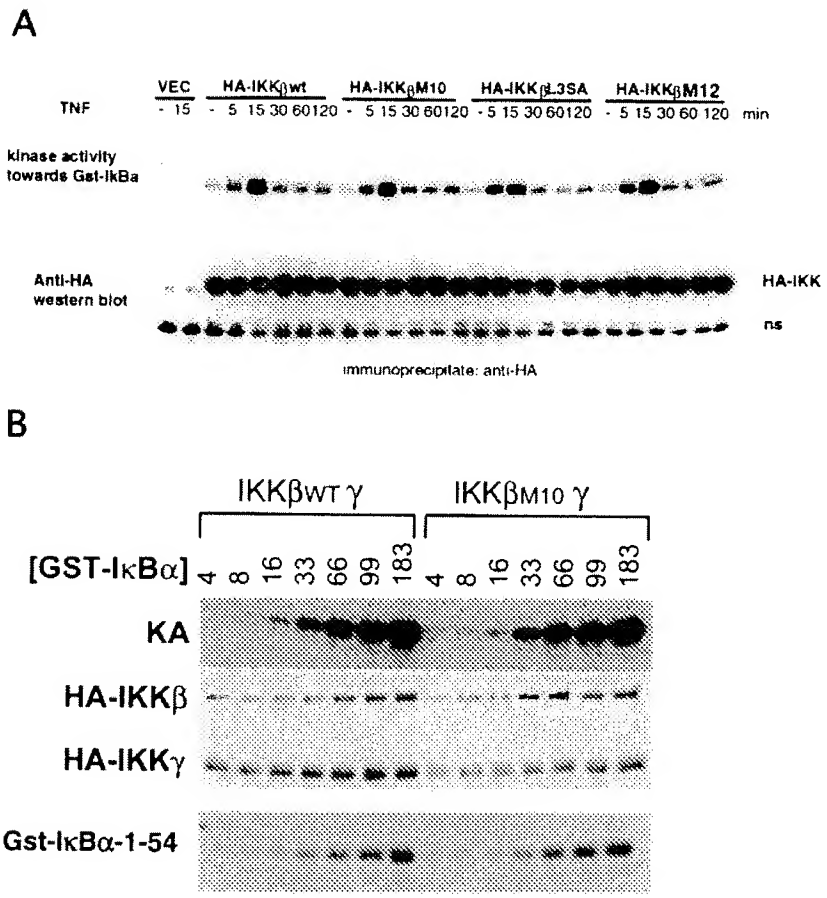

FIGURE 1. **The C-terminal serine residues of IKKβ do not play a role in the down-regulation of the IKK complex after activation.** *A*, MEFs deficient in IKKβ were transfected with the indicated HA IKKβ wild-type (*wt*) or mutants (*M10*, all 10 serines between amino acids 664–707 mutated to alanine; L3SA, serines 733, 740, and 750 mutated to alanine; M12, all serines between amino acids 664–707 as well as serines 740 and 750 mutated to alanine). Stable pools of cells were established by drug selection. The activities of IKK complexes in these cells after TNFα stimulation for the times indicated were determined by immune kinase complex assay using anti-HA antibodies. The *top panel* shows the kinase assay data, the *bottom panel* shows the Western blot analysis of the immunoprecipitated HA-IKK proteins. *B*, activity of wild-type IKKβ + γ is similar to the activity of IKKβ M10 + γ. IKKs were expressed in yeast and purified by gel filtration. IKK activity was tested over a range of GST-IκBα-(1–54) concentrations (from 4–183 μg/ml). The *upper panel* shows kinase activity (KA), and the *middle panel* shows the level of HA-IKKβ and HA-IKKγ assessed by immunoblot, and the *bottom panel* shows a Coomassie Blue stain of GST-IκBα substrate.

We further examined *in vitro* whether there is a difference in activities between wild-type IKKβ and IKKβM10 in the absence of IKKα. IKK complexes containing IKKγ with either wild-type IKKβ or IKKβM10 were expressed in yeast and partially purified by gel filtration. The activities were compared over a range of concentrations of IκBα substrate (from 4 to 183 μg/ml, Fig. 1*B*). The activity of the IKKβM10 was similar to the activity of wild-type IKKβ over the whole range of substrate concentrations. This indicates that rendering the serines at the C terminus of IKKβ unphosphorylatable neither increases nor decreases kinase activity toward IκBα. For this kinase assay, there was a 10 min. incubation of enzyme in the presence of substrates, and the level of IKKβ seemed to be significantly lower at the end of the assay for samples incubated with low concentrations of IκBα (compared with the level of IKKβ after incubation in high concentrations of IκBα). This indicates that somehow, the higher concentrations of substrate stabilized the enzyme during the assay. Because of this, it was not possible to quantitatively compare the kinetic parameters of the wild-type IKKβ to IKKβM10 containing complexes. Nevertheless, qualitatively, both complexes show very similar activities.

The C Terminus of IKKβ Is Autophosphorylated in Yeast in an IKKγ-dependent Manner—Previous work (1) suggested that the C terminus of IKKβ becomes phosphorylated following IKK activation via autophosphorylation in mammalian cells. Here we used the IKK reconstituted in yeast to examine IKKγ-dependence of the autophosphorylation of the C terminus of IKKβ. A routine Western blot of IKKs expressed in yeast using HA antibodies revealed a pronounced band shift of IKKβ when co-expressed with IKKγ (Fig. 2*A*). This marked band shift induced by the presence of IKKγ occurred for wild-type IKKβ and IKKβ γBD AA (a mutant of IKK in which serines 740 and 750 are changes to alanine, see also Fig. 3*A*) but was not observed for the M10 and M12 mutants. This suggests that the serine residues C-terminal to the helix-loop-helix are phosphorylated. The greatly reduced band shift for M10 and M12, in which most of the C-terminal serines are rendered incapable of phosphorylation, suggests that much of the phosphorylation occurs in the 10 serines immediately C-terminal to the helix-loop-helix, and it requires IKKγ.

To confirm that the band shift seen in IKKβ when co-expressed with IKKγ was caused by phosphorylation, extracts were treated with alkaline phosphatase. IKKβ co-expressed with IKKγ migrates slower compared with IKKβ (expressed alone) on SDS-PAGE (Fig. 2*B*, compare *lanes 1* and *3*). However, after treatment with alkaline phosphatase the IKKβ expressed with IKKγ migrates at the same rate as IKKβ expressed alone (Fig. 2*B*, *lane 4*), suggesting that the band shift was caused by phosphorylation. The migration of IKKβM10 (with or without IKKγ) (Fig. 2*B*, *lanes 5–8*) was unaffected by the alkaline phosphatase treatment. This indicates that the extent of phosphorylation of IKKβM10 mutant is significantly lower than wild-type IKKβ. It further indicates that much of the phosphorylation observed during co-expression of IKKγ with IKKβ must occur in the 10 serines immediately following the HLH domain.

The alkaline phosphatase experiment also indicates that IKKγ is phosphorylated. IKKγ is seen as a doublet when co-expressed with either IKKβ or IKKβM10; the size of the bands is similar for either complex. Treatment of IKKβ+γ or IKKβM10+γ with alkaline phosphatase caused IKKγ to migrate predominantly as the faster migrating band, indicating that the slower migrating band is phosphorylated.

To further demonstrate that the C terminus of IKKβ is phosphorylated and the majority of the phosphorylation occurs on the ten serines

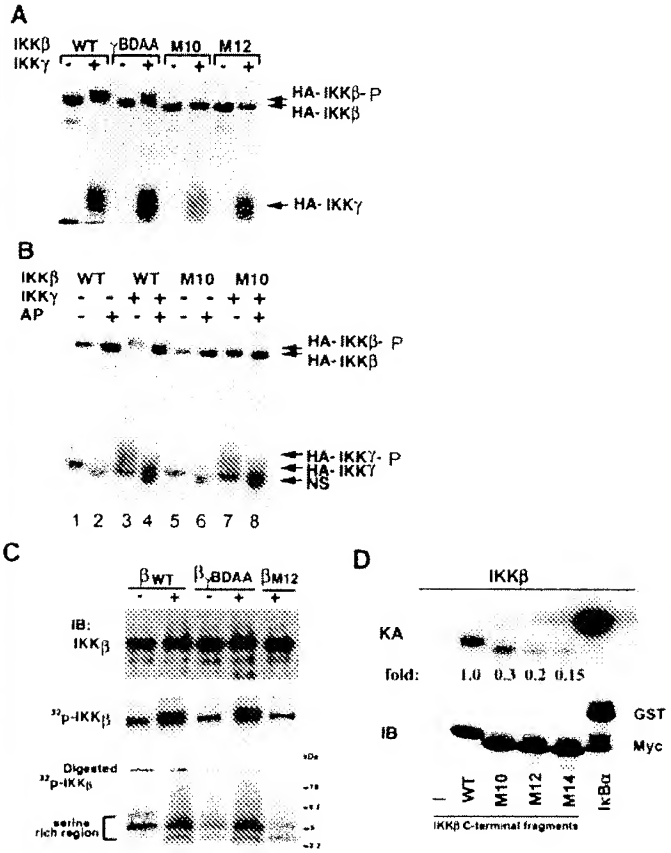

FIGURE 2. **Activation of IKKβ is required for it to be phosphorylated at its C terminus, and this phosphorylation is enhanced by IKKγ.** *A*, co-expression of IKKγ with IKKβ leads to autophosphorylation of IKKβ as assessed by a band shift assay. Wild-type or various mutant forms of HA-IKKβ were expressed alone or along with HA-IKKγ in yeast, and lysates were separated by SDS-PAGE and analyzed by immunoblot. Co-expression with HA-IKKγ results in the delayed migration of IKKβ; the absence of this band shift where the serines were mutated to alanines (for M10 and M12) suggests that the slower migration resulted from phosphorylation of C-terminal serines. *B*, treatment of extracts with alkaline phosphatase indicates that the band shift induced by IKKγ is caused by increased phosphorylation. Wild-type and IKKβ M10 was expressed alone or co-expressed with IKKγ in yeast. Extracts were either untreated or dephosphorylated using alkaline phosphatase (*AP*) before immunoblotting with antibodies directed against HA. *C*, IKKγ-dependent *in vivo* phosphorylation of C-terminal IKKβ wild type and IKKβ-γBDAA, but not IKKβ-M12. IKK proteins were labeled in yeast with [^{32}P]orthophosphate, immunoprecipitated and digested with CNBr, and separated on a Tris-Tricine gel as described under "Experimental Procedures." *Top panel* shows the immunoblot using HA antibodies. *Middle panel* shows undigested ^{32}P-labeled IKK proteins. The *bottom panel* shows CNBr-digested ^{32}P-labeled IKK peptides. Molecular weight markers are indicated at the *right*. *D*, IKKβ is able to phosphorylate its own C terminus. Purified IKKβ from Sf9 cells was tested for kinase activity (*KA*) using GST-IκBα-(1–54) or various peptides of its own C terminus as substrate.

between the HLH and the γBD, we labeled wild type, IKKβ-γBDAA, and IKKβM12 in yeast with [^{32}P]orthophosphate. Wild-type IKKβ and IKKβ-γBDAA were expressed with or without IKKγ, and IKKβM12 was expressed with IKKγ (Fig. 2*C*). The IKKβs were immunoprecipitated using HA antibodies, gel-purified, and cleaved by CNBr for phosphopeptide mapping as described (1). As shown in Fig. 2*C*, *top panel*, similar levels of IKKβs were immunoprecipitated. Wild-type and IKKβ-γBDAA are phosphorylated weakly when expressed alone (Fig. 2*C*, *middle panel*). Their level of phosphorylation increases significantly when expressed with IKKγ. The phosphorylation of the IKKβM12 mutant in the presence of IKKγ is low and similar to the levels of wild type IKKβ-γBDAA in the absence of IKKγ expression. When co-expressed with IKKγ, the C-terminal fragment of IKKβ, the ^{32}P-labeled peptide band above the 5-kDa marker is seen in the wild type and IKKβ-γBDAA, but not in IKKβM12 mutant (Fig. 2*C*, *bottom panel*).

We further assessed whether IKKβ purified from Sf9 cells is capable of phosphorylating a peptide containing the C-terminal serines of IKKβ *in trans*. The entire C-terminal region of IKKβ including the HLH, serine-rich, and the NBD/γBDs were produced with a Myc tag and a His_6 tag at their C terminus in bacteria. For some of these peptides, ten or more of the serines were mutated to alanines. For M10, the first 10 serines after the HLH were substituted with alanine. For M12, twelve serines, including those in and near the NBD/γBD, were substituted with alanine. For M14, 14 serines were substituted with alanine. These peptides were expressed in bacteria and purified using nickel beads.[4]

As shown in Fig. 2*D*, purified IKKβ was able to phosphorylate the peptide containing the wild type and the M10, M12, and M14 peptides. The mutant peptides were phosphorylated 3–5 times less efficiently than the wild-type peptide. As a control, purified IKKβ strongly phosphorylated its known substrate IκBα. The phosphorylation of the C-terminal peptides by IKKβ was significantly weaker than phosphorylation of the IκBα. The data indicate that IKKβ can phosphorylate its C terminus. However, perhaps caused by the absence of IKKγ and conformational requirements only present within the IKK complex, phosphorylation of the C-terminal serines may not be as specific and efficient *in trans*. Phosphorylation of M10, M12, and M14 *in trans* by IKKβ could also occur on threonine residues in the C terminus of IKKβ. Taken together, data in Fig. 2 indicate that the C-terminal serines between HLH and NBD/γBD in IKKβ are autophosphorylated in an IKKγ-dependent manner.

IKKγ Induces Phosphorylation of the T-loop of IKKβ and Mimicks a Phosphorylation State of the NBD/γBD That Reduces IKK Activation Significantly—As shown above, autophosphorylation of ten serines between the HLH and NBD/γBD of IKKβ does not seem to play a role in regulating IKK complex activity. May *et al.* (33) suggested that phosphorylation of serines 740 in the NBD/γBD may down-regulate IKK activity. We used the yeast reconstitution of IKK to examine whether mimicking the phosphorylation state of the serines 740 and 750 in the NBD/γBD has a negative effect in IKKγ-induced activation of IKK complex. Substituting serine to glutamate to mimic a negative charge has resulted in constitutively active MAP kinases (36). In the case of IKK kinases, phosphorylation of the regulatory serines in the T-loop activation region in the kinase domain has resulted in constitutive activity (3). We generated yeast expression vectors for HA-IKKβ-γBDEE (in which serines 740, and 750 are mutated to glutamate) and HA-IKKβ-γBDAA (in which serines 740 and 750 are mutated to alanine, see Fig. 3*A*). We also generated yeast expression vectors for HA-IKKβ-T-loopEE, HA-IKKβ-T-loopAA, and HA-IKKβ-T-loopEE-γBDEE (Fig. 3*A*). Each IKKβ was expressed alone or with IKKγ on the same vector in yeast, and IKK complexes were partially purified by gel filtration. IKKβ reconstituted with IKKγ (Fig. 3*B*, *lane 2*) has higher activity than IKKβ alone (Fig. 3*B*, *lane 1*), indicating that IKKγ facilitates self-activation of IKK. Mutating the T-loop regulatory serines to glutamate to mimic the phosphorylated state results in high activity (Fig. 3*B*, *lane 3*), which is not further activated by co-expression with IKKγ (Fig. 3*B*, *lane 4*). This indicates that the regulatory role of IKKγ is upstream of the phosphorylation of the T-loop serines. Mutation of the T-loop serines to alanines makes the kinase completely inactive (Fig. 3*B*, *lane 5*), and this mutated IKKβ T-loop AA cannot be activated at all by the presence of IKKγ (*lane 6*). When the serines 740 and 750 in the NBD/γBD are mutated to glutamate, IKKβ still has a low level of kinase activity (Fig. 3*B*, *lane 7*), similar to wild-type IKKβ (Fig. 3*B*, *lane 1*). However, reconstitution with IKKγ does not allow IKKβ-γBDEE to become activated (*lane 8*). This

[4] Y-K. Lee and E. Zandi, unpublished data.

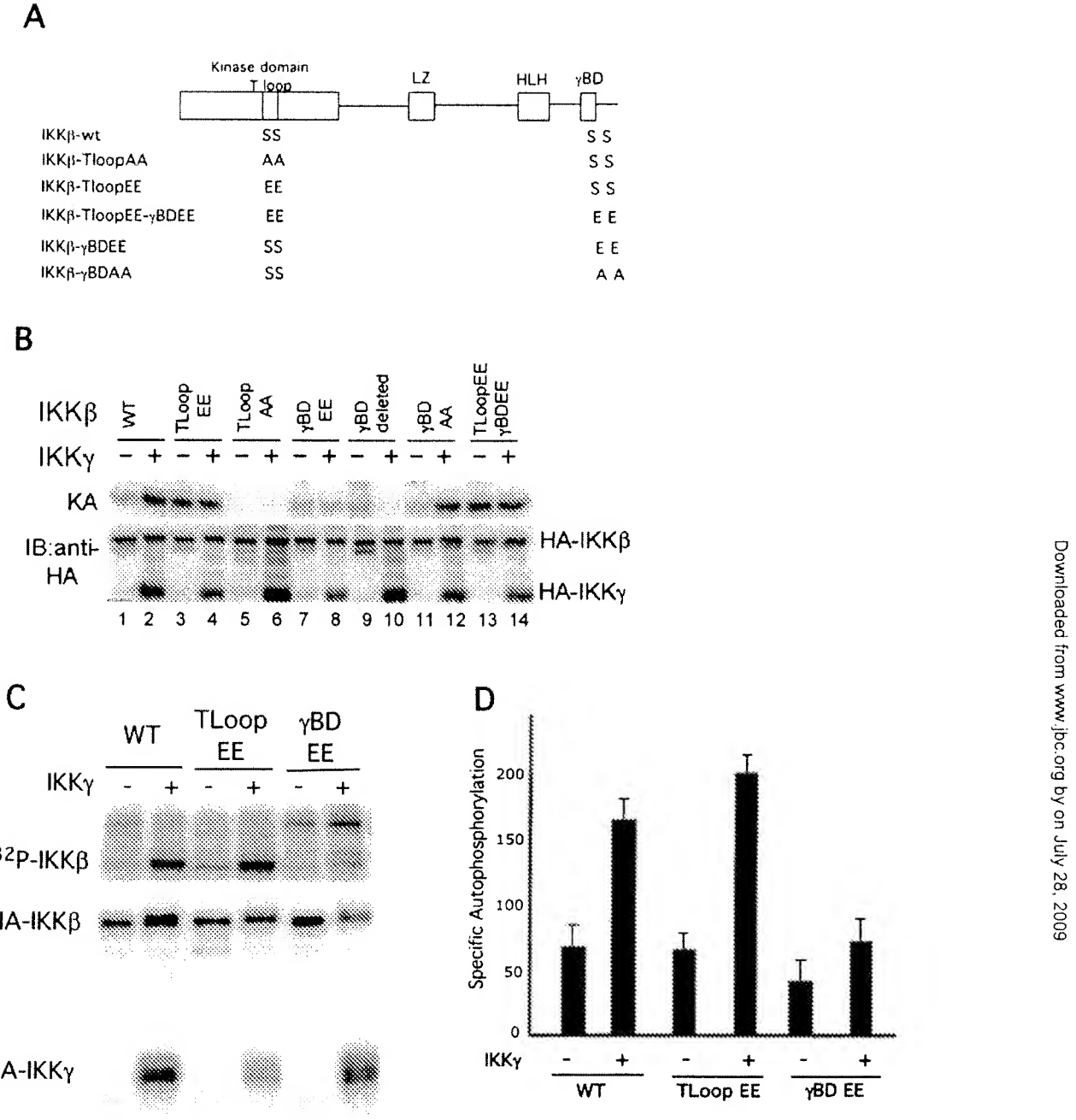

FIGURE 3. **Mimicking the phosphorylation state of serines in and adjacent to the γBD of IKKβ prevents IKKγ-induced activation of IKK complex in yeast.** *A*, schematic diagram showing the IKKβ T-loop and C-terminal mutant constructs. In wild-type IKKβ, there are 2 serines in the T-loop (Ser^{537} and Ser^{541}) and a series of serines following the HLH domain. These serines were mutated to alanines (to prevent possible phosphorylation) or to glutamic acids (to make them mimic the phosphorylated state). These constructs were transformed into and used to express full-length IKKβ (with an HA tag at the N terminus) in yeast. *B*, kinase assay comparing activity of wild-type and mutant forms of IKKβ. Wild-type or mutant forms of HA-IKKβ were expressed alone or co-expressed with HA-IKKγ in yeast. Partially purified IKK complexes were tested for IKK kinase activity (*KA*), and the amounts of HA-IKKβ and HA-IKKγ were determined by anti-HA immunoblot (IB-anti-HA). *C*, phospholabeling of IKKβ in yeast. Untransformed (YPD) yeast or yeast transformed with expression plasmids for various forms of IKKβ (with or without IKKγ) were simultaneously induced and labeled with [^{32}P]orthophosphate. Yeast pellets were lysed, IKK was isolated by immunoprecipitation, and the level of autophosphorylation in IKKβ was assessed by SDS-PAGE followed by PhosphorImager. *D*, scans from three independent experiments shown in *C* were quantified, and the data are shown as specific autophosphorylation of IKKβ. For each data point, the density of autophosphorylation was normalized based on the density of the corresponding signal in the immunoblot. The normalized autophosphorylation values of three independent experiments were averaged, and standard deviations were calculated.

indicates that the analog of phosphorylated serines in the γBD prevents IKKγ from facilitating self-activation of IKK and supports the hypothesis that phosphorylation of these amino acids is a mechanism to maintain IKK in a state of low level of activity. IKKβ with the 6 amino acids in the NBD/γBD domain at the C terminus (LDWSWL) deleted had a low level of activity (Fig. 3*B*, *lane 9*), similar to wild-type IKKβ, but IKKγ could not allow the complex to self-activate (Fig. 3*B*, *lane 10*). This further indicates that the γBD is required for self-activation of the complex. IKKβ-γBDAA, in which serines at the NBD/γBD (740, 750) were mutated to alanine, had a similar level of IKK activity to wild type (Fig. 3*B*, *lane 11*), and IKKγ facilitates its self-activation (Fig. 3*B*, *lane 12*) similar to wild type. Finally, when both the T-loop serines and NBD/

γBD serines are mutated to glutamate to mimic phosphorylation, IKKβ has a high activity (Fig. 3*B*, *lane 13*), and its activity is not further enhanced by the presence of IKKγ (Fig. 3*B*, *lane 14*). These results indicate that interaction of IKKγ with the NBD/γBD of IKKβ is upstream to the phosphorylation of the T-loop serines, which can occur intramolecularly within the IKK complex.

Gel filtration analyses of the above complexes showed that IKKβ containing point mutations in the NBD/γBD form similar size complexes to the wild type and native IKK from HeLa cells (data not shown). This indicates that mutating serines to alanine or glutamate in the NBD/γBD did not affect IKK complex formation.

To further confirm that mimicking the phosphorylation state of the γBD results in decreased IKK activity *in vivo*, we examined autophosphorylation of IKKβ in yeast labeled with [^{32}P]orthophosphate. We compared the autophosphorylation of the wild-type, T-loop EE, and γBD EE IKKβ. Yeast were incubated in [^{32}P]orthophosphate for 5 h, induced to synthesize IKKs, harvested, and lysed, immunoprecipitated, separated by SDS-PAGE, and analyzed by autoradiography and Western blot. A representative experiment is shown in Fig. 3*C* and autophosphorylation data from three independent experiments were normalized based on the signal intensities of corresponding Western blots, and the results are shown in Fig. 3*D*. The wild-type IKKβ expressed alone was only weakly autophosphorylated (Fig. 3, *C* and *D*), but when co-expressed with IKKγ, the level of autophosphorylation increased by 2.3-fold. The IKKβ T-loopEE (which has constitutively high activity toward IκBα, see Fig. 3*B*) when expressed alone showed similar level of autophosphorylated to the wild type. The autophosphorylation of the T-loop EE increased by 3-fold when co-expressed with IKKγ. This result support the data in Fig. 2*C* that show IKKγ facilitates increased phosphorylation of the C-terminal serines, even under conditions where its presence is not needed to activate IKKβ. The IKKβ T-loopEE mutant cannot be phosphorylated in the T-loop, so this phosphorylation is most likely due to C-terminal phosphorylation, providing further support for the findings shown in Fig. 2. The level of autophosphorylation in IKKβ-γBDEE whose kinase activity toward IκBα is low, even in the presence of IKKγ (Fig. 3*B*) did not increase much when co-expressed with IKKγ (Fig. 3, *C* and *D*). In summary, these data suggest that IKKγ facilitates the C-terminal phosphorylation of IKKβ within the IKK complex. This is true even under conditions where IKKβ is constitutively active. Furthermore, the data support the May *et al.* (33) findings in that phosphorylation of the NBD/γBD in IKKβ plays a regulatory role in IKKγ-dependent regulation of IKK complex.

Effect of the NBD/γBD Mutations in IKKβ on the Activity of Reconstituted IKK in MEFα$^{-/-}$β$^{-/-}$—To investigate whether the data shown in Fig. 3*B* can be recapitulated in mammalian cells, we generated HA-tagged mammalian expression vectors for IKKβ-γBDEE and IKKβ-γBDAA. To avoid the interference of the endogenous IKKα or IKKβ, we utilized the MEFα$^{-/-}$β$^{-/-}$ (35). Stable pools of MEFα$^{-/-}$β$^{-/-}$ expressing HA-tagged IKKβ-wt, IKKβ-γBDEE, or IKKβ-γBDAA were generated, and the activity of IKK complex was examined before and after treatment with IL-1β for 10 min (Fig. 4*A*). Using anti-IKKγ antibody, IKKβ·IKKγ complexes were isolated and the kinase activity was assessed by immune kinase complex assay. The activity of IKKβ-wt was induced by IL-1β as expected (Fig. 4*A*). The IKKβ-γBDEE has a similar basal level of activity like the wild-type IKK, but its activity is not induced by IL-1β (Fig. 4*A*). This is consistent with the yeast experiments in Fig. 3*B*, and supports the hypothesis that a negative charge(s) in the NBD/γBD of IKKβ can prevent induction of IKK. Preventing the phosphorylation of the serines in the NBD/γBD should allow constitutive activity of the complex, at least to some degree. IKKβ-γBDAA has significantly higher basal level kinase activity compared with the wild type, and this activity is only marginally induced by IL-1β (Fig. 4*A*). It is important to note that in the presence of endogenous IKKα similar mutations in the NBD/γBD of IKKβ did not allow constitutive activity of the complex (see Fig. 1*A*), though the activation was faster. This indicates that a wild-type NBD/γBD in one of the kinase subunits within the IKK complex could be sufficient to allow IKKγ to regulate the basal level of IKK complex.

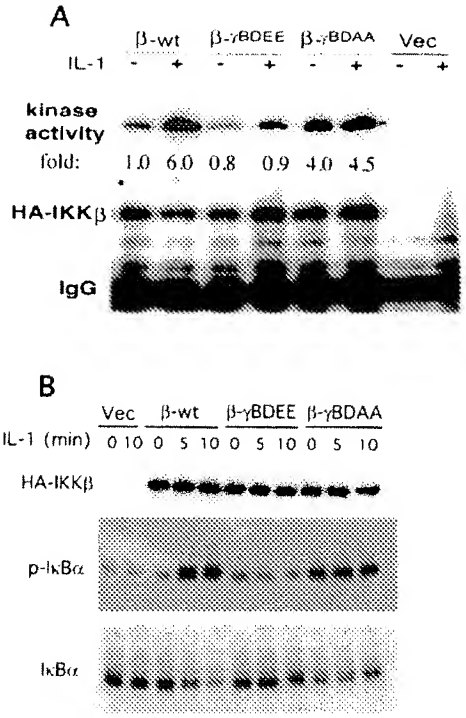

FIGURE 4. **Reconstitution of IKK complex in MEFα$^{-/-}$β$^{-/-}$.** *A*, MEFα$^{-/-}$β$^{-/-}$ were transfected with HA-tagged mammalian expression vectors of IKKβ-wt, IKKβ-γBDEE, or IKKβ-γBDAA, and stable pools were selected using G418. The kinase activities of IKK was assessed by immune kinase complex assay using anti-IKKγ antibodies in cells left untreated or treated with IL-1β for 10 min. Anti-IKKγ antibody was used to isolate the IKKβ·IKKγ complex. *KA*, kinase assay of the immunoprecipitated IKK toward GST-IκBα; *IB*, immunoblot using anti-HA to show that similar levels IKKβ proteins were pulled-down in IKK complex. The HA-IKK amounts were determined by Western blot using anti-HA antibodies. *B*, IL-1-induced phosphorylation of the endogenous IκBα was determined in cells described in *A*. To prevent rapid degradation of phosphorylated IκBα, cells were treated with 5 μM MG-132 (a proteasome inhibitor) for 30 min prior treatment with IL-1β (2 ng/ml) for indicated times in minutes. For immunoblot analysis, 30 μg of whole cell extracts were used. Levels of HA-IKKβ was determined using anti-HA (*top panel*). Phosphorylated IκBα was detected using the phospho-IκBα (Ser^{32}) antibody (Cell Signaling) (*middle panel*). Total IκBα protein levels was determined using an IκBα antibody (Cell Signaling) (*bottom panel*).

To compare the *in vivo* activities of wild-type and mutant IKKβs in the cell lines, we determined the phosphorylation of endogenous IκBα using phospho-IκBα antibodies before and after treatment with IL-1β for 5 and 10 min (Fig. 4*B*). Because phosphorylated IκBα is ubiquitinated and degraded rapidly, proteasome was inhibited by treating the cells with MG-132 (5 μM) for 30 min prior to IL-1 treatment. The phospho-IκBα antibody detects a background band that is present even in the cells transfected with vector. Treating cells with IL-1 did not increase the intensity of the background band in vector-transfected cells (Fig. 4*B*). Because MEFα$^{-/-}$β$^{-/-}$ are devoid of any known IKK activity, the band detected by phospho-IκBα antibody is most likely a weak interaction of this antibody with unphosphorylated IκBα. On the other hand, in cells expressing the wild-type IKKβ, phosphorylation of IκBα increased significantly after IL-1 treatment (Fig. 4*B*). In cells expressing IKKβ-γBDEE, IL-1 treatment did not increase phosphorylation of IκBα

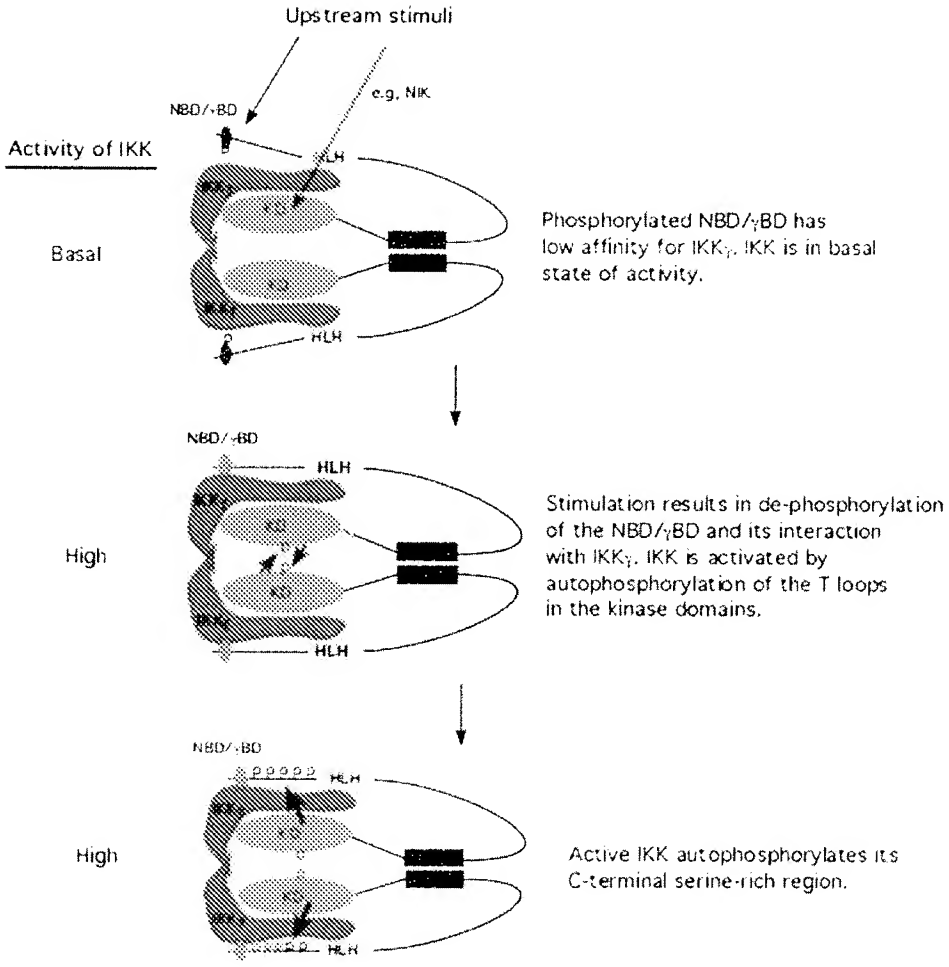

FIGURE 5. **A model for IKKγ-dependent activation of IKK complex by autophosphorylation.**

(Fig. 4*B*). In cells expressing the IKKβ-γBDAA and not treated with IL-1, phosphorylation of IκBα is significantly higher than the wild-type IKKβ (Fig. 4*B*). Treatment of these cells with IL-1 did not increase phosphorylation of IκBα further (Fig. 4*B*).

Taken together, the data in Fig. 4 support the hypothesis that phosphorylation of the NBD/γBD in IKKβ and possibly in IKKα plays a role in regulation of the IKK complex.

DISCUSSION

There are at least 16 serine residues in IKKβ, which may be involved in up-regulating and down-regulating IKK activity. These consist of two serine residues in the T-loop and 14 serines following the HLH domain, including 2 serines in and adjacent to the NBD/γBD. NIK activates IKKα by direct phosphorylation of T-loop serines (19). However, many other stimuli activate IKK via IKKγ and may not act by direct phosphorylation of T-loop serines. Rather many stimuli may act by altering the interaction of IKKγ with the NBD/γBD at the C terminus of IKKβ. As shown in Fig. 3*B*, when the serine residues in the NBD/γBD of IKKβ are mutated to resemble phosphoserine, the kinase is no longer stimulated by IKKγ in the yeast reconstitution system. Expression of a similar IKKβγBDEE in MEF$\alpha^{-/-}\beta^{-/-}$ could only be weakly stimulated by IL-1. Furthermore, IKKβγBΔAA (where NBD/γBD serines cannot be phosphorylated) was either constitutively active or showed more rapid activation kinetics than wild-type IKK. Altogether, these data suggest that phosphorylation of NBD/γBD serines may be a mechanism by which IKK is maintained in a low activity state, and upstream stimuli may regulate IKK by altering the phosphorylation status of NBD/γBD serines. Phosphorylation of serines in the region where IKKγ binds to IKKβ may alter the interaction between the two subunits, thereby altering its capacity to become activated.

Data presented here and previously (33) indicate that phosphorylation of the NBD/γBD maintains IKK in a basal state, but it is unclear what kinase is responsible for catalyzing this phosphorylation. The results of this study demonstrate that IKKβ can phosphorylate a peptide substrate containing the serines in the NBD/γBD of IKKβ, indicating that indeed IKKβ can phosphorylate its NBD/γBD. However, this phosphorylation is relatively weak (compared with the activity of IKK toward IκB, see Fig. 2*D*). Perhaps the level of phosphorylation observed is low because IKKβ is phosphorylating exogenous C termini, and the kinase normally autophosphorylates its NBD/γBD within the same complex. Perhaps this phosphorylation is weak because IKKγ is needed for this autophosphorylation. Alternatively, it is possible that while IKKβ can indeed autophosphorylate its NBD/γBD, in mammalian cells there exists another kinase whose role is to phosphorylate the NBD/γBD of IKKβ.

It is clear that phosphorylating the NBD/γBD serines can diminish IKK activity, but these are not the only serines phosphorylated in the C terminus of IKKβ. As in mammalian cells, the 10 serines immediately following the HLH are heavily phosphorylated in the yeast reconstitution system. This study indicates that this is due to autophosphorylation, requires active IKKβ, and is strongly enhanced by IKKγ. Previous work using mammalian cells indicated that inactivating mutations in

the kinase domain (K44A) or T-loop (S177A and S181A) of IKKβ completely prevented IKKβ phosphorylation at the C terminus, suggesting that the mechanism of C-terminal phosphorylation is autophosphorylation (1). However, it remained plausible that only native, active IKK could be recognizable by a putative exogenous IKK C-terminal kinase. Co-expression of IKKγ with IKKβ in the yeast system results in increased phosphorylation of IKKβ, primarily in the 10 serines immediately following the HLH as evidenced by direct *in vivo* labeling as well as by band shift during gel electrophoresis (Figs. 2 and 3). This result is not surprising since expression of IKKγ is known to activate IKKβ, and IKKβ has been shown to autophosphorylate its C terminus. However, when IKKβ is made constitutively active by mutation of T-loop serines to glutamic acids, it is not phosphorylated very strongly. In contrast, when this same form of IKKβ T-loop EE is co-expressed with IKKγ, a strong phosphorylation of the C terminus is seen. This result indicates that while having active kinase is sufficient for IKKβ autophosphorylation, IKKγ is somehow involved in augmenting the phosphorylation of C-terminal serines beyond the HLH. As shown in Fig. 1, phosphorylation of these serines does not appear to affect IKK activity, nor does it appear to have a previously reported down-regulatory function (1).

In studies involving mammalian cells, mutation of T-loop serines to glutamic acids resulted in constitutively high activity (1, 3). However, because these cells have an NF-κB activation pathway, it was possible that these phosphorylated residues attracted other molecules to the IKK complex, resulting in activation. Yeast cells lack the NF-κB system (and presumably other factors involved in activating IKK). Nonetheless, when IKKβ with phospho-mimicking residues in the T-loop is expressed in yeast (Fig. 3*B*), it is constitutively active and does not require IKKγ. Mutation of the T-loop serines to alanines makes the kinase inactive, even in the presence of IKKγ. When both the NBD/γBD serines and the T-loop serines were mutated to glutamic acids (Fig. 3*B*), the kinase was constitutively active (with or without co-expression with IKKγ). This indicates that phosphorylation of the T-loop serines is the dominant factor governing whether IKKβ is active or inactive; if the T-loop serines are phosphorylated, the kinase is not affected by changes in the phosphorylation status of the C terminus.

These data suggest that there are possibly dual mechanisms for activating IKK (see Fig. 5). Certain pathways (such as NIK) may activate IKK by directly phosphorylating the T-loop serines. Other stimuli may act via IKKγ and the NBD/γBD to cause conformational changes in the IKK complex, facilitating autophosphorylation of T-loop serines and increasing kinase activity. Phosphorylation of the NBD/γBD serines may prevent IKKγ from facilitating autophosphorylation and self-activation during periods of basal activity.

Acknowledgments—We thank Dr. Michael Karin for generously providing the IKKβ serine to alanine C-terminal mutants and the MEFβ$^{-/-}$ cells. We thank Dr. Inder Verma for generously providing the MEFα$^{-/-}$β$^{-/-}$. We thank Dr. Chih-Lin Hsieh for reading and comments on the manuscript.

REFERENCES

1. Delhase, M., Hayakawa, M., Chen, Y., and Karin, M. (1999) *Science* **284,** 309–313
2. DiDonato, J. A., Hayakawa, M., Rothwarf, D. M., Zandi, E., and Karin, M. (1997) *Nature* **388,** 548–554
3. Mercurio, F., Zhu, H., Murray, B. W., Shevchenko, A., Bennett, B. L., Li, J., Young, D. B., Barbosa, M., Mann, M., Manning, A., and Rao, A. (1997) *Science* **278,** 860–866
4. Zandi, E., Rothwarf, D. M., Delhase, M., Hayakawa, M., and Karin, M. (1997) *Cell* **91,** 243–252
5. Rothwarf, D. M., Zandi, E., Natoli, G., and Karin, M. (1998) *Nature* **395,** 297–300
6. Yamaoka, S., Courtois, G., Bessia, C., Whiteside, S. T., Weil, R., Agou, F., Kirk, H. E., Kay, R. J., and Israel, A. (1998) *Cell* **93,** 1231–1240
7. Ghosh, S., and Karin, M. (2002) *Cell* **109,** (suppl.) S81–S96
8. Siebenlist, U., Franzoso, G., and Brown, K. (1994) *Annu. Rev. Cell Biol.* **10,** 405–455
9. Yaron, A., Hatzubai, A., Davis, M., Lavon, I., Amit, S., Manning, A. M., Andersen, J. S., Mann, M., Mercurio, F., and Ben-Neriah, Y. (1998) *Nature* **396,** 590–594
10. Strack, P., Caligiuri, M., Pelletier, M., Boisclair, M., Theodoras, A., Beer-Romero, P., Glass, S., Parsons, T., Copeland, R. A., Auger, K. R., Benfield, P., Brizuela, L., and Rolfe, M. (2000) *Oncogene* **19,** 3529–3536
11. Miller, B. S., and Zandi, E. (2001) *J. Biol. Chem.* **276,** 36320–36326
12. Zandi, E., Chen, Y., and Karin, M. (1998) *Science* **281,** 1360–1363
13. May, M. J., D'Acquisto, F., Madge, L. A., Glockner, J., Pober, J. S., and Ghosh, S. (2000) *Science* **289,** 1550–1554
14. Takeda, K., Takeuchi, O., Tsujimura, T., Itami, S., Adachi, O., Kawai, T., Sanjo, H., Yoshikawa, K., Terada, N., and Akira, S. (1999) *Science* **284,** 313–316
15. Hu, Y., Baud, V., Delhase, M., Zhang, P., Deerinck, T., Ellisman, M., Johnson, R., and Karin, M. (1999) *Science* **284,** 316–320
16. Li, Q., Van Antwerp, D., Mercurio, F., Lee, K. F., and Verma, I. M. (1999) *Science* **284,** 321–325
17. Dejardin, E., Droin, N. M., Delhase, M., Haas, E., Cao, Y., Makris, C., Li, Z. W., Karin, M., Ware, C. F., and Green, D. R. (2002) *Immunity* **17,** 525–535
18. Claudio, E., Brown, K., Park, S., Wang, H., and Siebenlist, U. (2002) *Nat. Immunol.* **3,** 958–965
19. Senftleben, U., Cao, Y., Xiao, G., Greten, F. R., Krahn, G., Bonizzi, G., Chen, Y., Hu, Y., Fong, A., Sun, S. C., and Karin, M. (2001) *Science* **293,** 1495–1499
20. Huynh, Q. K., Boddupalli, H., Rouw, S. A., Koboldt, C. M., Hall, T., Sommers, C., Hauser, S. D., Pierce, J. L., Combs, R. G., Reitz, B. A., Diaz-Collier, J. A., Weinberg, R. A., Hood, B. L., Kilpatrick, B. F., and Tripp, C. S. (2000) *J. Biol. Chem.* **275,** 25883–25891
21. May, M. J., Larsen, S. E., Shim, J. H., Madge, L. A., and Ghosh, S. (2004) *J. Biol. Chem.* **279,** 45528–45539
22. Lomaga, M. A., Yeh, W. C., Sarosi, I., Duncan, G. S., Furlonger, C., Ho, A., Morony, S., Capparelli, C., Van, G., Kaufman, S., van der Heiden, A., Itie, A., Wakeham, A., Khoo, W., Sasaki, T., Cao, Z., Penninger, J. M., Paige, C. J., Lacey, D. L., Dunstan, C. R., Boyle, W. J., Goeddel, D. V., and Mak, T. W. (1999) *Genes Dev.* **13,** 1015–1024
23. Krappmann, D., and Scheidereit, C. (2005) *EMBO Rep.* **6,** 321–326
24. Wang, C., Deng, L., Hong, M., Akkaraju, G. R., Inoue, J., and Chen, Z. J. (2001) *Nature* **412,** 346–351
25. Sun, L., Deng, L., Ea, C. K., Xia, Z. P., and Chen, Z. J. (2004) *Mol. Cell* **14,** 289–301
26. Deng, L., Wang, C., Spencer, E., Yang, L., Braun, A., You, J., Slaughter, C., Pickart, C., and Chen, Z. J. (2000) *Cell* **103,** 351–361
27. Abbott, D. W., Wilkins, A., Asara, J. M., and Cantley, L. C. (2004) *Curr. Biol.* **14,** 2217–2227
28. Huang, T. T., Wuerzberger-Davis, S. M., Wu, Z. H., and Miyamoto, S. (2003) *Cell* **115,** 565–576
29. Brummelkamp, T. R., Nijman, S. M., Dirac, A. M., and Bernards, R. (2003) *Nature* **424,** 797–801
30. Kovalenko, A., Chable-Bessia, C., Cantarella, G., Israel, A., Wallach, D., and Courtois, G. (2003) *Nature* **424,** 801–805
31. Trompouki, E., Hatzivassiliou, E., Tsichritzis, T., Farmer, H., Ashworth, A., and Mosialos, G. (2003) *Nature* **424,** 793–796
32. Prajapati, S., Verma, U., Yamamoto, Y., Kwak, Y. T., and Gaynor, R. B. (2004) *J. Biol. Chem.* **279,** 1739–1746
33. May, M. J., Marienfeld, R. B., and Ghosh, S. (2002) *J. Biol. Chem.* **277,** 45992–46000
34. Li, Z. W., Chu, W., Hu, Y., Delhase, M., Deerinck, T., Ellisman, M., Johnson, R., and Karin, M. (1999) *J. Exp. Med.* **189,** 1839–1845
35. Li, Q., Estepa, G., Memet, S., Israel, A., and Verma, I. M. (2000) *Genes Dev.* **14,** 1729–1733
36. Brunet, A., Pages, G., and Pouyssegur, J. (1994) *Oncogene* **9,** 3379–3387